THE GEOLOGY AND GEOCHEMISTRY OF THE GLENTIG, SWAERSHOEK AND ALMA FORMATIONS IN THE LIMPOPO PROVINCE, SOUTH AFRICA

By

MAKULANA MULALO MELTON

[redacted]

Dissertation submitted in fulfilment of the requirement for the degree of

MASTER OF SCIENCE

In

GEOLOGY

In the

DEPARTMENT OF GEOLOGY AND MINING

SCHOOL OF PHYSICAL AND MINERAL SCIENCES

FACULTY OF SCIENCE AND AGRICULTURE

UNIVERSITY OF LIMPOPO, SOUTH AFRICA

SUPERVISOR: DR CHRISTOPHER BAIYEGUNHI

NOVEMBER 2020

DECLARATION

I, Melton Mulalo Makulana, declare that this research dissertation entitled “The geology and geochemistry of the Glentig, Swaershoek and Alma Formations in the Limpopo Province, South Africa” to be my unaided work. The research reported in this dissertation, except where otherwise indicated, contain the original research results and has not been previously accepted or concurrently submitted to any other university for any degree award or examination purposes.

Mulalo Melton Makulana 20/11/2020

University of Limpopo, Mankweng Date

DEDICATIONS

To God be the Glory

ACKNOWLEDGEMENTS

First and foremost, Praises and Honour to Jesus Christ for His overflowing protection, love and guidance.

My wife, Livhuwani Makulana all this was possible because of your superlative love, your enduring support, not overlooking the faith you have in me and providing a home to run to after a long day's work. Orifunaho Phathutshedzo Makulana there is no words to ascertain how much you inspired me.

My supervisor Dr C Baiyegunhi, I thank you for your support, words of advice, guidance, and encouragement which built me into a better if not a competitive scientist and for sharing your grandiose expertise with me. Ḽ meela Daalụ

A warm appreciation to my whole family especially my mom Mrs Nyaluvhani Emily Makulana and my father Mr Engedzani Frans Makulana, I thank you for giving me your endless love, guidance, and support from the beginning of this journey, even through it and to its ultimate fulfilment. Mazekeen thanks for the negative energy, it pushed me to be better than who I am, for that am grateful.

To my field buddy, colleague, and friend extraordinaire, Mr S Masango, I am grateful and highly appreciate of your assistance, guidance, unwavering support and having so much faith in me.

I would like to extend my great appreciation to the Mining Qualification Authority (MQA) for financial assistance.

ABSTRACT

The Glentig, Alma and Swaershoek Formations were deposited after the emplacement of the Bushveld igneous complex (BIC). The sediments accumulated in what is termed as the proto-basin of the Waterberg Group. The Glentig Formation is an unconformity-bounded formation that is overlain by the Swaershoek and Alma Formations of the Waterberg Group. This study revisited the stratigraphy and put perception on the petrography, lithofacies, provenance, paleoweathering, tectonic setting and source rock characteristics of the lower parts of Waterberg Group (Swaershoek and Alma Formations) and Glentig Formation. The methodologies employed in achieving the aforementioned goals include stratigraphical analysis, petrographical and modal composition analyses, lithofacies analysis and geochemical analysis. In the study area (northeast of Modimolle town), the Glentig Formation lies or bounded between the Swaershoek Formation and Schrikkloof Formation of the Rooiberg Group. The Glentig, Swaershoek and Alma Formations attained a maximum thickness of about 400 m, 300 m and 190 m, respectively. Based on the stratigraphical analysis, the Swaershoek, Alma and Glentig Formations can be correlated. The basis for the correlation rests solemnly on the similarities in the lithological characteristics that can be found in the three formations.

Six facies were identified based on lithofacies analysis. The lithofacies are grouped into 2 facies association (FA1 and FA2). The two facies associations are FA1: Conglomerate and massive sandstone, and FA2: Cross-bedded sandstone, and planar cross-bedded sandstone. Sedimentological characteristics of the identified facies associations are interpreted as debris flow, and longitudinal and transverse bars (fluvial channel deposits). Petrography and modal composition analyses indicate that the detrital components of the sandstones are dominated by monocrystalline quartz,

feldspar and lithic fragments. The sandstones of the Swaershoek, Alma and Glentig Formations can be classified as subarkosic arenite and lithic arkosic arenite. Also, provenance analysis indicates that the sandstones are derived from both felsic igneous provenance and intermediate igneous provenance. The modal composition analysis and geochemical tectonic setting discrimination diagrams show that the sediments are from both the passive and active continental margin tectonic settings. Also, the geochemical data of major and trace elements suggested that the studied formations have been derived from the same provenance source area. The indices of weathering indicated that the studied rocks have been subjected to moderate to the high degree of chemical weathering.

Keywords: *Geology, geochemistry, Glentig, Swaershoek, Alma, Waterberg Group, South Africa*

TABLE OF CONTENTS

LIST OF FIGURES

LIST OF TABLES

CHAPTER 1

GENERAL INTRODUCTION

1.1 Background of the study

The Glenting, Swaershoek and the Alma Formations are the least studied formations. The aforementioned formations exist in the least studied hiatuses in the world. The Vaalian Era was characterized by a long period of comparative craton stability and marked by cyclic epeirogeny during which the Transvaal Supergroup was deposited in shallow-marine environments; due to barrage of the Kaapvaal Craton (Maré et al., 2006). The extrusion of the Rooiberg Group of the Bushveld Igneous Complex (BIC) marked the end of the Vaalian Era (Maré et al., 2006). The development or formation of intracratonic basins in the north of the Kaapvaal Craton resulted in the deposition of the red beds of the Waterberg Group. During the hiatus, at the end of the Vaalian Era and beginning of the Mokolian Era, deposition of the proto-Waterberg units, which includes Loskop, Rust de Winter and Glentig Formations occurred (van der Nuet et al., 1991; Maré et al., 2006).

The Glentig Formation is an unconformity-bounded formation that is overlain by the Swaershoek Formation of the Waterberg Group and underlain by the Sckrikkloof Formation of the Rooiberg Group (Figure 1.1). Jansen (1970) proposed the name Glentig Formation and indicated the locality to be on the farm Glentig (Figure 1.2). The Waterberg Group was deposited in gently subsiding intracratonic basins in the north of the Kaapvaal Craton during the Paleoproterozoic (Mokolian) era (Callaghan et al., 1993). The “red beds” Waterberg Group were deposited unconformably on the

Transvaal Supergroup, felsic and mafic rocks of the Bushveld Complex and Archaean basement of the Kaapvaal Craton (Johnson et al., 2006).

Martini (1998) reported that, in the Witbank-Cullinan Basin, the Rooiberg Group grades conformably to Loskop Formation. Eriksson et al. (2005) included the Loskop Formation in the Transvaal Sequence, while Kent (1980) documented that the Loskop Formation and its correlatives i.e. the Glentig and Rust de Winter Formations are stand-alone units not belonging to neither the Transvaal Supergroup, Bushveld Igneous Complex nor the Waterberg Group (Figure 1.1).

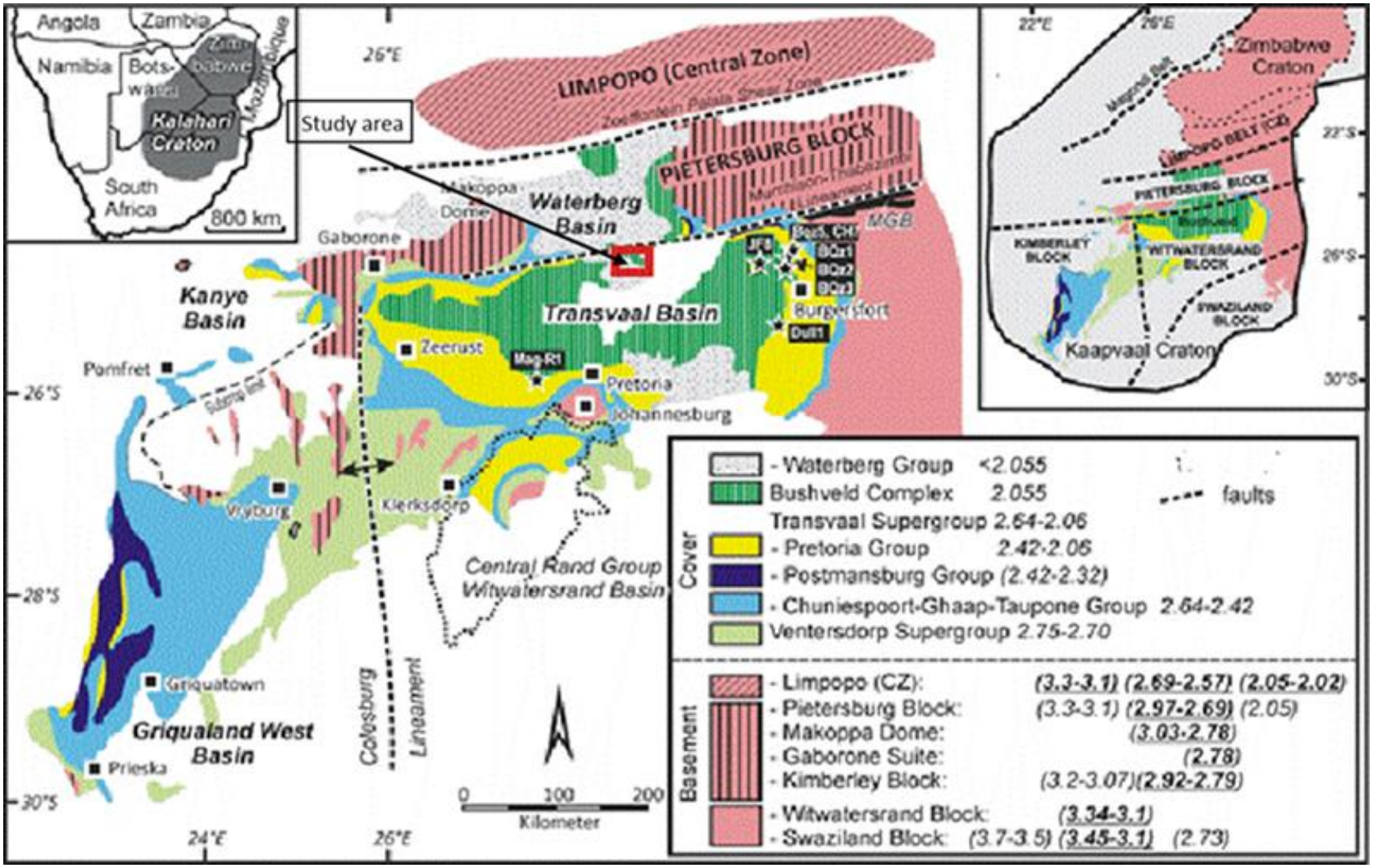

Figure 1.1 Geological map of the study area (after Zeh et al., 2016).

The Swaershoek Formation is the lowermost formation of the Nylstroom Subgroup (Johnson et al., 2006). As documented by SACS (1980), the Swaershoek Formation is subdivided into a lower and upper part. The lower part is reported to have been deposited immediately after the emplacement of the Bushveld Complex, and it is made up mostly of arenites and rudites. On the other hand, the upper part of the Swaershoek Formation comprises of arenites and rudites intercalated with lutites and occasional quartz porphyry (Johnson et al., 2006). The Glentig, Swaershoek and Alma Formations are one of the least studied formations in South Africa. Research work carried out by Jansen (1970) is the only reported study on the Glentig, Swaershoek and Alma Formations.

The deposition of the Glentig and Swaershoek Formations occurred in the period between the last magmatism of the Bushveld Igneous Complex and the deposition of Paleoproterozoic red beds of the Waterberg Group (Martini, 1998). The correlation of the Glentig Formation and Loskop Formation was based on the upper and lower contact relationships and lithological similarities (SACS, 1980). The Loskop Formation has been a subject of more studies than the Glentig Formation (Masango, 2014; Barker et al., 2006; Martini, 1998; Mellor, 1997). Nevertheless, none of these researchers correlated the Loskop, Glentig, Swaershoek and Alma Formations as well as report on their stratigraphy, facies, tectonic provenance and depositional environments.

The purpose of this study is to investigate the geology and geochemistry of the aforementioned formations to unravel their provenance and tectonic setting. In addition, the study is intended to provide more detailed information on the main characteristics of lithologies, sedimentary structures and vertical sequence patterns

and depositional paleo-environments of the Glentig, Swaershoek and Alma Formations. The results or datasets generated from this research work could be used to tease out an interpretation of the sedimentary history and evolution of the basin as well as enhance the understanding of the development of geological events during the last 2 billion years.

1.2 Location of the study area

The study area is located approximately 54 km north of Modimolle town (previously called Nylstroom) and 143 km south-southwest of Polokwane. Geographically, it is bounded within latitudes 24˚24'04.89" S and 24˚30'05.33" S and longitudes 28˚20ˈ0" E; 28˚30ˈ0" E (Figure 1.2). Specifically, the only outcrop of the Glentig Formation in South Africa is situated within longitudes 28˚25ˈ58.12" E and 28˚29ˈ22.13" E and latitudes 24˚28'04.89" S and 24˚26'05.33" S in the Limpopo Province (Figure 1.3). The study area is a sparsely populated farming area and majority of the farms are operated as either as game hunting areas, farming or as game reserves. Furthermore, the average annual temperature is about 18.4 ℃ (climate-data.org). In a year, the average rainfall is approximately 630 mm, with most rainfall occurring during summer. The estimate terrain elevation above sea level is about 1378 m.

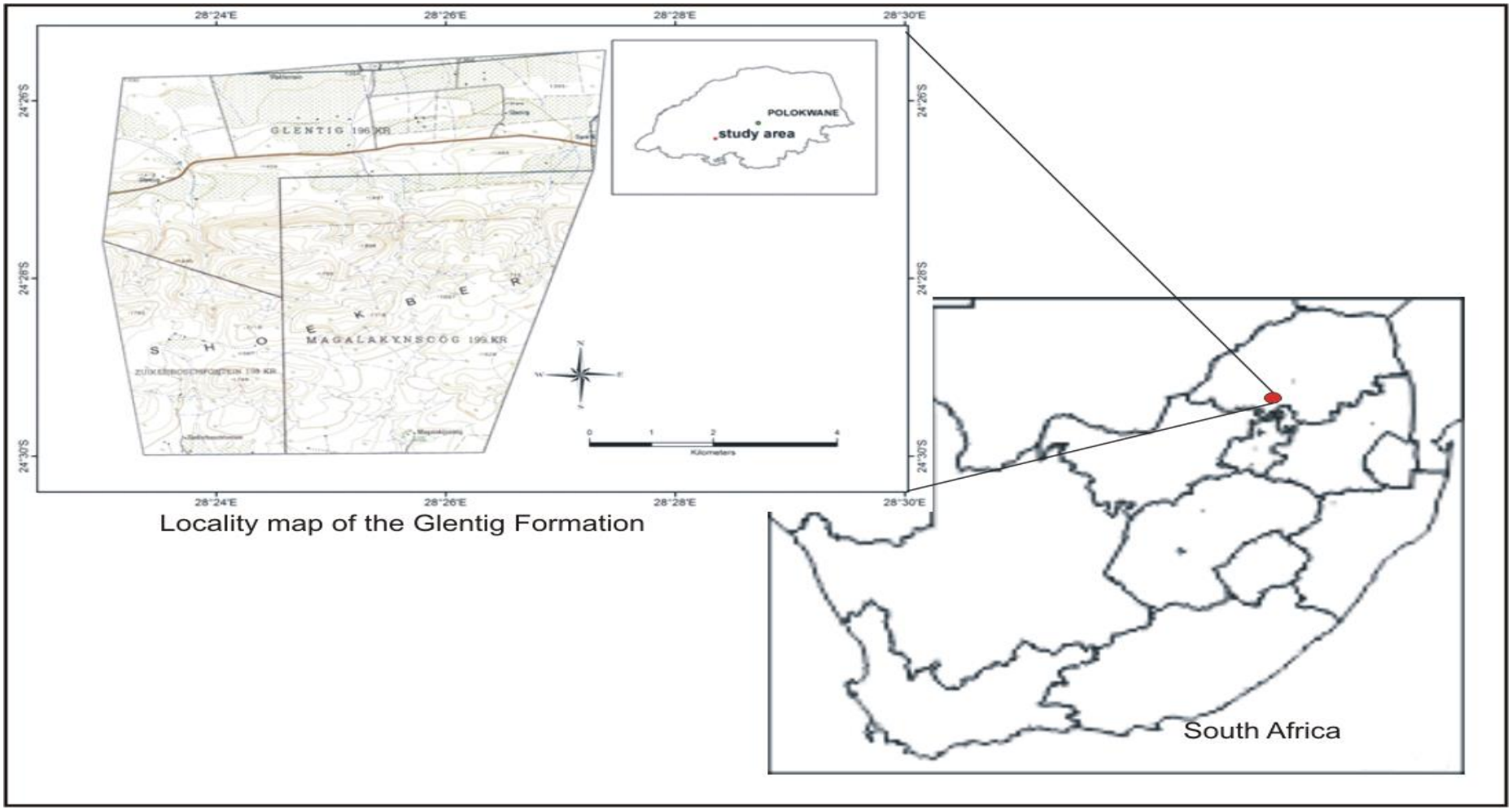

Figure 1.2: Location of the study area within the Yellowwood game lodge, Magalakynsoog north and south Farms, Limpopo Province (after Twist and French, 1983).

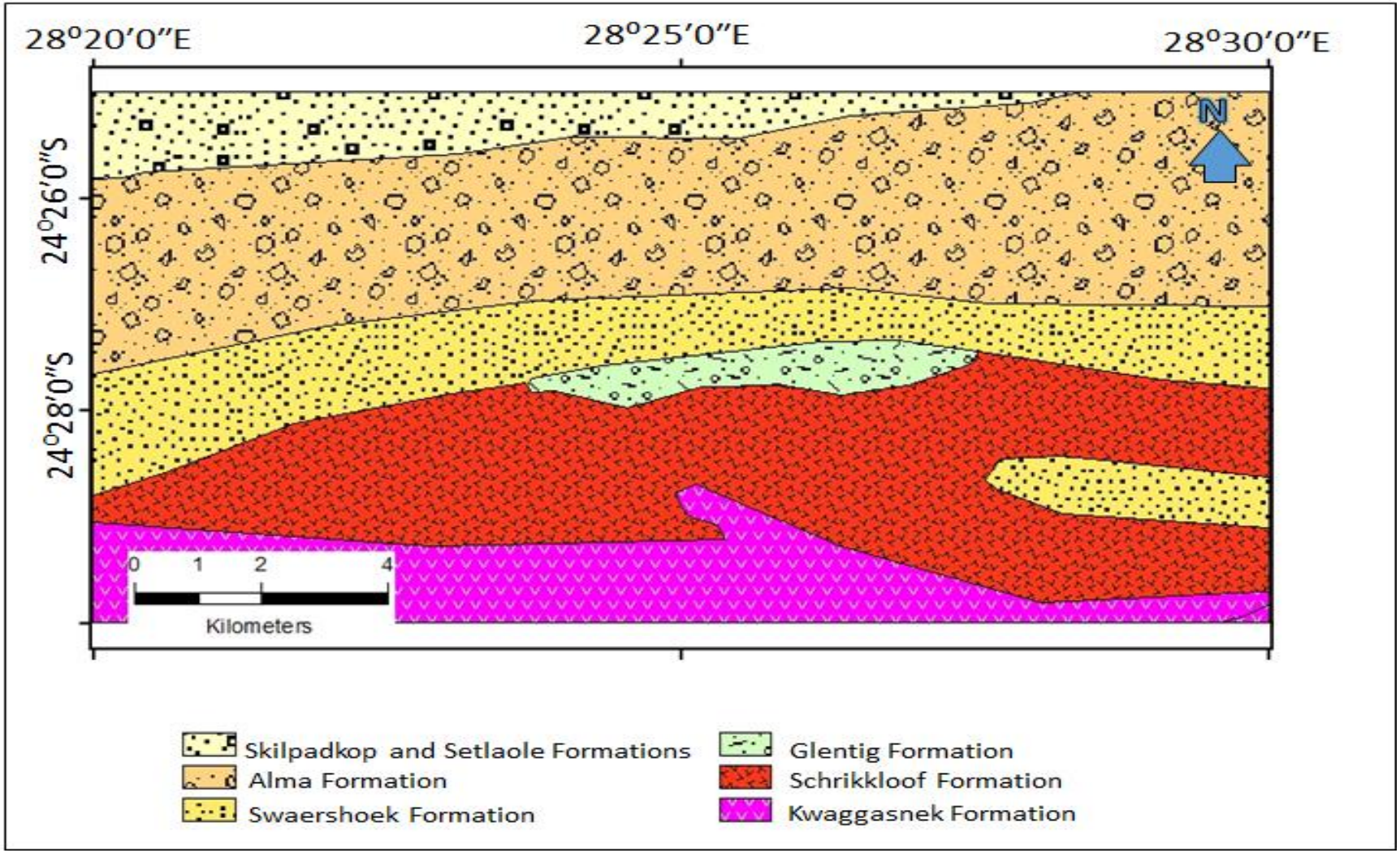

Figure 1.3: Geological map of the study area (modified after Masango, 2014).

1.3 Problem statement

Previous studies carried out on the Glentig, Swaershoek and Alma Formations including those of Jansen (1970), Jansen et al. (1977), SACS (1980), Cheney and Twist (1986), and Johnson et al. (1997) mainly focused on the stratigraphy and age of the formations. The South African Committee of Stratigraphy (SACS, 1980) and Johnson et al. (1997) only reported that the Glentig Formation is a proto-basin to the Waterberg Group. The depositional environment of the Glentig Formation has neither been a subject of study in the past nor the provenance determined. Up to date, little is known of the stratigraphy, depositional processes, sedimentary facies and provenance of the Glentig Formation. Even though more work has been carried out on the Swaershoek and Alma Formations, up to date, their provenance, tectonic setting and source rock characteristics of these formations are still poorly understood or documented. Again, there is a general absence of a cohesive analysis of sedimentary and geochemical data of the rocks of the Swaershoek, Alma and Glentig Formations.

1.4 Aim and objectives

This research project aims to investigate the geology and geochemistry of the Glentig, Alma and Swaershoek Formations to provide information on their source rock characteristics, provenance and tectonic setting. The objectives of the study are to:

i. determine the lithology and measure the stratigraphic successions of the Glentig, Alma and Swaershoek Formations
ii. investigate the sedimentary facies that are present in the formations and deduce their depositional environments

iii. carry out and modal composition to unravel the tectonic provenance of the formations

iv. use the geochemistry (major oxides and trace elements) to investigate the tectonic setting and paleoweathering conditions of the rocks.

1.5 Research limitations

The major challenge faced during this research work is gaining access to the farms where the Glentig, Alma and Swaershoek Formations outcropped. The aforementioned formations are only exposed in the Glentig, Magalakynsoog (north and south), Geelhoutkloof (Yellowwood game Lodge), Vlakfontein, and Gemsbokfontein farms. Most of these farms are game farms, except for the Magalkynsoog south which is a cattle breeding farm. Accessibility to the Glentig, Vlakfontein, and Gemsbokfontein farms was denied after several attempts. Hence, in this study, stratigraphic measurements and sampling were only carried out in the Magalakynsoog (north and south) and Geelhoutkloof (Yellowwood game Lodge) farms where access was granted.

CHAPTER 2

LITERATURE REVIEW

2.1 Geological background

The Glentig Formation is an unconformity-bounded formation that is overlain by the Swaershoek Formation of the Waterberg Group and underlain by the Schrikkloof Formation of the Rooiberg Group (Figure 1.1). An unconformity-bounded unit is interpreted as a unit of rocks bounded above and below designated discontinuities in the stratigraphic succession preferably of regional or inter-regional extent (Salvador, 1987). Previous geological studies in South Africa, especially in the Waterberg and Rooiberg groups, focused mostly on the economically potential lithologies and less work was carried out on other formations such as the Glentig, Swaershoek and Alma Formations (SACS, 1980). Special attention needs to be drawn to these kinds of units since they represent neither lithostratigraphic, biostratigraphic nor chronostratigraphic units (Salvador, 1949). Thus, they are termed unconformity-bounded units.

The basic unconformity-bounded units are called synthems (Hong Chang, 1975) with names related to their geographical position. These synthems are regional units bounded by major unconformities regardless of whether they are lithologically homogenous or heterogeneous (Chang, 1975). The unconformity-bounded units are always diachronous (Whittaker et al., 1991). Chang (1975) indicated that the nature of the bounding unconformities should be recognised to the areal extent they overlap each other. Furthermore, the bounding unconformities should be extensive and distinctive to deserve the status of boundaries of an unconformity-bounded unit. In light of the above, SACS (1980) indicated the upper contact of Glentig Formation and

the lower part of the Swaershoek Formation (Waterberg Group) are separated by an angular unconformity.

The Rooiberg Group is the youngest stage of the Bushveld Igneous Complex (BIC) magmatism and it is widely known for hosting some platinum and chrome deposits (Schweitzer and Hatton, 1995). The Waterberg Group mainly outcrops west of Limpopo Province and in the east of Botswana, with smaller outcrops in Gauteng and Mpumalanga Provinces, South Africa (Johnson et al., 2006). The age of the Waterberg Group is placed or estimated to be between 1900 Ma and 1700 Ma (Jansen, 1970). Although no radiometric dating was conducted, the age was largely based on the relationship or correlation of the group with surrounding dated rocks. Mare (2003) suggested that the deposition of the Waterberg Group started during the emplacement of the Bushveld Complex and sporadically continued throughout several tectonic events in the pre-existing Transvaal Basin up until just before the Umkondo thermal event at about 11607- 1112 Ma (Barker et al., 2006). The Loskop Formation, which has been correlated to the Glentig Formation, contains detritus of the Rustenburg Layered Suite (Kinnaird, 2006).

2.2 Waterberg Group

The Waterberg Group is a mildly deformed succession of well- lithified red beds. These “red beds” Waterberg Group were deposited unconformably on the rocks of Transvaal Supergroup, felsic and mafic rocks of the Bushveld Complex and Archaean basement of the Kaapvaal Craton (Johnson et al., 2006). The “red beds” of the Waterberg Group are preserved in two main structural domains on the Kaapvaal Craton. They are an east-west elongated domain (bounded by the Zoetfontein-Melinda faults in the north,

the Thabazimbi-Murchison Lineament (TML) in the south. The second one is a north-northwest elongated domain situated between the eastern and western lobes of the Bushveld Complex termed the Central Bushveld Domain (de Kock, 2006). The domain between the Zoetfontein Fault and Thabazimbi-Murchison Lineament comprises of the main outcrop areas of the Waterberg Group (Waterberg Plateau), with two smaller outcrop area to the west of Kanye in eastern Botswana (Barker et al., 2006). Central Bushveld Complex domain comprises the Nylstroom Syncline outcrop areas to the west of Waterberg Plateau and the Middleburg area (Figure 2.1). The Rust de Winter, Loskop and Glentig Formations are erosional outliers between the Middelburg and Nylstroom (Lenhardt and Eriksson, 2011).

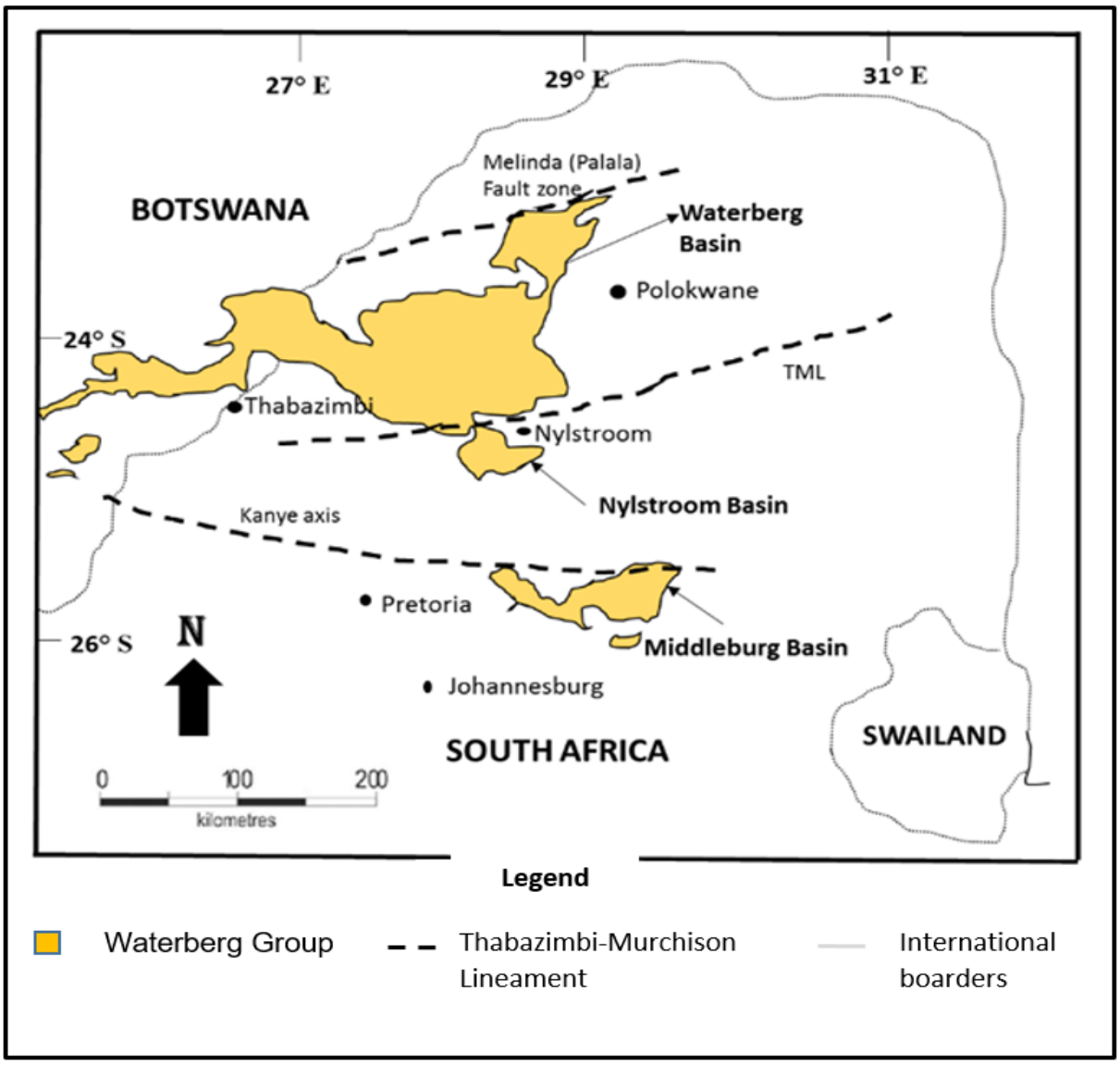

Figure 2.1: Geological map of the Waterberg Group (after Mtimkulu, 2009).

There are different schools of thought regarding the age of the Waterberg Group (Table 2.1). The ages outlined by several researchers are related to the different techniques used for dating. Eriksson et al. (2006) constrained the Waterberg Group within the age limits of 2.06-1.88 Ga. On the other hand, Dorland et al. (2006) reported the age of the Waterberg Group to be 2054 ± 4Ma. Catuneanu et al. (2005) indicated that the Waterberg Group was deposited between the time frame of 3.0 to 1.8 Ga, whereas Callaghan (1986) presented the age of the Waterberg Group to be 1800-

1900 Ma. The Waterberg Group is preserved within the Main and Middleburg Basin on the Kaapvaal Craton and it was deposited largely by alluvial/braided-fluvial with the secondary paleo-desert environment, within fault-bounded, possibly pull-apart type depositories (Catuneanu et al., 2005).

Table 2.1: Comparison of proposed ages of the Waterberg Group by different researchers.

Author	Age of the Waterberg	Dating Methods
Eriksson and Reczko (1997)	1900 – 1700 Ma	No method provided
Dorland et al. (2006)	2054 $\pm$ 4 Ma	Precise Shrimp U-Pb Zircon
Eriksson et al. (2006)	2.0 – 1.9 Ga	No method provided
Eriksson et al. (2008)	2.0 – 1.8 Ga	No method provided

The Waterberg Group made up of three basins, the Main Waterberg Basin, Nylstroom Basin and the Middleburg Basin (Figure 2.1). It is documented by Callaghan et al. (1991) that the Waterberg Group is made up of twelve formations, some of which grades laterally into others. The Main Waterberg Basin hosts eleven formations that are categorized into three subgroups, namely the Nylstroom, Matlabas and Kransberg subgroups (SACS, 1980). The Middleburg Basin hosts only one formation which is the Wilge River Formation. The Nylstroom Basin is the focus of this study and it is made up of only two formations, which are the Swaershoek and Alma Formations. Cheney and Twist (1986) also arranged the Waterberg Group into five subdivisions, namely, Waterberg Unconformity Bounded Sequence (WUBS) I, II, III, IV, and V (Figure 2.2). The WUBS I (Lower Swaershoek Formation) is correlated to Loskop, Rust de Winter,

and Glentig Formations. Cheney (1986) further subdivided the northern outcrop into the Nylstroom Basin and the Main Waterberg Basin.

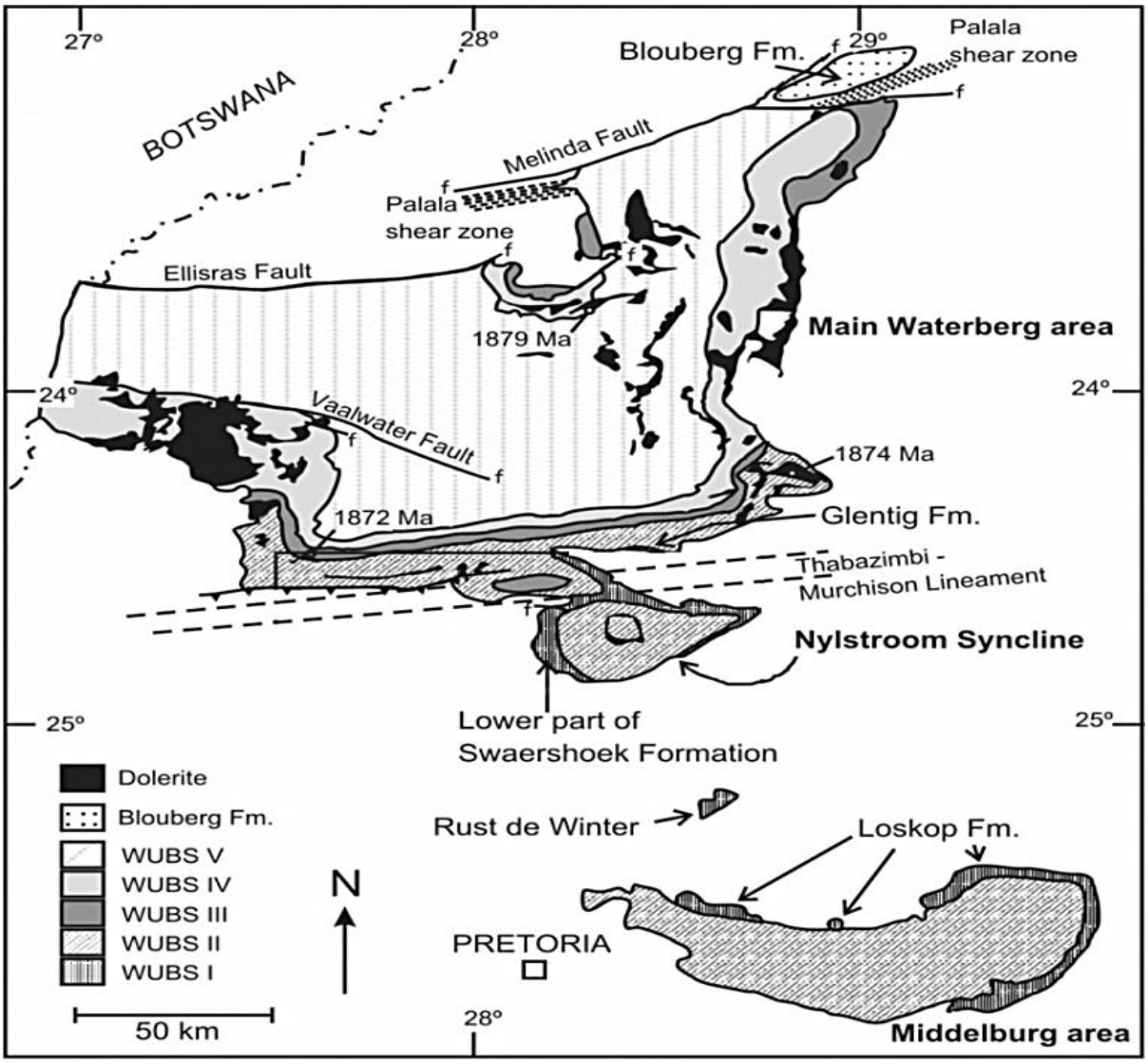

Figure 2.2: Geological Map of the Waterberg Group and surrounding geology (Cheney and Twist, 1986). The Waterberg Group is categorized as WUBS I to WUBS V. WUBS I-Lower Swaershoek, WUBS II-Alma, Upper Swaershoek, WUBS III-Skilpadkop and Setlaole, WUBS IV-Aasvoëlkop and Makgabeng and WUBS V-Vaalwater Cleremont Sandriviersberg and Mogalakwena.

2.2.1 The Waterberg Group in the Nylstroom Basin

2.2.1.1 Alma Formation

The Alma Formation consists mainly of sandstones and it attains a maximum thickness of approximately 1800 m in the Nylstroom Basin (Figure 2.3). The depositional environment of Alma Formation is envisaged to be a combination of alluvial fans that form a bajada along a scarp due to the uplifted block on the southern parts of the Murchison strike-slip fault zone (Callaghan, 1993). The Alma Formation overlies the Swaershoek Formation in the Nylstroom Basin.

2.2.1.2 Swaershoek Formation

The Swaershoek Formation overlies the Glentig Formation unconformably in the Nylstroom Basin (Callaghan, 1993). It is a 2500 m succession of arenites and rudites, with intercalations of lutites. The Swaershoek Formation is divided into the upper and the lower parts, wherein it has been thought that the lower parts of the formation is thought to have been deposited immediately after the intrusion of the Bushveld granites (Maré et al., 2006). As reported by Du Plessis (1987), the Swaershoek Formation overlies the Rooiberg Group conformably in the Modimolle (Nylstroom) area. The lower part of the Swaershoek Formation is correlated to the Loskop Formation, Rust de Winter Formation, and Glentig Formation by Cheney and Twist (1986) (Figure 1.1). Marě (2003) outlined that the Swaershoek Formation is mainly made up of reddish sandstone with minor interactions of conglomerate, purple and reddish-brown shale and red amygdaloidal lava (Figure 2.4). Furthermore, Marě (2003) indicated that the rudites have pebbles to boulders of rhyolite, arenite, quartz vein, chert, iron-formation, Jasper, rudite and lutite.

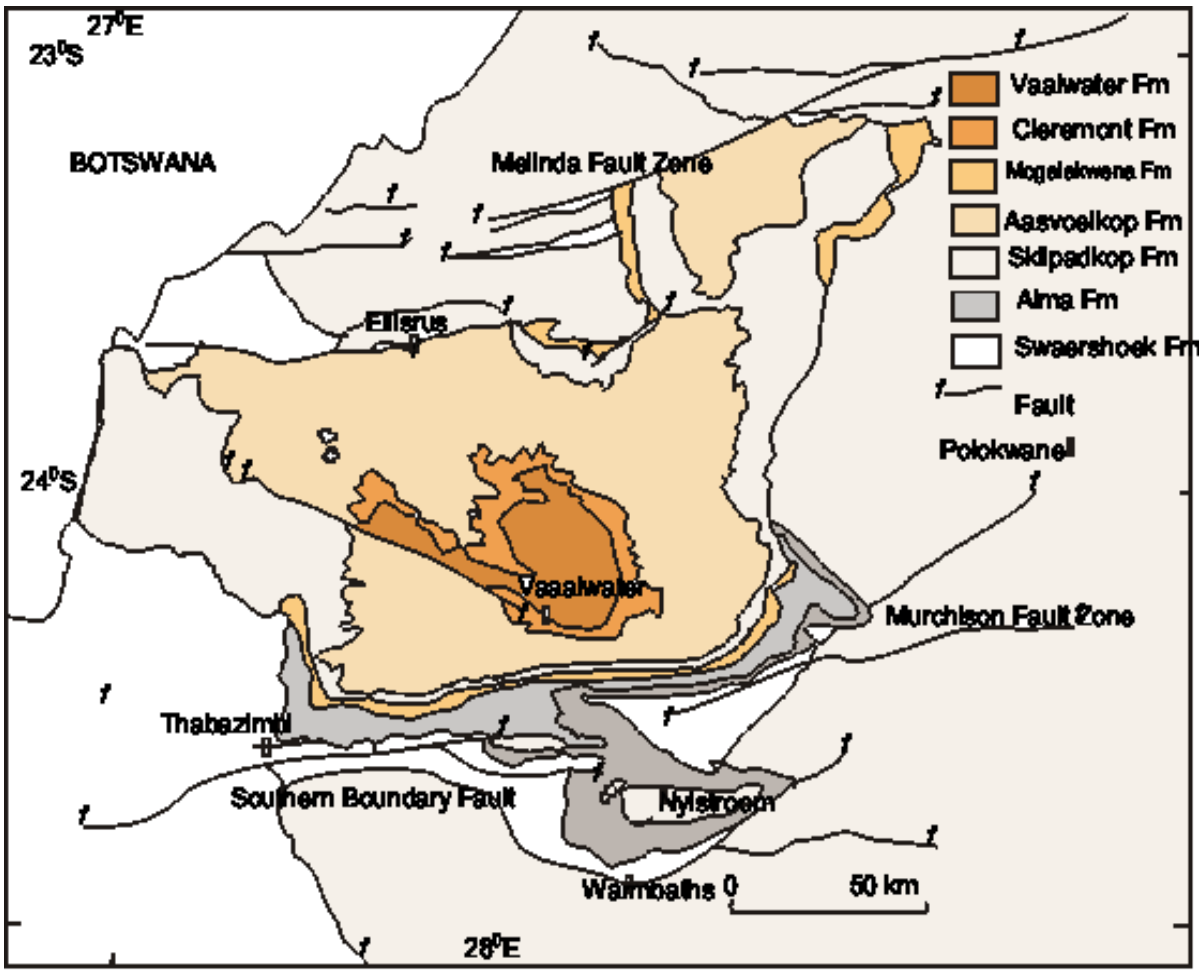

Figure 2.3: The distribution of the Waterberg (Baker et al., 2006).

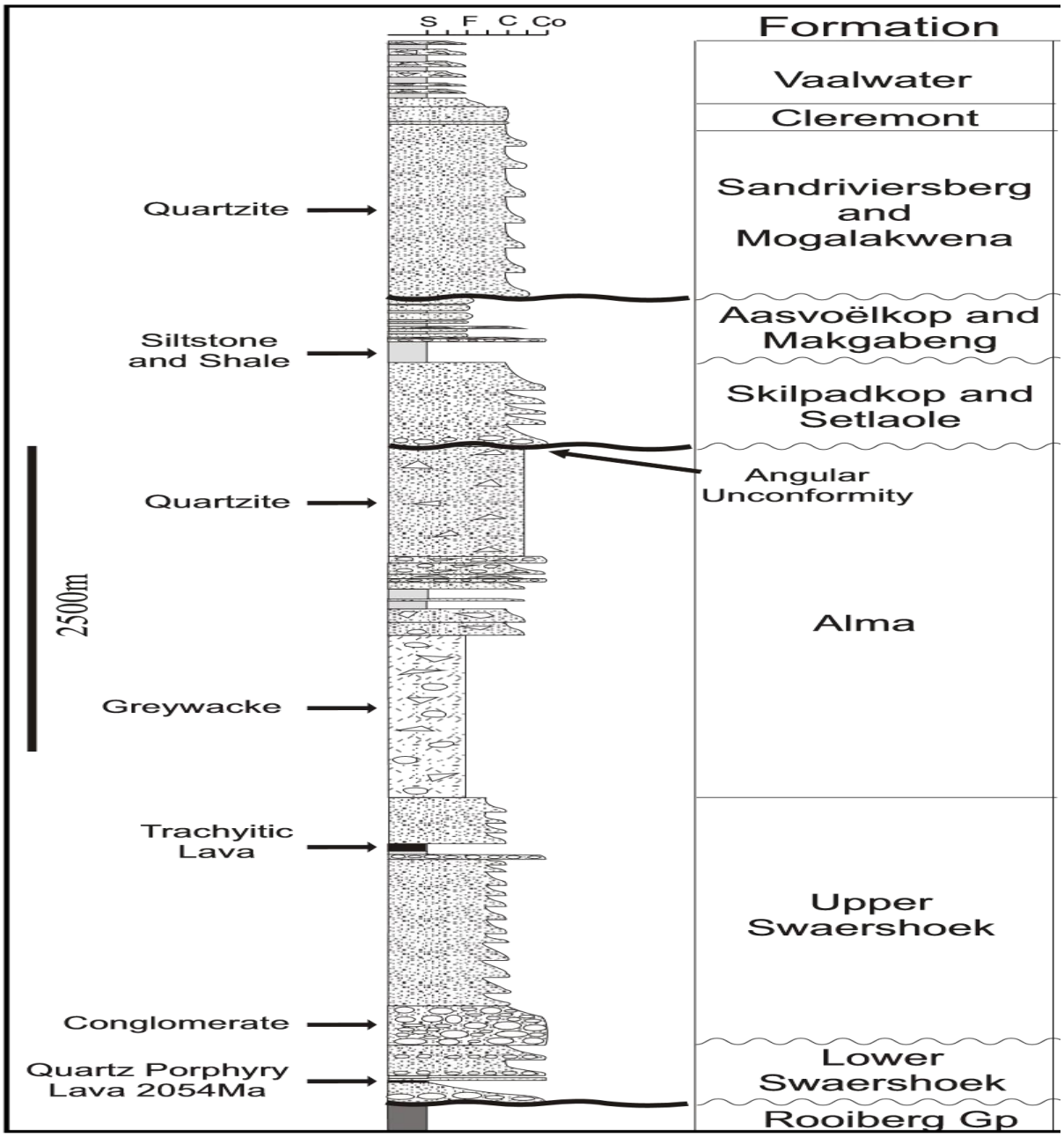

Figure 2.4: Stratigraphical subdivision of the Waterberg Group (Dorland, 2006).

2.2.1.3 Waterberg Group and its relation to the Glentig Formation

The Waterberg Group has been a subject of several studies by researchers like de Kock (2006), Callaghan (1986) and Eriksson et al. (1995). The group has an estimated thickness, varying from 7 km to 10 km (Callaghan, 1993). The Waterberg Group is part

of the red-bed succession that is widespread in southern Africa (Dorland et al., 2006). The Waterberg Group was deposited unconformably on the rocks of the Soutpansberg Group, Transvaal Supergroup, Rooiberg Group (U-Pb zircon age of 2061± 2 Ma) and the Archean basement of the Kaapvaal Craton (Callaghan, 1993). The contact between the Glentig Formation and Waterberg Group is an angular unconformity (Martini, 1998; Figure 1.3).

2.4 Rooiberg Group

The Paleoproterozoic Rooiberg Group is the most extensive siliceous igneous body in the world (Schweitzer and Hatton, 1995; Figure 2.5). Twist and French (1983) estimated that the volume of the Rooiberg Group to be around 300,000 km^3 and covers an area extent of approximately 50,000 km^2. The estimated thickness of the group ranges from 3 km to 5 km (Von Gruenewaldt, 1968; Du Plessis, 1987). The Rooiberg Group is made up of Dullstroom, Damwal, Kwaggasnek and Schrikkloof Formations (Twist and French, 1983; Schweitzer and Hatton, 1995). The Dullstroom Formation forms the base of the Rooiberg Group (Schweitzer et al., 1997). The Dullstroom Formation is composed of an estimated 1500 m thick of intermediate felsic rocks, mafic to volcanic ranging from basalts to dacites (Buchanan et al., 2004). The Damwal Formation is a 1500 m thick, massive succession, characterized by dark coloured flow (with subordinate high-Fe-Ti-P lava flows), rhyolites, intercalated quartzite and pyroclastic flow at the bottom of the formation (Buchanan and Reimold, 1998).

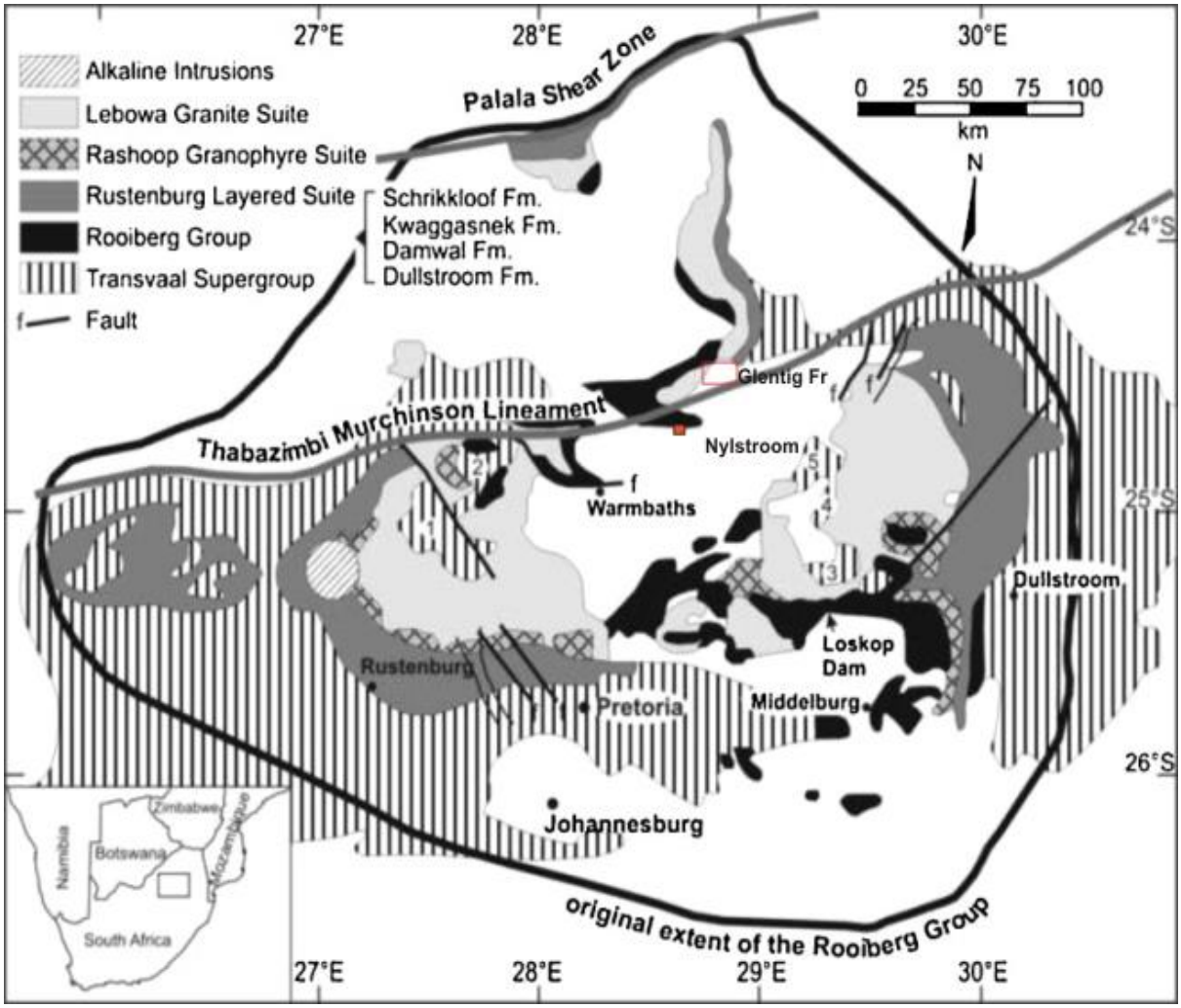

Figure 2.5: The distribution of the Rooiberg Group (Lenhardt and Eriksson, 2011).

2.4.1 Rooiberg Group in the Nylstroom Area

The exposed formations of the Rooiberg Group in the Nylstroom area are the Kwaaggasnek and Scrikkloof Formations, with the latter being conformably overlain by the Glentig Formation and Swaershoek Formation (Figure 2.5). Mare et al. (2003) reported the presence of clasts of rhyolites in the Swaershoek Formation. The same clasts were also reported in the Glentig Formation.

2.4.2 Schrikkloof Formation

Masango (2014) reported that the base of the Schrikkloof Formation is mainly composed of porphyritic rhyodacite marked by a range of 5 to 25% phenocrysts. The top of this formation is dominated by the presence of phenocrysts. The margins of this formation are marked by 10% vesicles and also has prominent flow banding (Jolayemi et al., 2015). The observed rhyodacite clasts in the Glentig Formation displayed the lack of phenocrysts and prominent flow banding, which could suggest the eroded clasts could be from the Schrikkloof Formation (Masango, 2014).

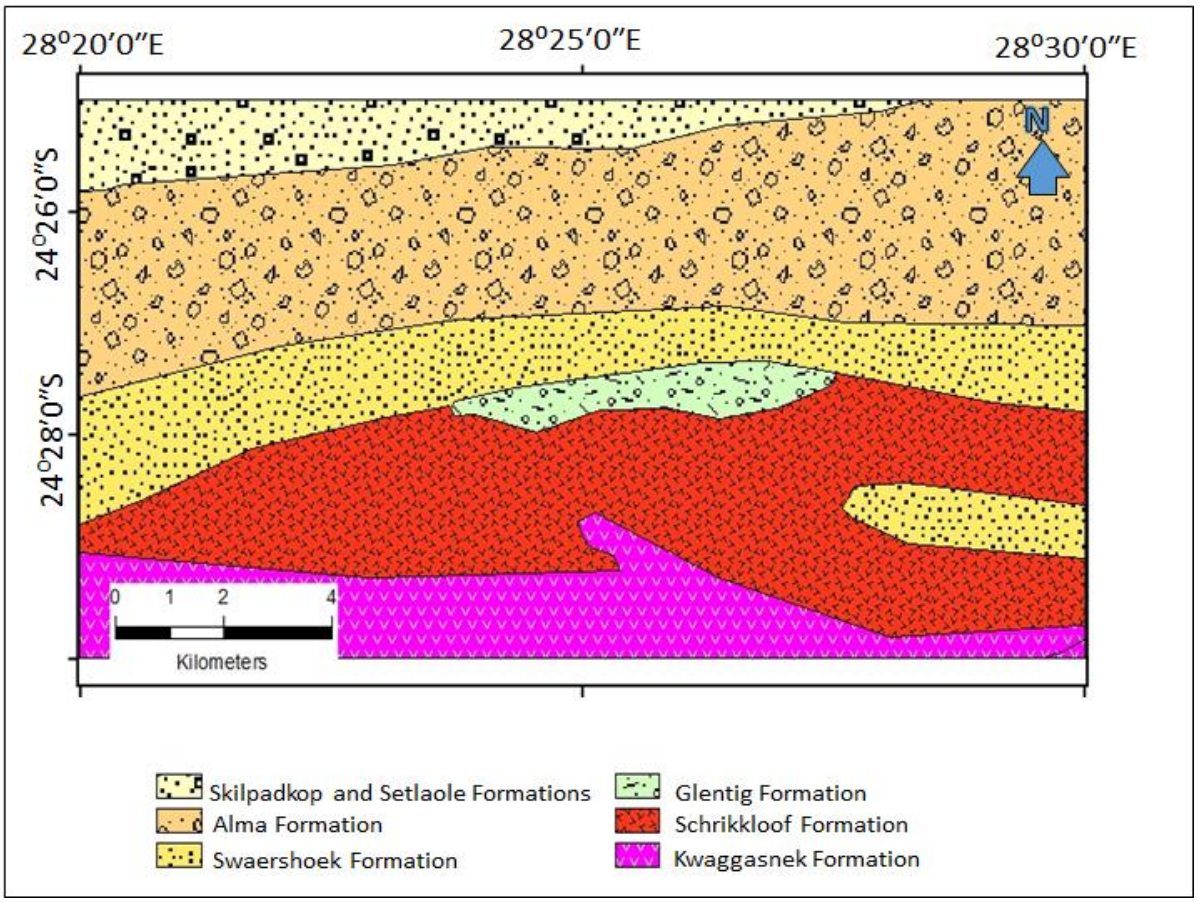

Figure 2.6: The geological map showing the relationships of Schrikkloof and Kwaagasnek Formations (Rooiberg Group), Glentig Formation and Swaershoek, Alma and Skilpad Formations (Waterberg Group) (after Masango, 2014).

2.5 Possible correlatives of the Glentig, Swaershoek and Alma Formations

The Loskop, Rust de Winter and Glentig Formations are not in contact with each other, but share many lithostratigraphic features (SACS, 1980). These formations are viewed as proto-Waterberg deposits (Barker et al., 2006). The previously accepted stratigraphic status of the Loskop, Rust de Winter and Glentig Formations is that they are the uppermost beds of the Transvaal Supergroup, concordantly overlying the Rooiberg lavas (Jansen, 1970). The correlation of the Glentig Formation, the Loskop Formation, Rust de Winter and the lower parts of the Swaershoek Formation was outlined by (Martini, 1998; Cheney and Twist, 1986). Visser et al. (1961) reported the occurrence of a conglomerate at the base of Loskop Formation and this was concurred by Masango (2014). The clast provenance reported by Martini (1998), classified the Loskop siliciclastics into different categories that include: polygenic conglomerate and greywackes, monogenic felsite conglomerate, and quartzite.

Mare (2003) reported that the lower parts of the Swaershoek sedimentation were deposited penecontemporaneous with the intrusion of the Bushveld granites. Furthermore, Mare (2003) emphasized that the Swaershoek Formation has no clasts of the Bushveld granite and overlies the rhyolites of the Rooiberg Group conformably in the Modimolle (Nylstroom) area. The lower parts of this formation contain a quartz-feldspar porphyry. Dorland et al. (2006) concurred that deposition of the lower Swaershoek was contemporaneous with the intrusion of the granites of Lebowa granites. furthermore, Dorland et al. (2006) found the isotopic ages of quartz porphyries of the lower Swaershoek and Rust de Winter Formations to be 2054 ± 4 Ma and 2051 ± 8 Ma, respectively. The ages are synchronous with the isotopic age of 2054.4 ± 1.8 Ma that was reported by Walraven and Hattingh (1993) for the Nebo

granites. Dorland et al. (2006) reported that there are erosional outliers between Nylstroom and Middelburg, wherein the largest of these is the Rust de Winter Formation. Coertze et al. (1977) outlined the stratigraphy of the Glentig Formation and its relation to the overlying Swaershoek Formation and underlying Rooiberg Group. In their discussion, they outlined the contact between the Swaershoek Formation and the Glentig Formation being a sharp contact. The Glentig Formation overlies the Rooiberg Group (Schrikkloof Formation) conformably.

2.5.1 Loskop Formation

The Loskop Formation is overlain conformably by the Wilge Formation of the Waterberg Group in the Middelburg area and is up to 1000 m thick north of Middelburg. The Loskop Formation consists of a basal conglomerate, which largely reflects the reworking of the volcanic parent material. The formation is predominantly composed of clastic sedimentary rocks interbedded with mafic to intermediate lavas in the basal part (SACS, 1980). The upper contact of the Loskop Formation with the Waterberg Group is marked by an angular unconformity (Martini, 1998). On the other hand, the lower contact with the Rooiberg Group is gradational (Coertze et al.,1977). Radiometric data from a granite porphyry intruded into the Loskop sediments indicate an age of greater than 2096 ± 35 Ma (Martini, 1998). Although SACS (1980) correlated the Glentig Formation with the Loskop Formation, there is no clear evidence to correlate these formations to the Rust de Winter Formation.

Russell (1997) reported that the Loskop Formation is located on the top portion of the Rooiberg Group, mainly due to the occurrence of a high amount of rhyolite clasts in the sediments. The Loskop Formation is found between the Rooiberg Group and

Waterberg Group, indicating that it is transition horizon from the volcanic succession of the Rooiberg Group to the clastic sedimentation of the Waterberg Group.

2.5.2 Rust de Winter Formation

Crocker (1985) argued that the term Rust de Winter Formation has been used in the past for two different lithologies, namely the Rust de Winter pyroclastic rock suite and the Rust de Winter Formation. In this study, the later name is adopted. The Rust de Winter Formation consists of cross-bedded sandstone, thin bands of shale and grit with numerous lenticular layers of conglomerate (SACS, 1980). The Rust de Winter sediments occupy a shallow basin, measuring 8 km by 14 km in area extent and rest conformably on the Rooiberg volcanic (Schweitzer et al., 1997).

CHAPTER 3

METHODOLOGIES

3.1 Introduction

The methodologies employed in this study were designed to achieve the aims and objectives of this study. To address the tasks of this research, literature review, field work, laboratory analysis and interpretation of the different datasets were carried out systematically.

3.2 Literature review

A review of the literature on the Glentig Formation, Swaershoek Formation, Alma Formation, Loskop Formation and Rooiberg Group in the Witbank-Cullinan Basin were done to have a synopsis of the geology of the area. Scientific articles and technical reports were used for the literature.

3.3 Fieldwork and sampling

Geological fieldwork was conducted during autumn and summer of 2019. The instruments used during the fieldwork included global positioning system (Garmin eTrex-10), compass, digital camera, measuring tape, grain size charter, sample bags, hand lens, permanent marker, masking tapes, pencils and field notebook. The outcrops were studied such that the different lithologies, sedimentary structures, vertical packing depositional styles and colour of the rocks were delineated and classified. The identified sedimentary structures on the outcrops were designated and measured with a measuring tape and where necessary, photographs were taken using a digital camera. A measuring tape was used to determine the thicknesses of the

stratigraphic units and the measurement was done perpendicular to the strike of the units. The collected rock samples were stored in clearly marked sample bags and these samples were used for thin sections preparation and geochemical analysis. Furthermore, the coordinates of the samples were taken using the Garmin eTrex-10 global positioning system and recorded in the field notebook.

3.4 Laboratory work

The laboratory work includes preparation of thin sections, petrographic study, modal compositional analysis, and X-ray fluorescence analysis.

3.4.1 Thin section preparation

The samples were chipped to remove any excess weathered material on the surface to attain a homogenous surface. The chipped samples were cut using a diamond saw, bonded to a glass thin section using petrobond. The rock slab was further ground until an even surface was attained at a thickness of or less than 30 µm. A total of 58 rock thin sections were prepared and the prepared thin section slides were neatly stored in a box to avoid contact with oil or any organic material.

3.4.2 Petrographic studies and modal compositional analysis

The prepared thin sections were studied using a Nikon Lv-UEPI-N petrographic light microscope at the University of Limpopo. Plane and cross-polarised light were used to identify the detrital and authigenic minerals based on their optical properties. Grain sizes, degree of sorting and roundness of the identified minerals were also recorded. The microscope is equipped with the digital camera, for attaining the

photomicrographs (Figure 3.1). Photomicrographs of the studied thin sections were taken with the aid of a built-in camera, equipped to a computer monitor.

Figure 3.1: Photograph showing analysis of thin section under a Nikon eclipse petrological microscope with a digital camera.

For the modal composition analysis, 400 points were counted per thin section in accordance with the Gazzi-Dickinson's point-counting method using the Nikon Lv-UEPI-N petrographic microscope coupled with an Olympus DP72 digital camera. Counting grids that are evenly distributed were deployed to cover the entire thin section such that mineral grains under the grid nodes can be counted. The grids were evenly spaced such that, individual grids would be bigger than the average grain size to avoid counting a particular grain twice or more. During the point counting, the

framework grains were grouped as monocrystalline quartz (Qm), polycrystalline quartz (Qp), plagioclase (P), K-feldspar (K) and lithic fragments (L). Thereafter, the detrital modes were recalculated to 100%, excluding the matrix, cement, mica, heavy minerals and carbonate grains (Dickinson and Suczek, 1979). Classifications of the sandstones were based on the methods proposed by Pettijohn (1974) and Folk (1954).

The QFL (quartz-feldspar-lithics) ternary diagrams were used to plot the recalculated values. The QFL diagrams employed were those of Dickinson et al. (1983), Yerino and Maynard (1984) and Hatano et al. (2019), which show compositional fields associated with different provenances (i.e., continental block provenances, recycled orogeny, magmatic arc provenances and collision suture sources). Additionally, the sandstones were classified based on the QFL ternary classification diagrams of Folk (1974).

3.4.3 X-ray fluorescence analysis

A total of thirty-eight representative samples were systematically collected from outcrops in the study area. The samples were cleaned with alcohol to remove any impurities, in preparation for geochemical analysis. The sampling position or geographic locations of the samples are presented in Appendix A. The major and trace element geochemistry of the rocks was determined by X-ray fluorescence analysis (XRF) at the Department of Geology and Mining, University of Limpopo. The collected samples were crushed and milled, wherein 12 g of the sample was taken in for whole-rock XRF analysis. An Epsilon 3^{XLE} EDXRF Spectrometer that uses a 50 kV 3 mA high-performance ceramic tube (Figure 3.2) was used to analyse the samples for major and trace elements. The milled samples (12 g) were placed in a sample holder.

The Epsilon software program was used to quantify for the major and trace elements. The major elements that were analysed are SiO_2, TiO_2, Al_2O_3, FeO, MnO, MgO, CaO, Na_2O, K_2O, P_2O_5 and Cr_2O_3. The analysed trace elements are As, Ba, Ce, Co, Cr, Cu, Ga, Hf, La, Mo, Nb, Nd, Ni, Pb, Rb, Sc, Sn, Sr, Ta, Th, Tl, U, V, W, Y, Yb, Zn, and Zr. The analysis was carried out at the Department of Mining and Geology, University of Limpopo. The data received from the software program were tabulated and plotted on binary and ternary diagrams for geochemical interpretation.

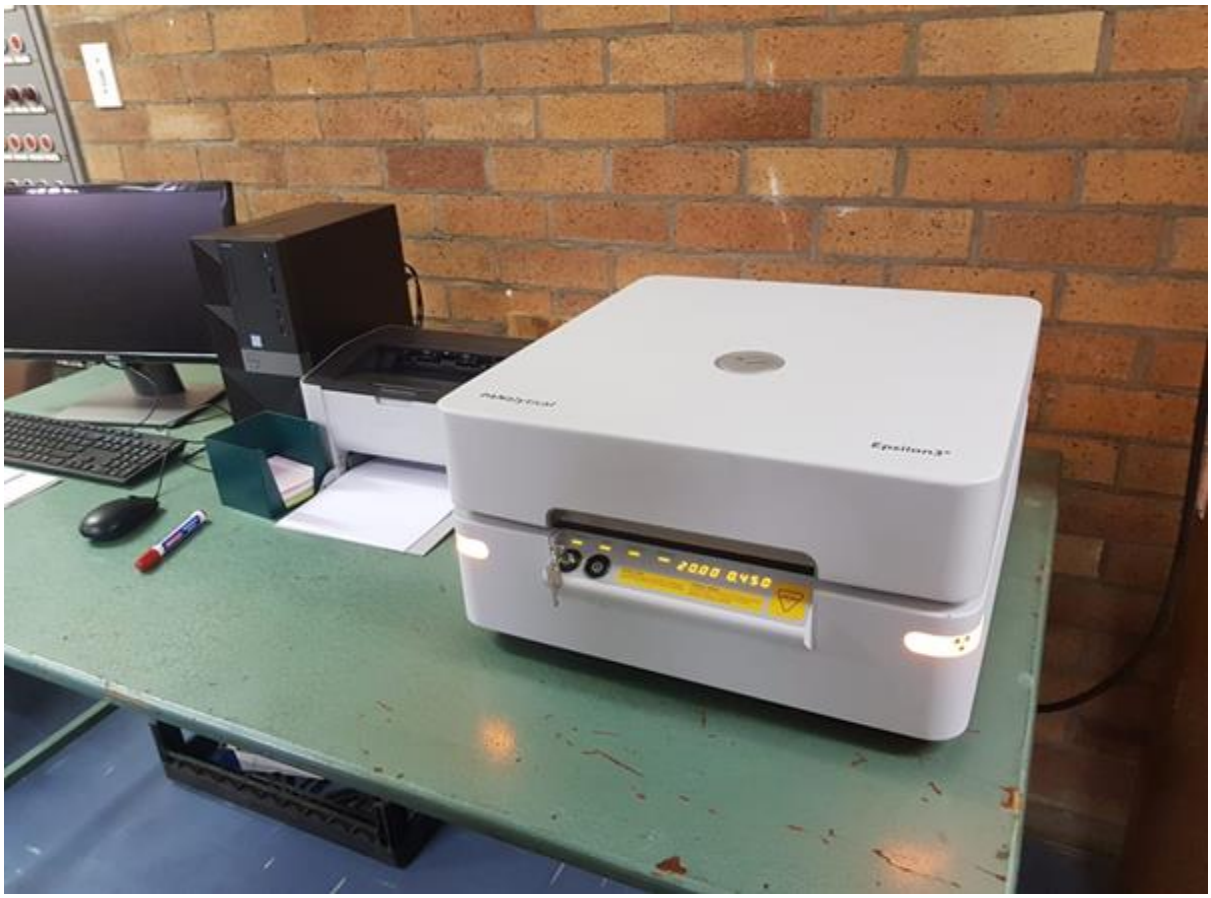

Figure 3.2: An image of an Epsilon 3 ^{XLE} EDXRF Spectrometer for XRF analysis.

CHAPTER 4

STRATIGRAPHY AND LITHOFACIES ANALYSIS

4.1 Introduction

Boggs (2009) defined stratigraphy as a branch in earth sciences that deals with the description, form, association, distribution, chronologic succession, and dating of lithological strata. Salvador (1949) offered a more concise definition of stratigraphy as the branch of geology that deals with the description, correlation, and interpretation of stratified sediments and rocks on and in the earth crust. Stratigraphy has different branches that are as follows: lithostratigraphy, pedostratigraphy, biostratigraphy, chronostratigraphy, geochronostratigraphy, magnetostratigraphy, chemostratigraphy and sequence stratigraphy (Boggs, 2009). The current study employs the use of lithostratigraphy, the use of lithostratigraphy focuses mostly on individual lithologies. Thus, entailing the arrangement of depositional sequence of the lithological units. Lithostratigraphy is used in the relation of lithological units in terms of individual characters.

The earliest use of the term lithofacies was by Gressly (1838), in Miall (1978) explained the genesis of sedimentary facies using the processes involved in depositional environments. Gressly (1838) demonstrated regular lateral facies transitions along beds and interpreted them as mosaics of environments along with depositional profiles value and that were useful for biostratigraphy (“index” or “zone” fossils). Gressly (1838) discussed the equivalency of vertical facies successions through a series of strata. The work forms the basis of Walther’s Law of the correlation of facies. In this chapter,

the sample principles of Walther's Law of Correlation were used in the correlation of Alma Formation, Glentig Formation and Swaershoek Formation.

Miall (1978) defined lithofacies as "a rock unit defined based on its distinctive lithological features, such as composition, grain size, bedding characteristics, and sedimentary structures". Lithofacies characterizes a specific depositional event. Lithofacies may be grouped into lithofacies associations, which exhibit traits of particular depositional environments. Lithofacies associations are the basis for identifying cyclic lithofacies. Biofacies are used for strata that have fossils within them. The current study employs the use of lithofacies. The Swaershoek Formation has been studied in the past, most of the work done on the formation never detailed the stratigraphy and facies of the Swaershoek Formation (Mare, 2003; Eriksson et al., 1994, 1995; 2006; Barker et al., 2006; Maré et al., 2006). The work done on the Swaershoek and Alma Formations related vaguely with the underlying less studied Glentig Formation. Barker et al. (2006) did not report on the stratigraphy of the Swaershoek Formation. This chapter focuses on the stratigraphy of the lower parts of the Swaershoek, Alma and Glentig Formations. A comprehensive review of the spatial stratigraphic changes of the sedimentary successions of the Glentig, Swaershoek and Alma Formations was performed. Strater software and Microsoft Office PowerPoint were used to process the stratigraphic data and the results are presented in the form of stratigraphic sections.

4.2 Results and discussion

4.2.1 Stratigraphy of the Swaershoek Formation

The Swaershoek Formation overlies the Rooiberg Group unconformably (Figure 4.1). The contact between the Swaershoek Formation and Rooiberg Group (Schrikkloof Formation) is not well defined (Figure 4.2). The measured thickness of the Swaershoek Formation is about 300 m. A fine to medium-grained massive sandstone of about 90 m forms the base of the formation in the Yellowwood Game Lodge. The thickness of the massive sandstone from the contact is about 96 m. The massive sandstone is overlain by clast supported conglomerate. The clast supported conglomerate is approximately 26 m thick. The matrix is fine to coarse-grained sandstone (Figure 4.3 B, C and D). Clast imbrications are occasionally observed in the conglomerate (Figure 4.3). This conglomerate is poorly to moderately well sorted with the cobble sized clasts at the bottom and the smaller clasts at the top, the diameter sizes range between 6.8 cm and 23 cm (Figure 4.4). The conglomerate a polymictic, with most of the matrix being quartzite pebbles. Some pebbles are elongated suggesting compression during depositions or after deposition. The top part of clast supported conglomerate is truncated by quartz veins. The quartz veins range between 2 cm and 20 cm in thickness (Figure 4.5).

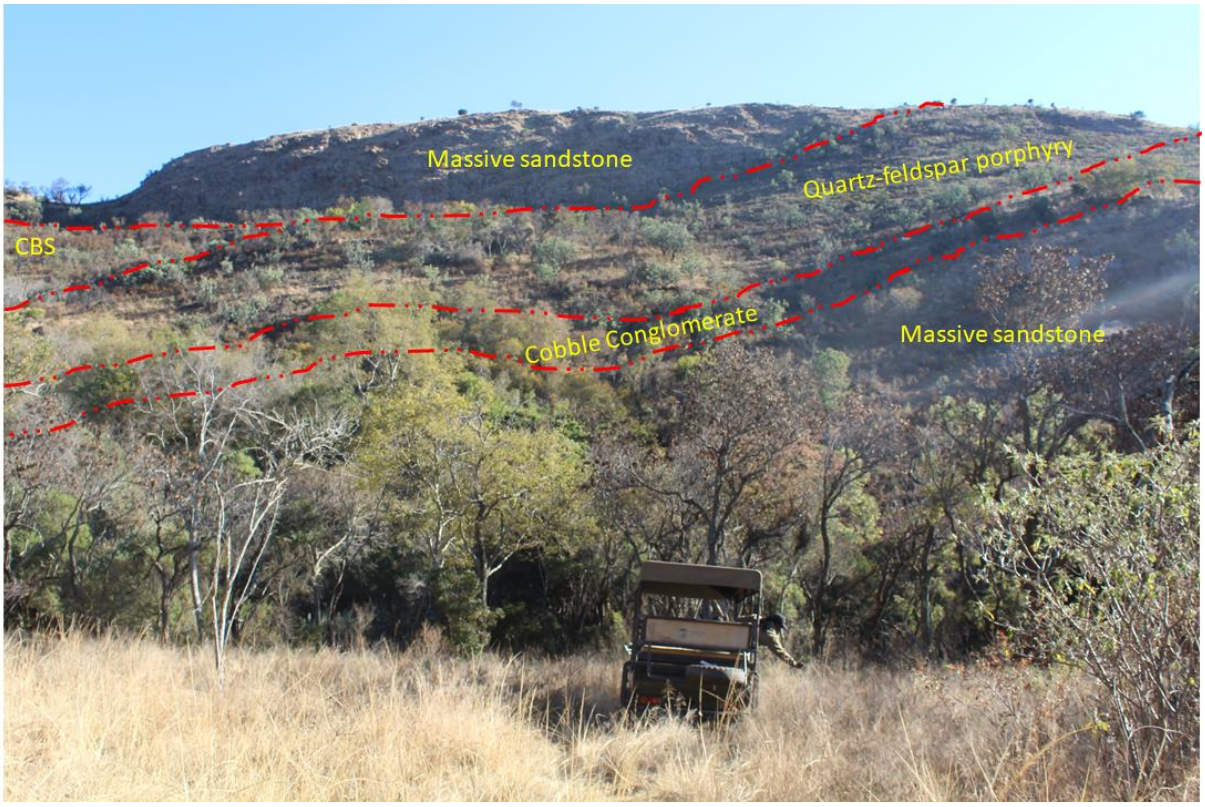

Figure 4.1: The lateral view of the Swaersberg mountain with the outline of the stratigraphy of Swaershoek Formation.

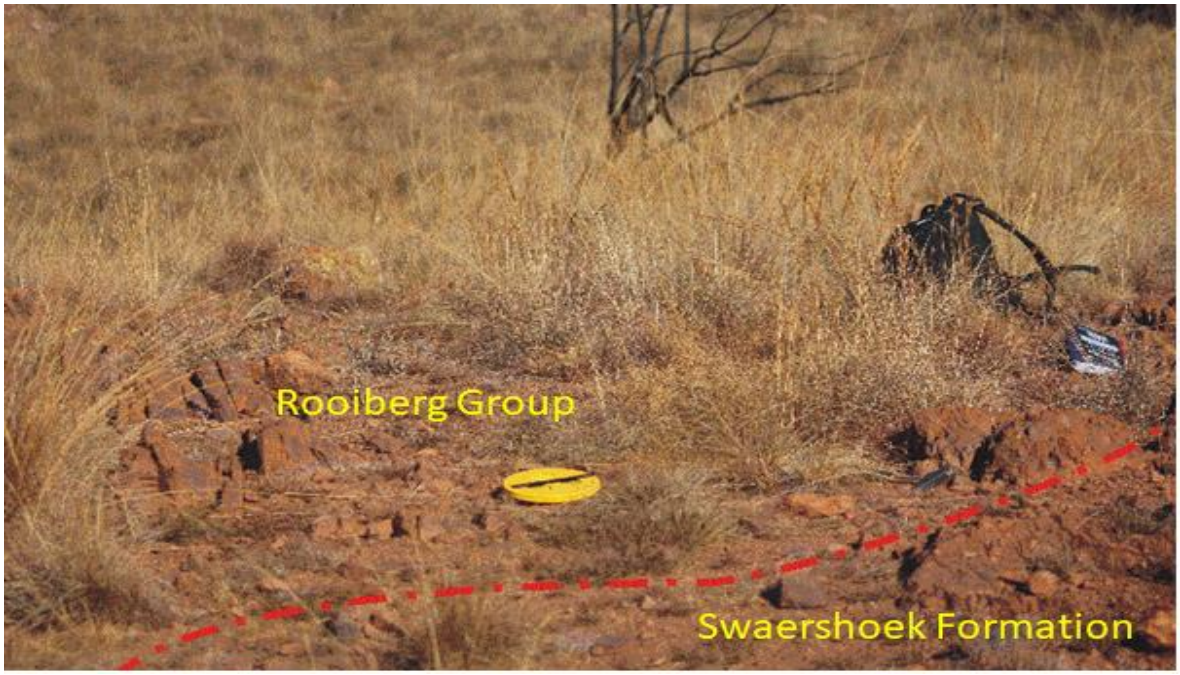

Figure 4.2: Photograph showing the contact between the Swaershoek Formation and Schrikkloof Formation (Rooiberg Group).

Figure 4.3: Photograph of the lower parts of the Swaershoek Formation showing; (A) massive sandstone; (B) Clast supported conglomerate; (C) matrix-supported cobble conglomerate with clast supported cobble conglomerate towards the top right of the image; (D) Cobble conglomerate truncated by quartz veins, the top part- the clast conglomerate grades to a matrix-supported conglomerate.

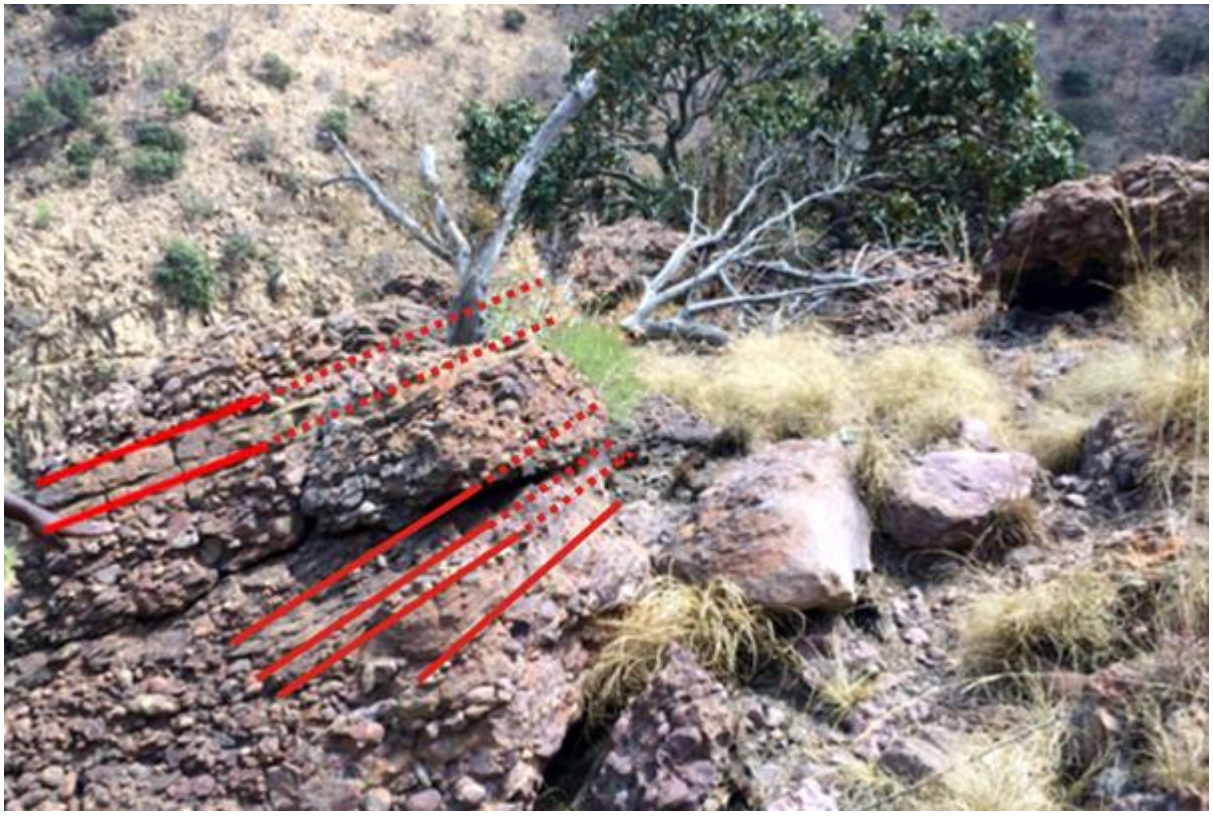

Figure 4.4: Clast supported conglomerate intercalated with massive sandstone.

Figure 4.5: Photograph showing clast supported conglomerate truncated by an east-west striking blocky quartz vein.

The conglomerate is overlain by a quartz-feldspar porphyry (Figure 4.6). The change in lithology is marked by a sharp contact between the feldspar-quartz porphyry and the clast supported conglomerate. The thickness of the quartz-feldspar porphyry is approximately 12 m. No chill margins were observed on the conglomerate nor the sandstone, this implies that the quartz-feldspar-porphyry is perhaps extrusive. The crystals of quartz are a bit circular, while feldspar crystals are elongated. A medium-grained planar cross-bedded sandstone of about 36 m thick overlies the feldspar-quartz porphyry (Figure 4.7). The contact between the planar cross-bedded sandstone and the feldspar-quartz porphyry is sharp. The medium-grained planar cross-bedded sandstone is overlain by a brownish coarse-grained massive sandstone (Figure 4.1).

The contact between the planar cross-bedded sandstone and the massive sandstone is gradational. The coarse-grained massive sandstone has a thickness of about 10 m in the Yellowwood lodge and it is characterized by the intrusion of multiple quartz veins. The thickness of the quartz veins varies between 1 cm and 6 cm. The stratigraphic section of the Swaershoek Formation in the Yellowwood Game Lodge is shown in Figure 4.7.

Figure 4.6: Photograph of part of the Swaershoek Formation showing quartz-feldspar porphyry.

SWAERSHOEK FORMATION SECTION (1) IN YELLOWWOOD GAME LODGE

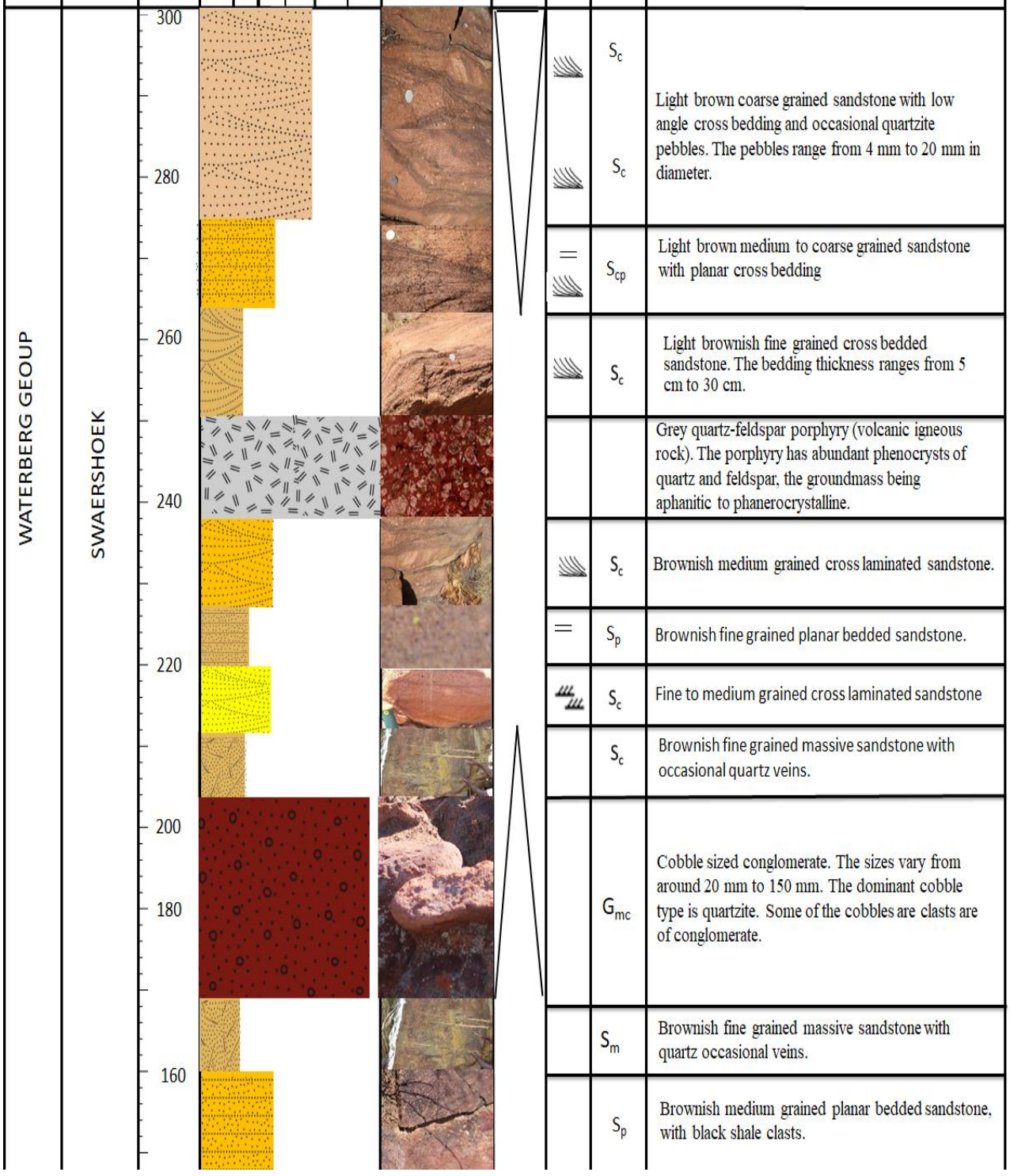

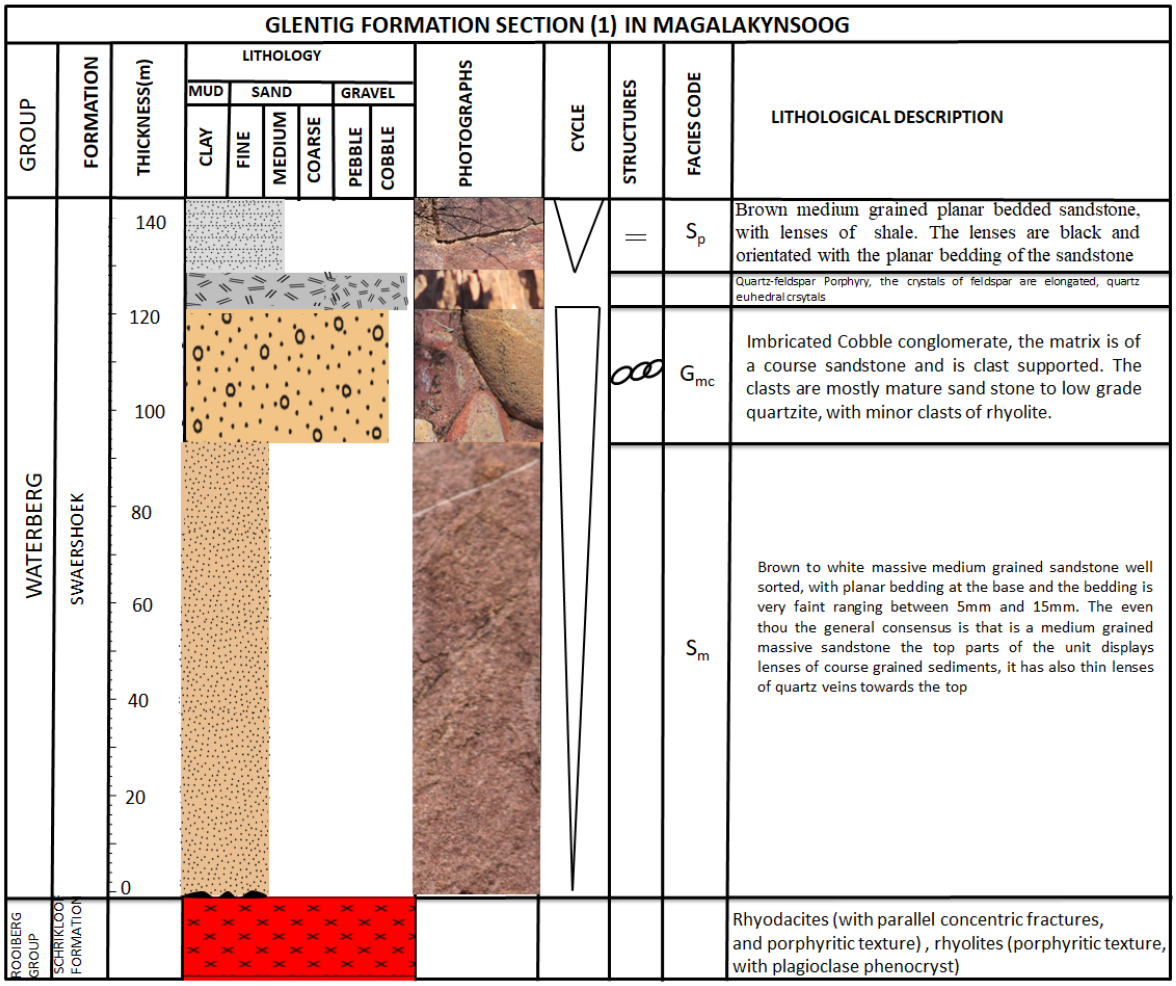

Figure 4.7: Stratigraphy of the Swaershoek Formation in the Yellowwood game lodge.

4.2.2 Stratigraphy of the Alma Formation

The Alma Formation rests conformably on the Swaershoek Formation in the Yellowwood Game lodge. The outcrop of the Alma Formation is present in the Yellowwood game lodge and extends into the Magalakynsoog north farm (Figure 4.8). The total measured thickness of the formation in the aforementioned places is about 190 m.

Figure 4.8: Photograph showing the contact between the Alma and Swaershoek Formations.

The bottom part of the formation is made up of a brown to light pink medium-grained massive sandstone. The unit has a maximum thickness of about 27 m. There is a sharp contact between the massive sandstone and the underlying rhyodacite (Schrikkloof Formation in the Rooiberg Group). The massive sandstone is overlain by

a 13 m thick matrix-supported conglomerate. The contact between the conglomerate and the underlying massive sandstone is sharp.

The polymictic pebble conglomerate is composed of quartzite, lava and sandstone. The clasts are subrounded to well-rounded. The matrix of the conglomerate represents the same fine to medium-grained massive sandstone. The unit attains a maximum thickness of about 11 m in the Magalakynsoog north farm. A gradational contact marks the change in lithology from a pebble conglomerate to a cobble conglomerate. The cobble conglomerate is a clast supported polymictic conglomerate. Most of the clasts are boulders since they have a diameter of over 256 mm. The bigger clasts are the quartzite and lesser in size are the sandstone. The clasts of lava that are presented are not as round as the other clasts.

A sharp contact marks the change from a cobble conglomerate to a massive sandstone similar to the one found at the bottom of the Alma Formation. The massive sandstone is brown to light pink and has a thickness of about 87 m. A cobble sized oligomictic conglomerate overlies the massive sandstone. The conglomerate clasts are of quartzite and their sizes range between 158 mm and 260 mm in diameter. The matrix is composed of very fine to medium-grained sandstone. The stratigraphic section of the Alma Formation in both Yellowwood Game lodge and Magalakynsoog north Farm is shown in (Figure 4.9).

ALMA FORMATION IN YELLOW WOOD GAME LODGE

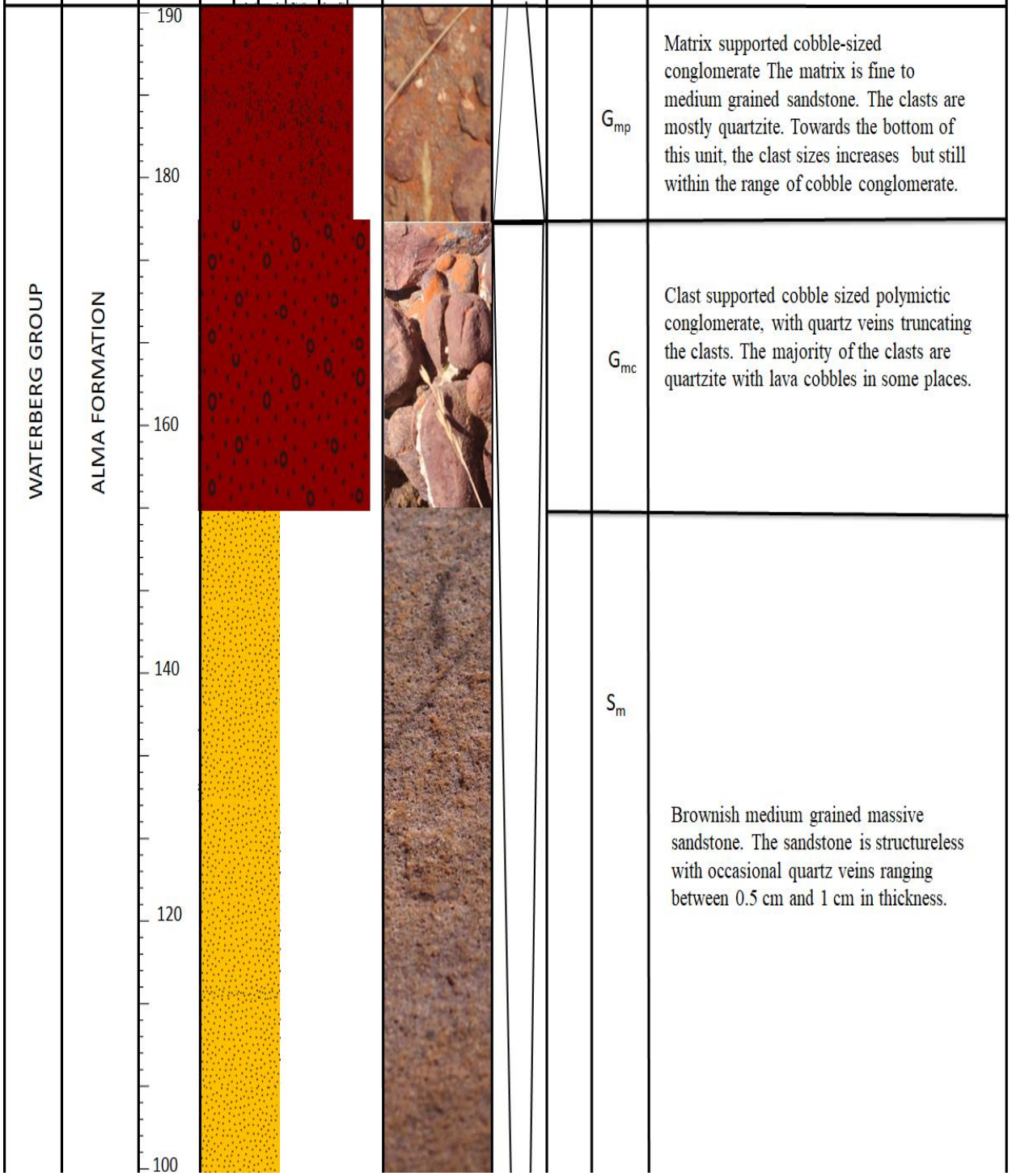

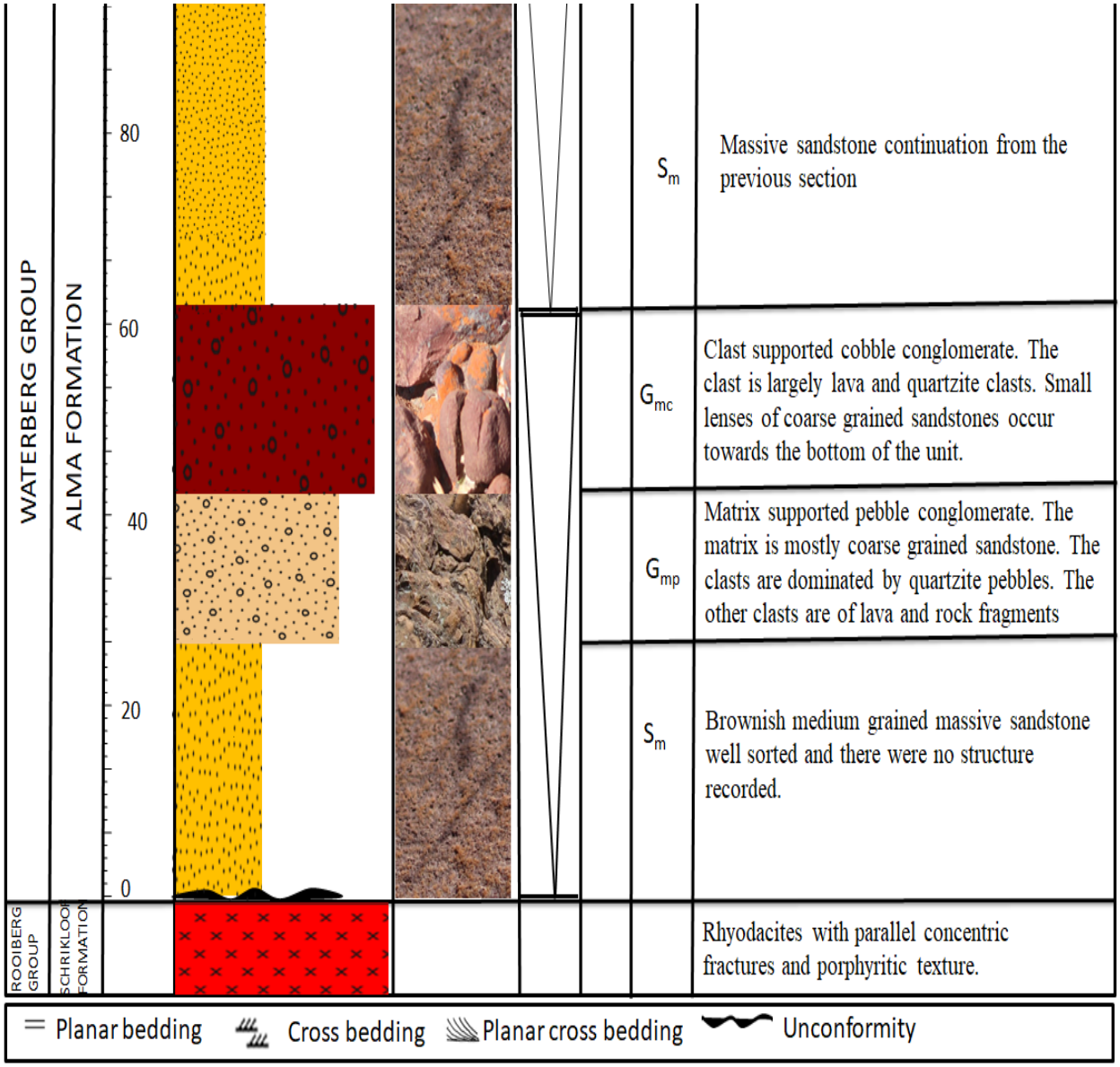

Figure 4.9: Stratigraphy of the Alma Formation in both Yellowwood Game lodge and Magalakynsoog North Farm.

4.2.3 Stratigraphy of the Glentig Formation

The Glentig Formation rests unconformably on the Rooiberg Group (Figure 4.10). It has a limited areal extent; in the sense that it is confined to the south-eastern edge of the Yellowwood Game lodge on the slopes of the Swaersberg mountains. The Glentig Formation is a 400 m succession of sandstones that are capped by a thick grey quartz-

feldspar porphyry (Figure 4.11). The lower unit of the Glentig Formation is composed of planar bedded fine-grained sandstone with minor siltstone. From the base, this unit is about 100 m thick and it is overlain by cobble size conglomerate. The contact between the underlying sandstone and the cobble conglomerate is gradational. The cobble conglomerate is a polymictic conglomerate, the clasts of the conglomerate ranges between 150 mm and 256 mm. The clasts of the conglomerate are mostly quartzite cobbles and lava, while the matrix is medium to coarse-grained sandstone. The conglomerate attained a maximum thickness of approximately 100 m in the Magalakynsoog North Farm. The cobble conglomerate is overlain by a greyish quartz-feldspar porphyry. The porphyry attains a maximum thickness of about 200 m in the study area. The porphyry trends east to west and thins towards the edges of the Glentig Formation in the east, while the maximum thickness is attained in the western side of the formation.

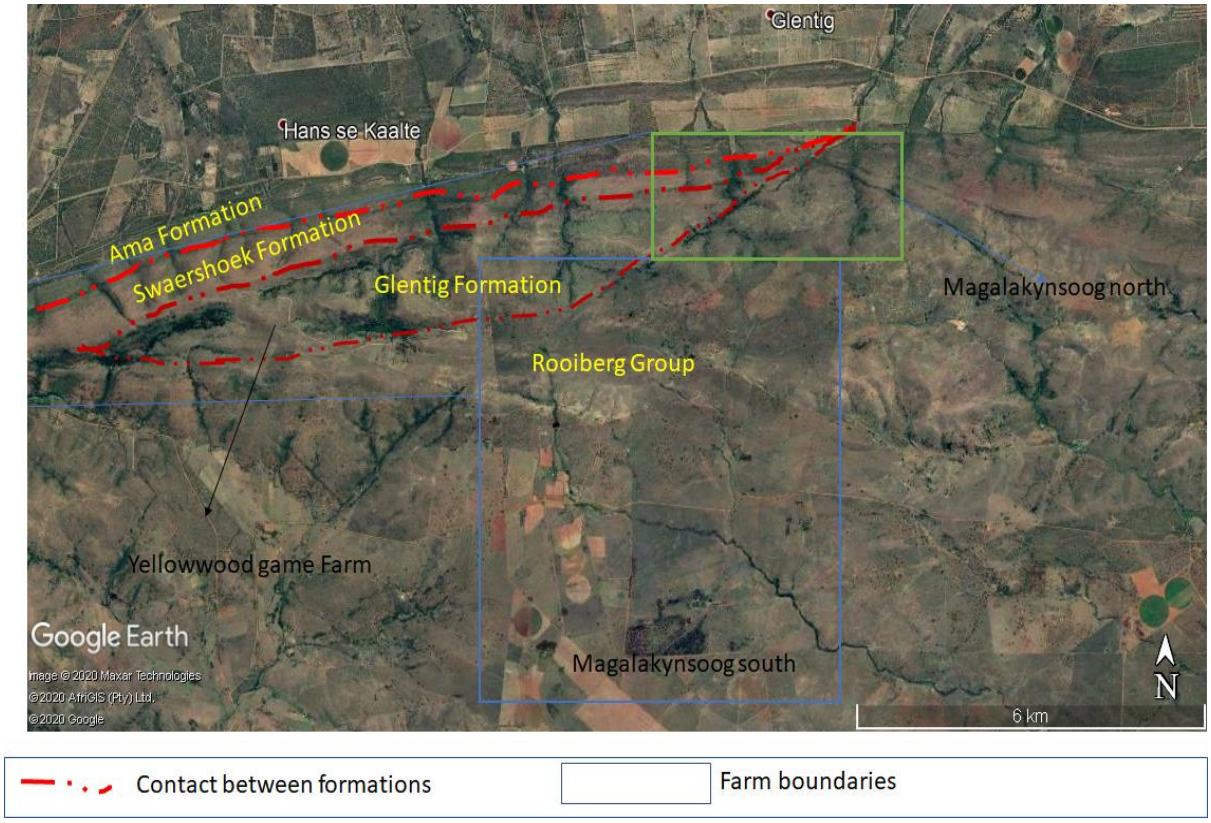

Figure 4.10: Google image showing the Glentig Formation. The blue and green lines are the farm boundaries.

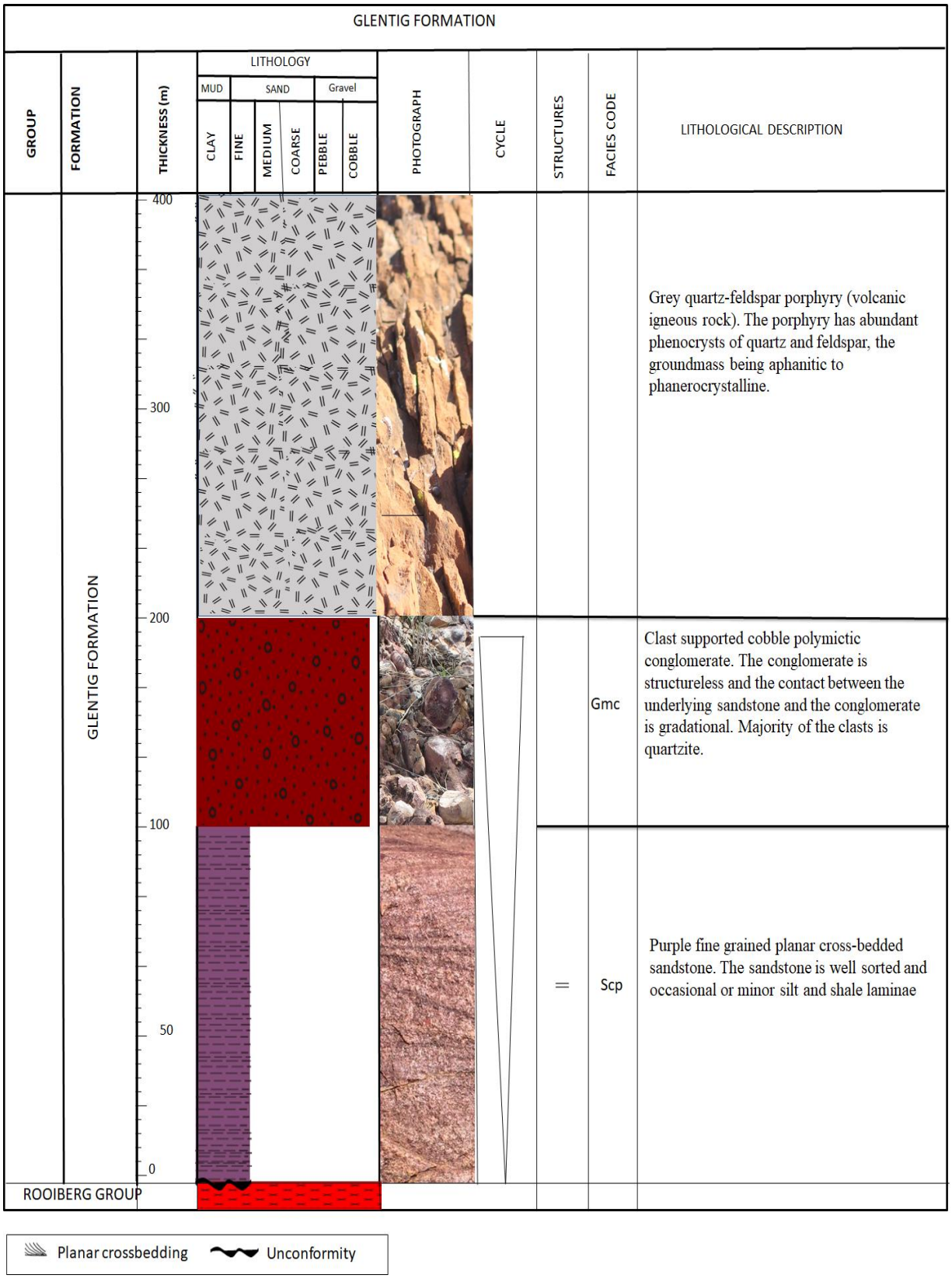

Figure 4.11: Stratigraphy of the Glentig Formation on the slopes of the Swaersberg mountains.

4.2.4 Correlation of the Glentig, Alma and Swaershoek Formations

The basis of correlation of the Glentig, Alma and Swaershoek Formations was coined by Cheney and Twist (1986). They based their correlation of the unconformities found at the base and top of the Swaershoek, Glentig and Alma Formations. The Glentig Formation is capped by a 400 m thick quartz-feldspar porphyry, which is present in the Swaershoek Formation. The quartz porphyry is absent in the Alma Formation, perhaps the unit has been eroded. The base of the Swaershoek is marked by the presence of a brownish massive sandstone that is consistent with the base of the Alma Formation. There is the presence of a polymictic cobble conglomerate, which is present in all the three formations in the study area (Figure 4.12). The upper parts of the Swaershoek Formation could not be correlated to any of the studied formations. This includes all lithological units above 205 m to 300 m on the Swaershoek Formation. The purple planar bedded sandstone at the base of the Glentig Formation is absent in both the Swaershoek Formation and Alma Formation. Stratigraphic correlation of the Glentig, Alma and Swaershoek Formations within the study is shown in Figure 4.13.

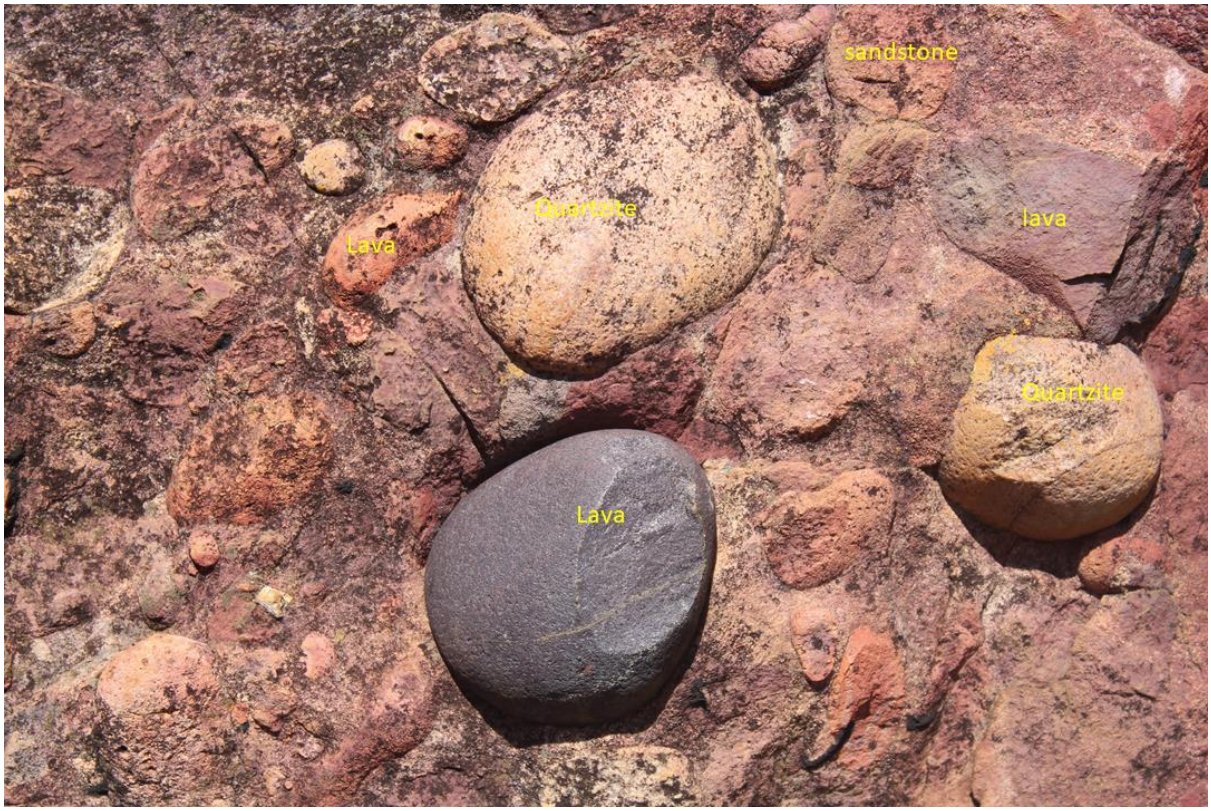

Figure 4.12: The polymictic cobble conglomerate that is prominent throughout the study area. it can be correlated in the Alma, Glentig and Swaershoek Formations.

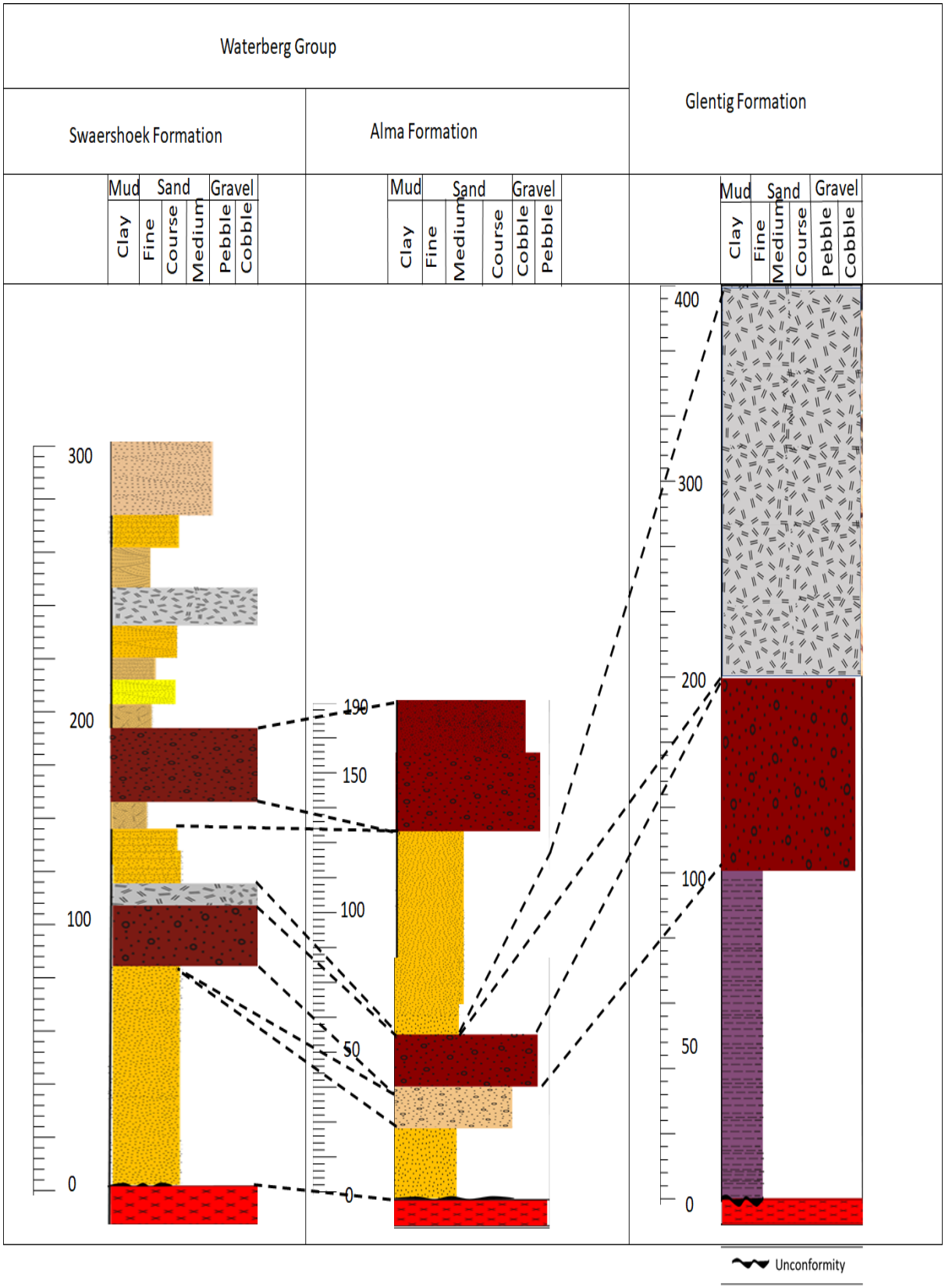

Figure 4.13: Stratigraphic correlation of the Swaershoek, Alma and Glentig Formations.

4.2.5. Sedimentary facies

Sedimentary facies analysis was conducted using the field sedimentological data. This data was mainly colour, grain sizes, rock types, and sedimentary structures. The sedimentological features were recorded or noted for the identification of sedimentary facies, so as to correlate strata in the different boreholes and to distinguish between the depositional environments/conditions. Facies analysis was undertaken using the modified version of the lithofacies classification scheme by Miall (1985, 1992, 1999, 2006). Facies associations were deduced by grouping the individual lithofacies, which in turn, represented the different depositional environments of the studied formations. In this study, the proposed lithofacies classification scheme Miall (1978) was followed to deduce the depositional environment for the Alma, Glentig and Swaershoek Formations. The standard facies architecture is shown in Appendix B. Six facies (Gmc, Gmp, St, Scp, Sp, and Sm) were identified and grouped into 2 facies associations as shown in Table 4.1.

Table 4.1: Lithofacies facies and facies association identified in the Swaershoek, Alma and Glentig Formations.

Facies code	Description	Structures	Facies association	Interpretation	Depositional environment
Gmc	Red cobble clast conglomerate, with polymictic clasts of quartzite, lava and chert, the matrix is coarse sandstone. Poorly sorted.	None	**FA1**	Debris flow. Massive to faintly laminated sandstones. Colour: brown Grain size: medium to course, poorly sorted. bars	Fluvial fan accumulation in response to uplift along a faulted margin or thermal subsidence
Gmp	Red clast supported Conglomerate, with pebbles of quartzite, sandstone, lava and chert. Well sorted.	Planar cross-beds			
Sm	Brown to light brown massive sandstone, with lenticular lenses of shale. Fine to medium-grained. Well sorted	None			
Sp	Brown planar bedded sandstone. Medium grained. Well sorted	Planar crossbedding	**FA2**	longitudinal, transverse bars,	Fluvial channel deposits
St	Brown trough cross-bedded sandstone	Trough Cross bedding			
Scp	Brown cross-bedded sandstone fine to medium-grained	Planar bedding			

The Gmc facies is made up of imbricated clast supported polymictic conglomerate (Figure 4.14). The major clast are quartzite and lava pebbles. The matrix is coarse sandstone. These facies varies in thickness throughout the different farms across the study area. On the other hand, the Gmp facies is a pebble conglomerate facies. These facies are restricted only to the Alma Formation. The facies Gmp is a clast supported conglomerate with lenses of coarse-grained sandstone (Figure 4.15). The maximum measured thickness of the Gmp facies is about 25 m in the Magalakynsoog north farm.

Figure 4.14: Photograph of the Gmc facies in the Yellowwood game lodge.

Figure 4.15: Photograph of the Gmp facies (clast supported conglomerate) in the Yellowwood Game Lodge.

The Sm facies is made up of fine-grained massive sandstone (Figure 4.16). These facies is structureless, but it has quartz veins that are present towards the top of this unit. The Sm facies is observed in all the three formations and it is often overlain by a cobble conglomerate and truncated by quartz veins (Figure 4.16). The St facies is a light brown coarse-grained sandstone with low angular cross-bedding (Figures 4.17 – 4.19). Occasionally, quartzite pebbles are present in the St facies. The quartz pebbles are sub-rounded, while the lava pebbles are moderately well rounded. The Scp facies is a light brown coarse-grained planar cross-bedded sandstone whereas the Sp facies is a fine to medium-grained planar cross-bedded sandstone.

Figure 4.16: Photograph showing the Sm facies (massive sandstone).

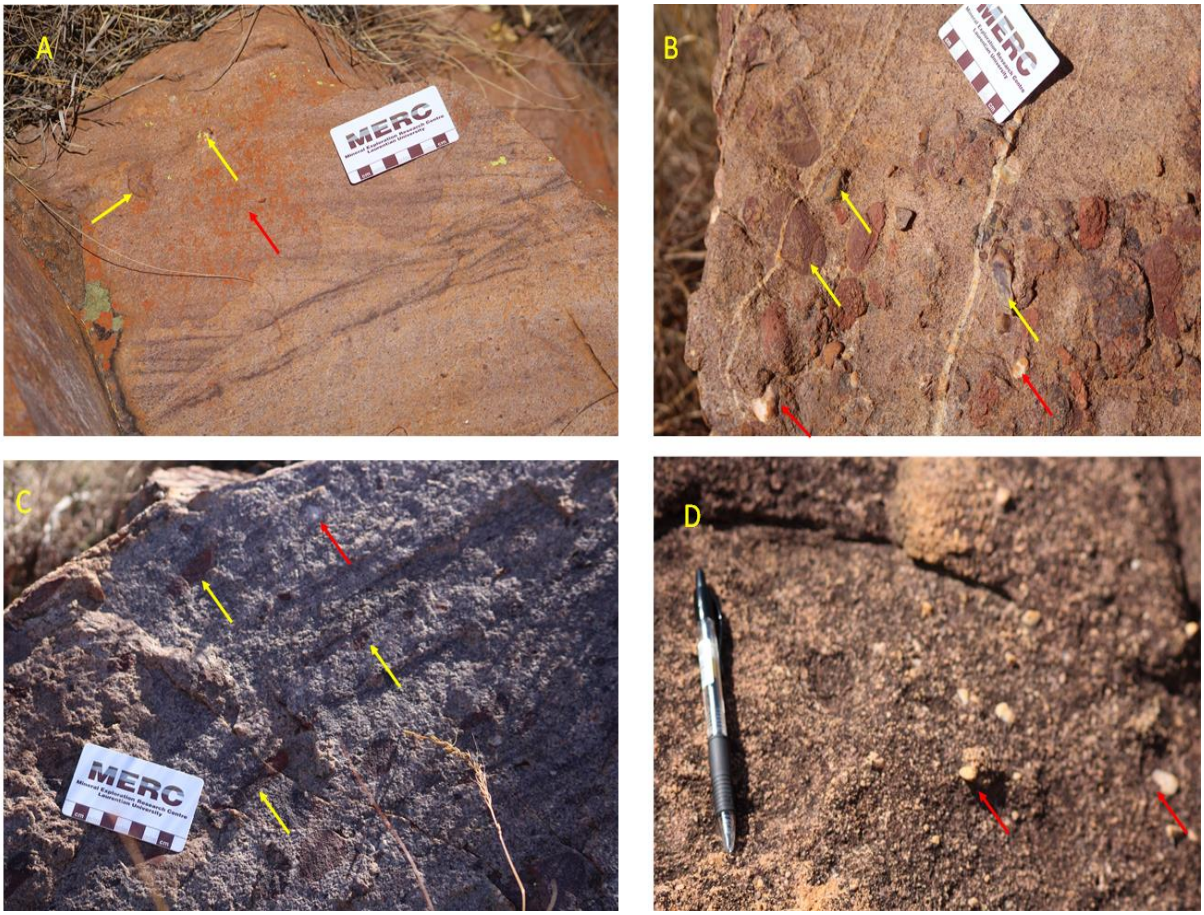

Figure 4.17: Photograph of the lower part of the Alma Formation showing: (A) trough cross-bedding (the yellow arrows show lava pebbles, while the red arrow indicates the quartzite pebbles); (B) massive sandstone with pebbles of lava and pebbles of quartzite; (C) low angle cross-bedded sandstone with pebbles of lava; (D) massive sandstone with pebbles of quartzite.

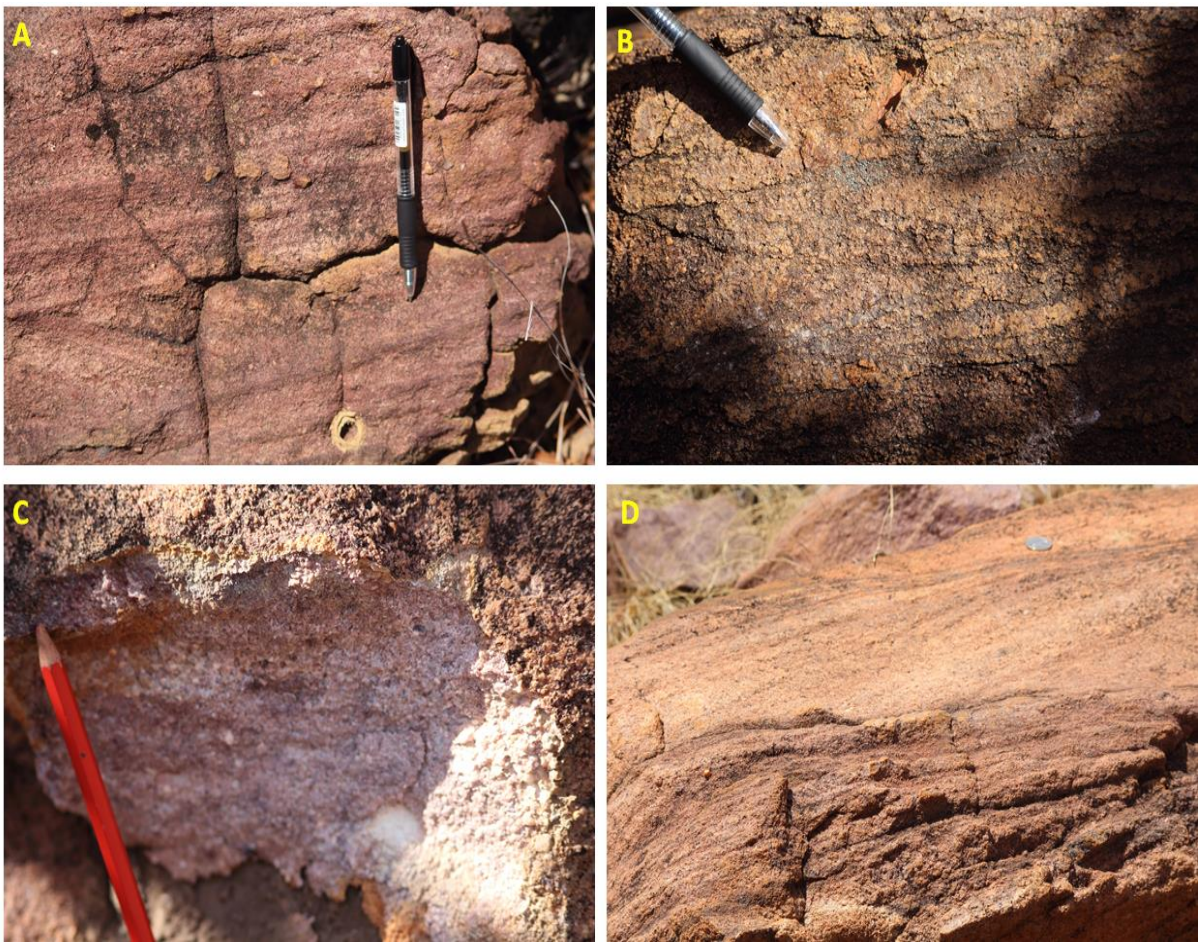

Figure 4.18: Planar bedded sandstone facies (Sp) showing: (A) Planar bedding in the Swaershoek Formation; (B) Trough cross-bedded sandstone in the Alma Formation; (C) Trough cross-bedded sandstones in the Alma Formation with random quartzite pebbles, D) Planar bedded sandstone of the Glentig Formation.

Figure 4.19: Photograph showing typical trough cross-bedded sandstone composed of seven troughs(St facies).

4.2.5.1. Facies association (FA1: Gmc, Gmp, Sm)

The FA1 is a representation of gravel sediments (unstratified conglomerates and imbricated conglomerates). The cobble conglomerates are abundant in the study area and attain a maximum thickness of about 80 m (Figure 4.20). FA 1 includes the pebble supported conglomerate with no sedimentary structures. In the Mgalakysnoog Farm, the lower parts of the Swaershoek Formation rests on the Rooiberg Formation, thus there are no traces of the Glentig Formation. The clasts are well rounded, except for a few that are sub-angular. Most of the sandstone grains in FA1 are well-rounded and moderately well sorted with few rock fragments. The sandstone lenses range between 2 cm to 5 cm in thickness. FA1 is also made up of massive sandstone, which attains a maximum thickness of 95 m in the Yellowwood Game Lodge. In some places, the sandstone has lenticular lenses of shale. The thickness of the lenticular lenses of shale

ranges between 3 cm and 5 cm. In Yellowwood Game Lodge, the massive sandstone has quartz veins that are orientated in a north-south direction. The thickness of the veins ranges from 20 cm to 60 cm. FA1 is interpreted as to be debris flow. Miall (1977) indicated that debris flow is as a result of channel flows that are associated with the fluvial deposit. The fluvial environment for the deposition of the sediments in the study area could have resulted due to uplift along a faulted margin or thermal subsidence.

Figure 4.20: Photograph showing different clasts in the polymictic cobble conglomerate in the lower parts of the Swaershoek Formation in the Magalakynsoog Farm; (A) Lava clast; (B) spherical weathering of clasts indicated by a blue arrow; (C) Conglomerate clast which has in turn pebbles of quartzite and lava; (D) Long axis ellipsoidal clast of lava; (E) Quartzite clast.

4.2.5.2 Facies Association (FA2: Sp, St, Scp)

FA2 is made up of the Sp, St and Scp facies (Figures 4.21 – 4.23). These facies are generally sandstones that are brownish with cross-beds and planar beds. Sometimes, both cross-beds and planar beds occur together as planar cross-beds. The St facies is a light brownish coarse-grained sandstone with low angular cross-bedding (Figure 4.17). Occasionally, quartzite pebbles are present in the St facies. The quartzite pebbles are subrounded, while the lava pebbles are moderately well rounded. The Scp facies is a light brownish coarse-grained planar cross-bedded sandstone and the Sp facies is a fine to medium-grained planar bedded sandstone. The thicknesses of the beds range from 1 cm to 3 cm for the cross-beds and 2 cm to 4cm for the planar beds. FA 2 is interpreted as longitudinal, transverse bars (fluvial channel deposits). These are deposited through channel flows and would contain cross-bedding as structures and also ripples. These may also contain dunes that have cross-bedded sandstone reflecting downstream migration of the avalanching face of the dune.

Figure 4.21: Photograph of FA 1 showing: (A) quartzite cobble; (B) gradational contact between the cobble conglomerate and massive sandstone (marked by a dotted orange line); (C) Contact between the cobble conglomerate and pebble conglomerate the dotted line represents the change in grading in the same bed that is upward fining; (D) Relative thickness of the cobble conglomerate.

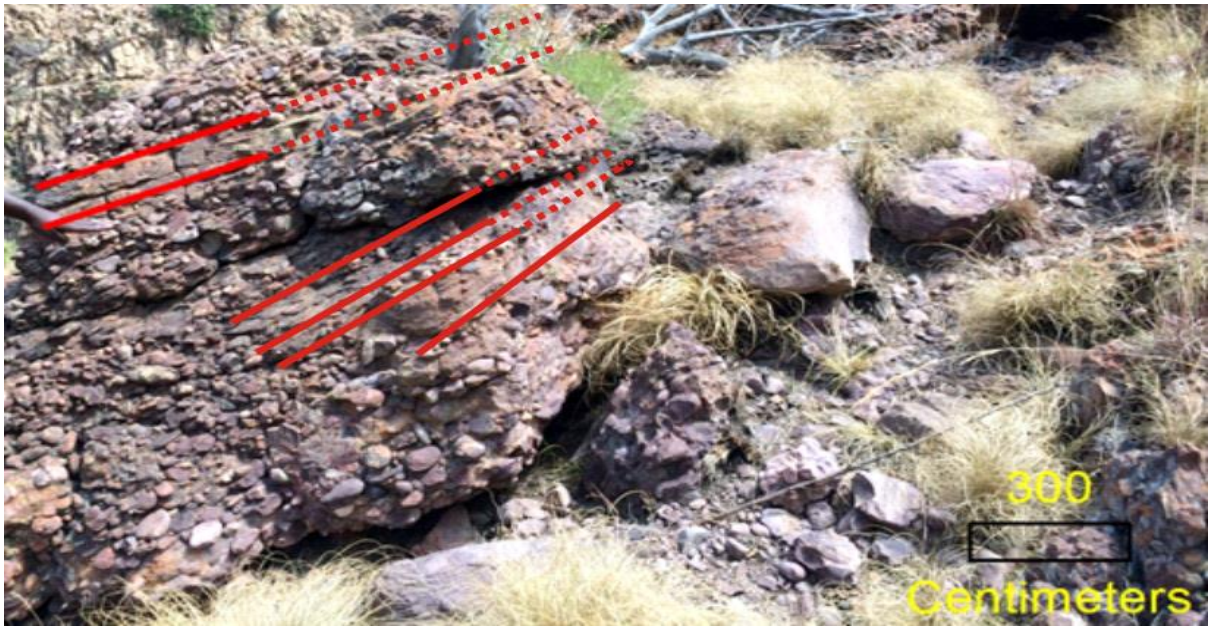

Figure 4.22: Photograph showing conglomerate with lenses of coarse-grained sandstone. The red lines indicate the location of the sandstones lenses within the conglomerate and the dotted lines indicate the possible continuation of the lenses.

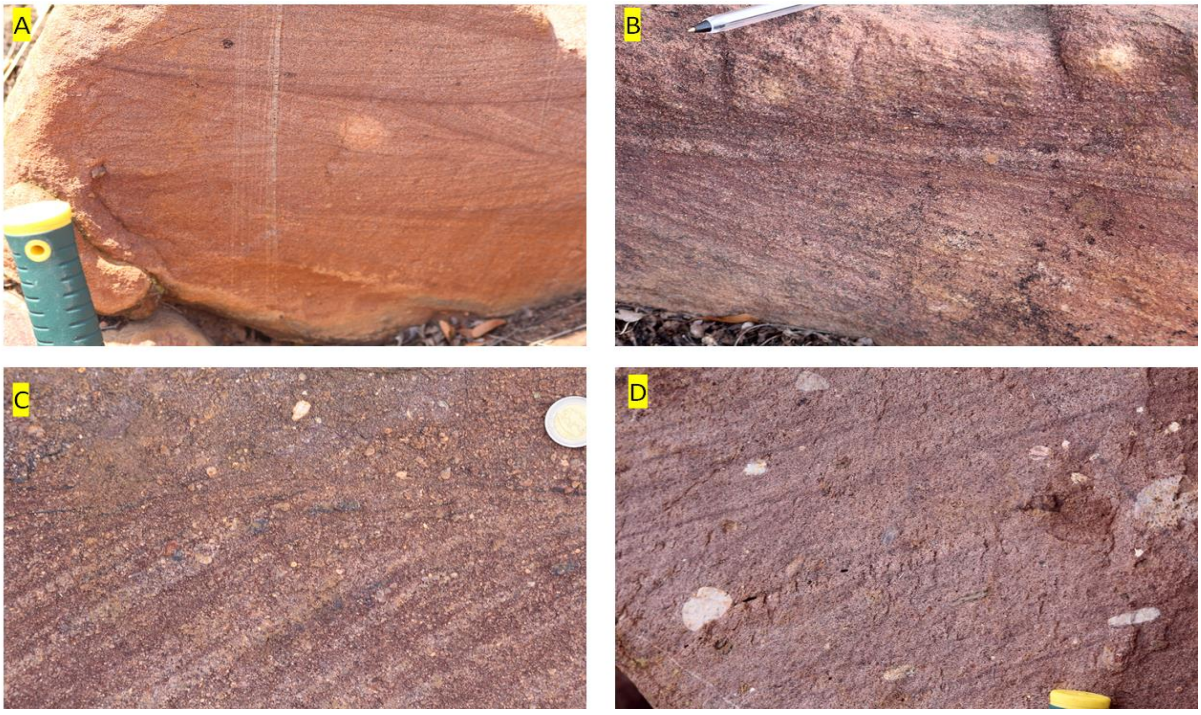

Figure 4.23: Photograph showing planar and cross-bedded units of FA2: (A) Low angle trough cross-bedded sandstone; (B) Trough cross-bedded sandstone; (C) cross-bedded sandstone with occasional pebbles of quartz; (D) Planar bedded sandstone with occasional pebbles of quartzite.

CHAPTER 5

PETROGRAPHY AND MODAL COMPOSITION

5.1 Introduction

The framework grain modal composition analysis (point counting) has been used in the classification of sedimentary rocks (i.e. sandstones) as well as to depicts their provenances (Dickinson, 1983; Boggs, 2009; Baiyegunhi, 2017). Quantitative modal composition analysis is for the determination of the volumetric proportions of minerals that make up the rock. This is often achieved by areal analysis of a thin section; thus point-counting is utilized to get an approximate modal composition of the rock. About 300-500 points on a thin section are systematically selected to record and describe what each point represents (Dickinson, 1983).

Modal composition analysis focuses on individual sediment that make up the bulk composition of the sample. The specific particles are Qm (monocrystalline quartz), Qp (polycrystalline quartz), F (feldspars; potassium feldspar + plagioclase grains) and L (lithics or rock fragments). Polycrystalline quartz and monocrystalline quartz are collectively they called quartz grains. These grains are pivotal in the construction of the Q-F-L plots as indicated by (Dickinson, 1983). Boggs (2009) defined sedimentary petrology study which entails the composition, characteristics and origin of sediments and sedimentary rocks. Dickinson (1983) proposed the relation of sandstones composition to the tectonic setting of the sedimentary basins in which they were deposited. The tectonic setting has a major effect on the composition of sediments in the depositional environment. Yerino and Maynard (1984) indicated different provenance tectonic settings for sediments studies. Sandstone composition was used

by Folk (1974) and Pettijohn (1954) for sandstone classifications. The classifications are based on the amount of quartz, feldspar and lithics that are present in a sample.

5.2 Results and discussion

5.2.1 Texture

The studied samples are sandstones and conglomerates. The sorting in these samples ranges from poorly sorted to moderately well-sorted. Grain morphology varies from subangular to moderately well rounded, depending on the stratigraphic positions. The contacts between individual grains are mainly; suture, long and concavo-convex (Figure 5.1).

5.2.2 Mineral composition

5.2.2.1 Quartz

The most abundant mineral in all the samples that were analysed is quartz. It usually appears in clear colour and it is less weathered compared to other minerals. The quartz content ranges from 62.3% to 89.5% of the total composition in the sandstones. Quartz minerals have been found to occur in three forms which are; monocrystalline grains (Qm), polycrystalline grains (Qp), and quartz cement as quartz overgrowth (Figure 5.2 C).

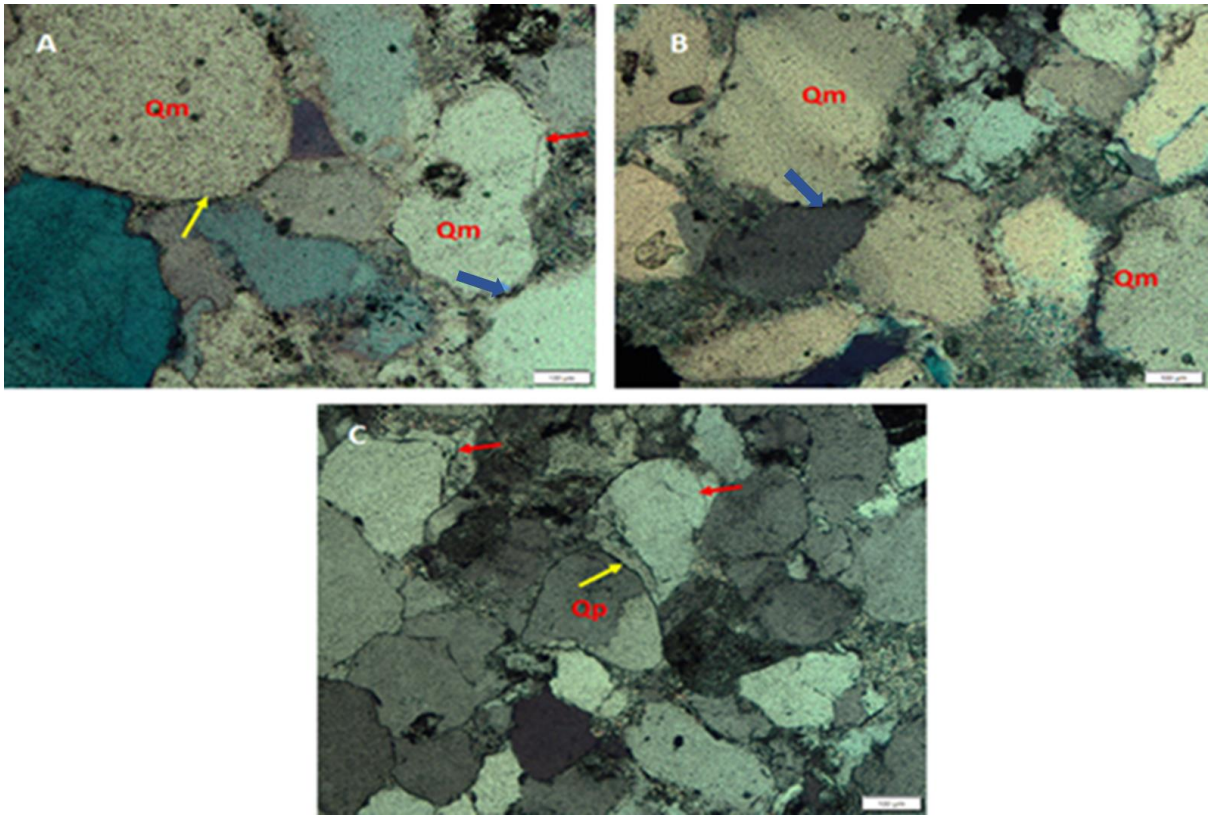

Figure 5.1: Photomicrograph of sandstone from the Swaershoek Formation showing: (a) Sub-rounded to rounded monocrystalline quartz (Qm) grains, quartz overgrowth (red arrow) and long (yellow arrow) and suture (blue arrow) contacts; (b) angular monocrystalline quartz (Qm) with suture contacts (blue arrow); (c) Polycrystalline quartz (Qp) with overgrowth.

The monocrystalline quartz has one or single crystalline quartz, whereas the polycrystalline quartz has more than one crystalline grain. The monocrystalline quartz grains account for about 83% of the total grains in most samples from the study area. Undulatory extinction is displayed in both the monocrystalline and polycrystalline quartz. This presence of monocrystalline and polycrystalline quartz depicts the variable source of these minerals (possibly igneous or from pre-existing sediments).

5.2.2.2 Feldspar

The second abundant mineral is feldspar, most grains of feldspars are altered and have only retained their shape and have been replaced by sericite or kaolinite. Alkali feldspar (orthoclase) and plagioclase feldspar (albite) are the feldspar minerals observed in the thin sections, with alkali feldspar being more abundant. These feldspars are much easily weathered compared to quartz minerals. Also, the feldspar grains are smaller in size and less rounded when compared to the quartz grains. Just like the quartz grains, both monocrystalline and polycrystalline feldspar grains are present and also there are feldspar overgrowths in some (few) of the studied thin sections. The feldspar overgrowth acts as cement in-between grains. Occasionally, there is reddish-brown stain, perhaps hematite rims around the original detrital feldspar grain. The feldspar constitutes an average of about 3.4% of grains in the matrix of conglomerate, and 8.2% of grains in sandstone. Microcline is present in only minor quantities, representing 0.4% in the conglomerates and 0.1% of the sandstones. Plagioclase (Albite) forms 2.6% of the matrix of the grain in conglomerate and 4.6% of the sandstone grains. Non-twinned K-feldspars are the most abundant recognizable feldspar in both the conglomerate (10.4%) and sandstone (14.7%) (Figure 5.2).

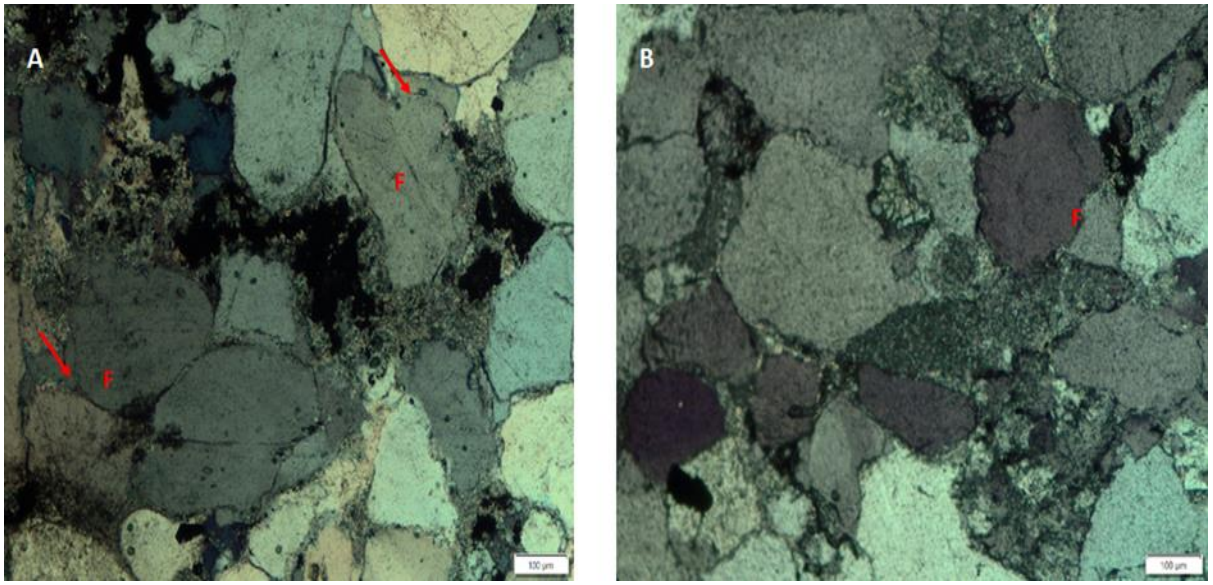

Figure 5.2: Photomicrograph of sandstone from Swaershoek Formation showing: (A) sub-rounded and rounded feldspar (F) grains and overgrowth (red arrow); (B) sub-rounded feldspar (F) grain being replaced by clay minerals.

5.2.2.3 Mica and rock fragment

The mica in the sandstones is muscovite and biotite, muscovite occurs more frequently when compared to biotite. The result of this is attributed to muscovite being chemically stable than biotite in the depositional environment. The identified rock fragments are sedimentary and these shards of rocks have been weathered to sand size particles and are now sand grains in the sedimentary rock (Figure 5.3).

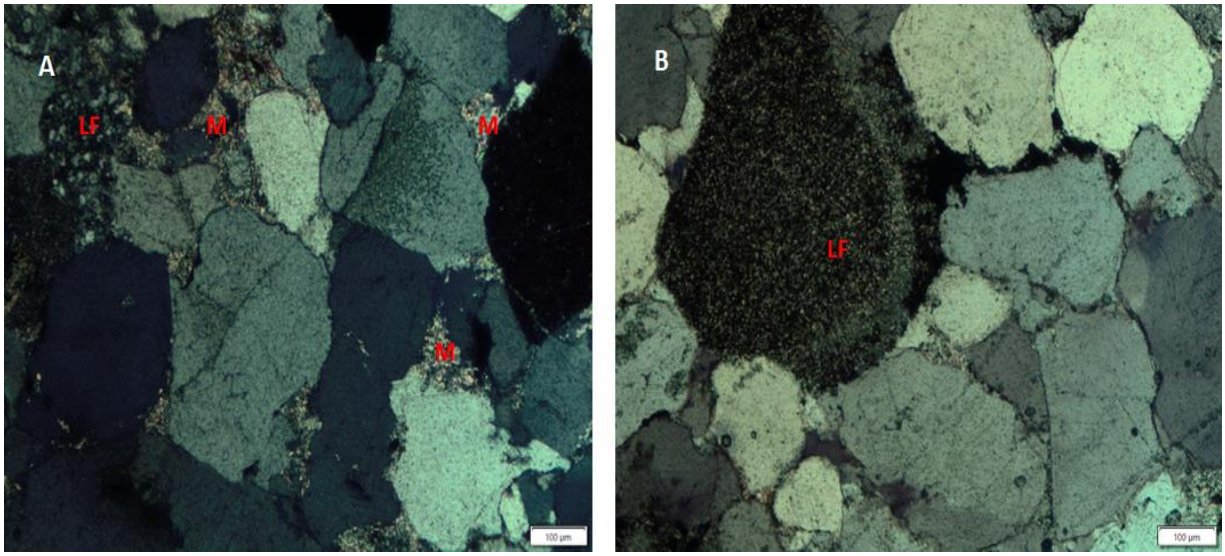

Figure 5.3: Thin sections photomicrograph of sandstone showing: (a) lithic fragments (LF); (b) mica (M).

5.2.2.4 Matrix and cement

The framework grains are bound together by both matrix and cement. The matrix is clay minerals and they are either detrital or diagenetic in form. The common cementing minerals are the clay, quartz overgrowth and feldspar overgrowth.

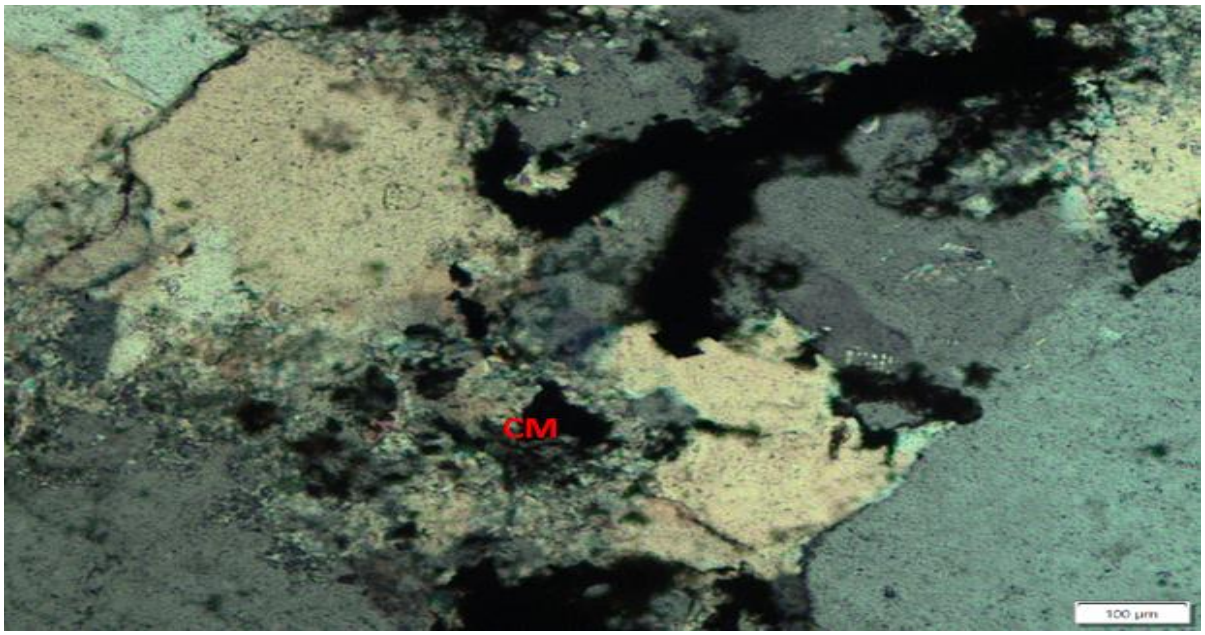

Figure 5.4: Thin section photomicrograph showing clay minerals (matrix).

5.2.3 Modal composition

The recalculated or normalized result of the framework detrital modes of the sandstones is presented in Table 5.1.

Table 5.1: Modal composition data (Recalculated QFL) for the studied sandstones.

Formation	Sample ID	Q (%)	F (%)	L (%)
Swaershoek Formation	PEB001	63,80	20,30	15,90
Swaershoek Formation	PEB002	62,30	10,60	27,10
Swaershoek Formation	PEB003	64,10	15,60	20,30
Swaershoek Formation	PEB004	75,50	17,50	7,00
Swaershoek Formation	PEB005	80,10	5,60	14,30
Swaershoek Formation	PEB006	66,40	22,50	11,10
Alma Formation	PEB007	73,40	9,50	17,10
Alma Formation	PEB0016	63,50	11,50	25,00
Alma Formation	MEL0012	62,30	16,90	20,80
Alma Formation	MEL0016	89,50	7,80	2,70
Alma Formation	MEL0017	83,60	11,50	4,90
Glentig Formation	MEL0018	82,50	6,60	10,90
Glentig Formation	MEL0026	66,80	14,50	18,70
Glentig Formation	MELS0016	74,50	13,50	12,00
Glentig Formation	Mels0028	65,50	15,60	18,90
	Average	71,59	13,30	15,11
	Standard Deviation	8,97	4,92	7,08

5.2.3.1 Sandstone classification

Using the proposed method of Pettijohn (1954), the studied samples were plotted on the Q-F-L diagram. Two samples from the Alma Formation plotted on the sub-arkose field indicating that more of quartz and less of lithics and feldspars (Figure 5.5). Two

samples from the aforementioned formation plotted on the sub-litharenite field, while the last sample plotted on the lithic arenite field. Four samples from the Glentig Formation plotted in the sub-litharenite and one sample plotted on the sub-arkose field. Three samples from the Alma Formation plotted within the sub-arkose field, while two more samples plotted within the sub-litharenite and the last sample plotted in the lithic arenite field (Figure 5.5A). In the background ternary diagram of Folk (1954), two samples from the Swaershoek Formation plotted in the sub-feldspathic arenite, while three samples plotted in the feldspathic litharenite field. One sample from the Glentig Formation plotted in sub-litharenite and lithic arkose fields, while the remaining three samples plotted in the feldspathic litharenite field. Three samples from the Alma Formation plotted in the lithic arkose field whereas the remaining two samples plotted in the feldspathic litharenite field (Figure 5.5B).

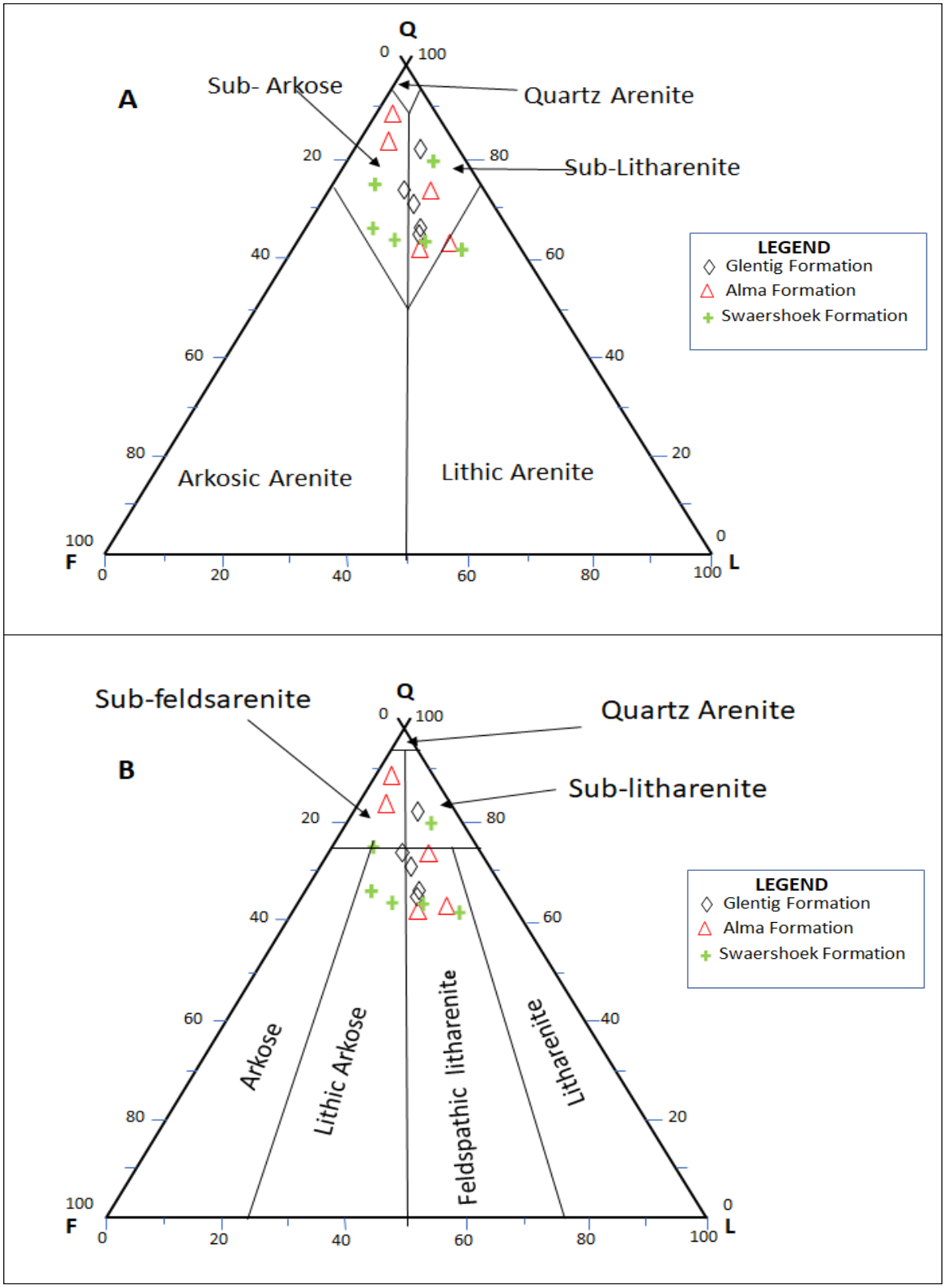

Figure 5.5: QFL ternary plots for sandstones from the Swaershoek, Alma and Glentig Formations (after Pettijohn, 1954 (A); Folk, 1954 (B)).

5.2.3.1. Tectonic setting

The provenance of sandstones composition can be categorized into a magmatic arc, recycled orogens, stable cratons, and basement uplifts (Dickinson et al., 1983). The background ternary plot of Dickinson et al. (1983) shows that the sandstones of the Alma Formation, Swaershoek Formation and Glentig Formation are of recycled Oregon (Figure 5.6). This indicates that the sandstones were mainly sourced from siliciclastic rocks with lesser volcanic rocks, to some extent, the rocks have been metamorphosed and open to erosion as a result of orogenic uplifted fold-belts and thrust sheets (Dickinson et al., 1983). As evidenced in the modal composition, Dickinson et al. (1983) reported that sands that are provenance from recycled orogen usually have low percentages of feldspar are since igneous rocks are not main sources. Also, the modal composition data plot of the studied formations on the background ternary diagram of Yerino and Maynard (1984) shows that the sandstones are related to trailing edge setting (Figure 5.7). Thus tectonically inactive and where the continental margin is facing a spreading centre or rifting resulting in the development of the Waterberg Basin on the trailing edge of the continent. The samples that plotted outside of the tectonic setting fields are possibly due to the effect of intense weathering that the sandstones underwent in the depositional basin.

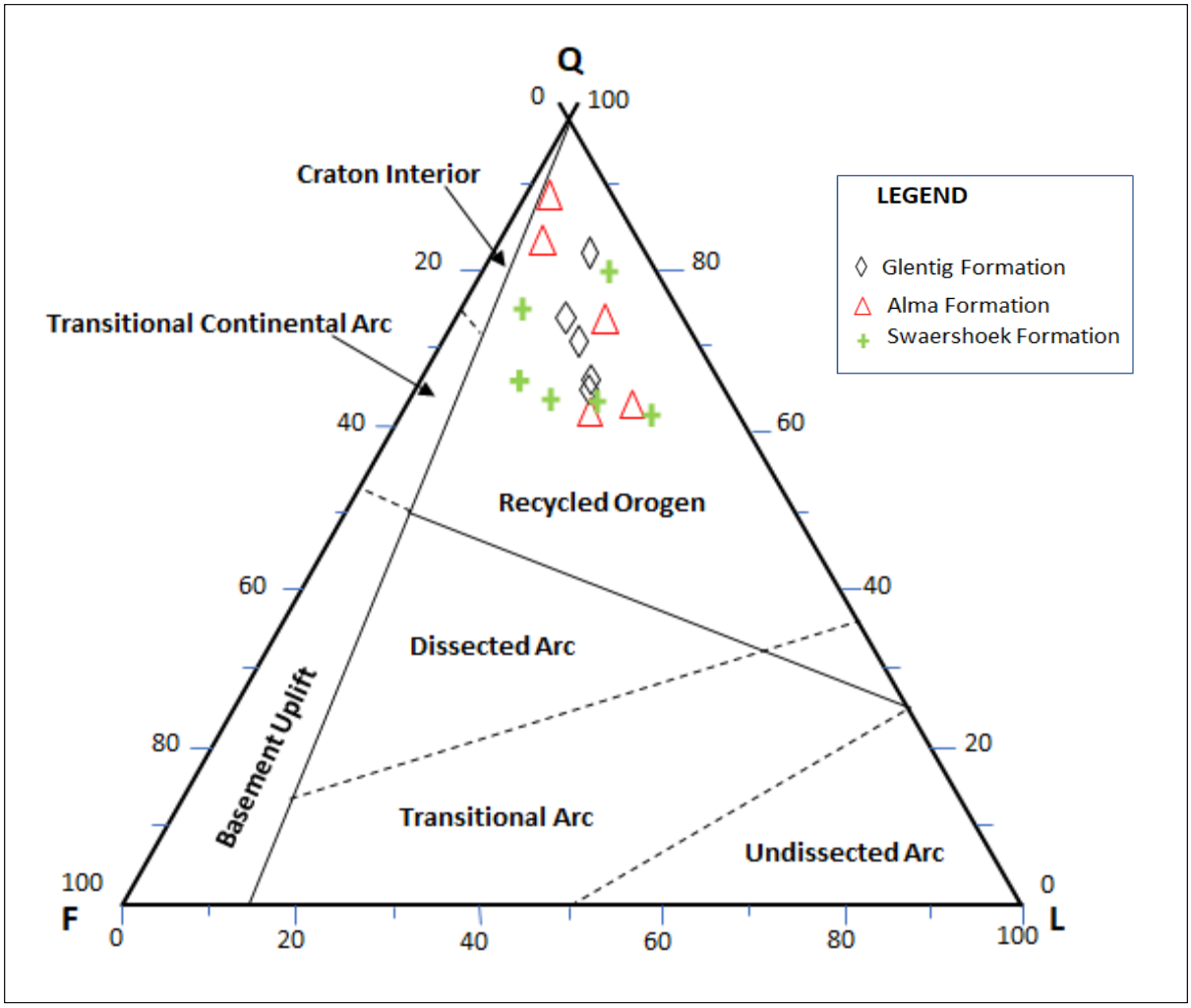

Figure 5.6: QFL ternary provenance plot of the modal composition of sandstones from Alma, Glentig and Swaershoek Formations (after Dickinson et al., 1983).

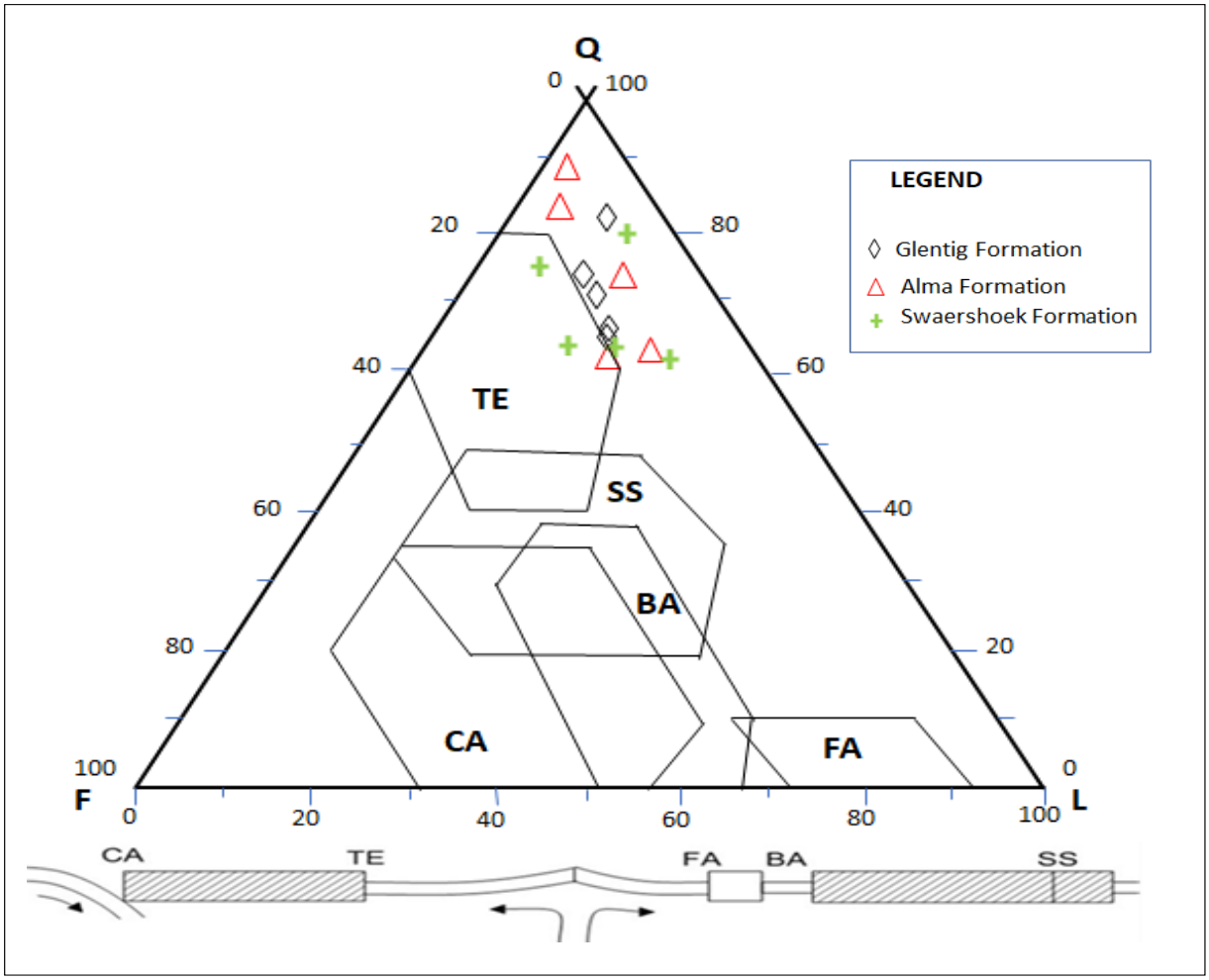

Figure 5.7: Q-F-L tectonic provenance diagram for Swaershoek, Alma and Glentig Formations sandstones (after Yerino and Maynard, 1984). The sandstones plot close and in the TE field. TE: trailing edge (also called passive margin); SS: strike-slip; CA: continental-margin arc; BA: back-arc to island arc; FA: fore-arc to island arcs.

The petrographic attributes of the sandstones of the Swaershoek, Alma and Glentig Formations suggest the following: 1) the sandstones can be classified as subarkosic arenite with a few been lithic arkosic arenite; 2) the provenance analysis indicates that the sandstones are largely derivatives of granites and granite–gneisses of a continental block tectonic provenance (craton interior and transitional continental), in a continental margin basin setting, suggesting that the sandstones were derived

from stable shields and uplifted areas. The aforementioned characteristics indicate that the sandstones were deposited on a passive continental margin that received an enormous amount of mature detritus from the surrounding areas.

CHAPTER 6

GEOCHEMISTRY

6.1 Introduction

The chemical and mineralogical composition of clastic sedimentary rocks is controlled by several factors that includes source rock composition, chemical and physical weathering, and sedimentation processes (i.e. mechanical sorting decomposition and diagenesis) (Boggs, 2009). The chemistry of siliciclastic sedimentary rocks has been long used for unravelling the source rock compositions, paleoclimatic conditions and tectonic setting. The composition of siliciclastic sediments and their tectonic setting and provenance have been studied by several researchers including Bhatia (1983b), Mclennan (1983), Roser and Korsch (1986, 1988), and Bhatia and Crook (1986) The geochemistry of siliciclastic sedimentary rocks can display traits about the parent materials. Furthermore, weathering, transportation, and diagenesis are parts of the determining factors of the chemical composition of clastic rocks. Emphasis has been put on the comparatively immobile elements such as Cr, Co, Th, Y, Zr, Hf, Nb and Sc (Fiantis et al., 2010). The relatively low mobility of these elements during sedimentary processes allows or supports the discrimination between different tectonic provenances and paleoweathering conditions.

In recent years, the use of geochemical techniques has advanced the determination of provenance of sediments. Sediments can come from three major sources, namely, the active continental margin, passive continental margin and Island arc (Roser and Korsch, 1988). The factors that control the mineralogical and chemical composition of clastic sedimentary rocks include (1) the composition of their source rocks, (2)

environmental parameters influencing the weathering of source rocks (i.e., atmospheric chemistry, temperature, rainfall and topography), (3) duration of weathering, (4) transportation mechanisms of the clastic material from the source region to depocentre, (5) depositional environment (e.g., marine versus freshwater), and (6) post-depositional processes (i.e., diagenesis, metamorphism) (Hayashi et al., 1997). Several investigations are substantiating the above aspects of the genesis of both ancient and modern siliciclastic sediments (i.e., Dickinson et al., 1983; Bhatia, 1983; Roser and Korsch, 1986; McCann, 1991; McLennan et al., 1993; Cullers, 2000; Condie et al., 2001; Hessler and Lowe, 2006; Aragón et al., 2013). Quite a number of studies have also been focused on the identification of palaeo-tectonic settings of provenances based on the geochemical signatures of siliciclastic rocks (e.g. Roser and Korsch, 1986; Bhatia, 1983; Bhatia and Crook, 1986)

Major and trace element geochemistry of sandstones and shales can be used as a powerful tool to determine provenance and tectonic setting of sedimentary basins (Bhatia, 1983b; Bhatia and Crook, 1986; Roser and Korsch, 1986). Herein, the major and trace element geochemistry of the sandstones were used to determine provenance and tectonic setting of the investigated formations using binary and ternary plots. The binary plots of TiO_2 versus Zr, TiO_2 against Ni, Th/Co versus La/Sc, La/Th against Hf, Cr versus TiO_2, TiO_2 versus $Fe_2O_3 + MgO$, Al_2O_3/SiO_2 versus $(Fe_2O_3 + MgO)$, K_2O/Na_2O against Fe_2O_3+MgO, $Al_2O_3/(Ca + Na_2O)$ versus (Fe_2O_3+MgO) and K_2O/Na_2O against SiO_2 (after Hayashi et al., 1977; Bhatia, 1983; Roser and Korsch, 1986; Floyd and Leveridge, 1987; Floyd et al., 1989; Hayashi et al., 1997; McLennan et al., 1993; Cullers, 2000) are employed in this study. The ternary-plots of V-Ni-Th×10, A-CN-K, Na_2O-CaO-K_2O, Th-Sc-Zr/10 and La-Th-Sc

(after Nesbitt and Young, 1984; Bhatia and Crook, 1986; Toulkeridis et al., 1999; Bracciali et al., 2007) were also attempted in this study.

6.2 Results and discussion

6.2.1 Major elements

The result of the major elements is presented in Appendix C. The concentration of SiO_2 in the samples ranges from 31% to 97%, averaging 71%. The TiO_2 displays a relatively low concentration in all the samples, the average concentration of TiO_2 is 0.40%. Sample oog41 has the lowest concentration of TiO_2, whereas sample oog18 has the highest concentration of 1.79% (Appendix C). Al_2O_3 has an average concentration of about 10% and the lowest concentration was found in oog23 with a concentration of 2.33% and the highest concentration was found in sample oog28 with a concentration of 26%.

Fe_2O_3 has an average concentration of 5.6%, the lowest concentration of 0.44% was found in sample oog41, while the highest concentration of 16% was found in sample oog7. MnO has an average concentration of 0.04% and in most of the samples range from 0.02 to 0.05%. MgO has an average of 5.6%, the lowest concentration of 0.1% was displayed in sample oog21, while no MgO was detected in sample oog6, the highest concentration of MgO was detected in sample oog34 with a concentration of 3.66%. CaO has an average concentration of 0.20%, whereas Na_2O has an average of 0.07% for all samples. The concentration of K_2O ranges between 0.48% and 5.66%, whereas the concentration of P_2O_5 varies from 0,011% up to of 1.28% in sample oog18. Al_2O_3 is inert and that is why it is less mobile unlike other oxides; hence its abundance was used in this study to compare with other oxides (Figure 6.1). The

detected major oxides in the analysed samples were plotted against Al_2O_3, to compare their mobility to Al_2O_3.

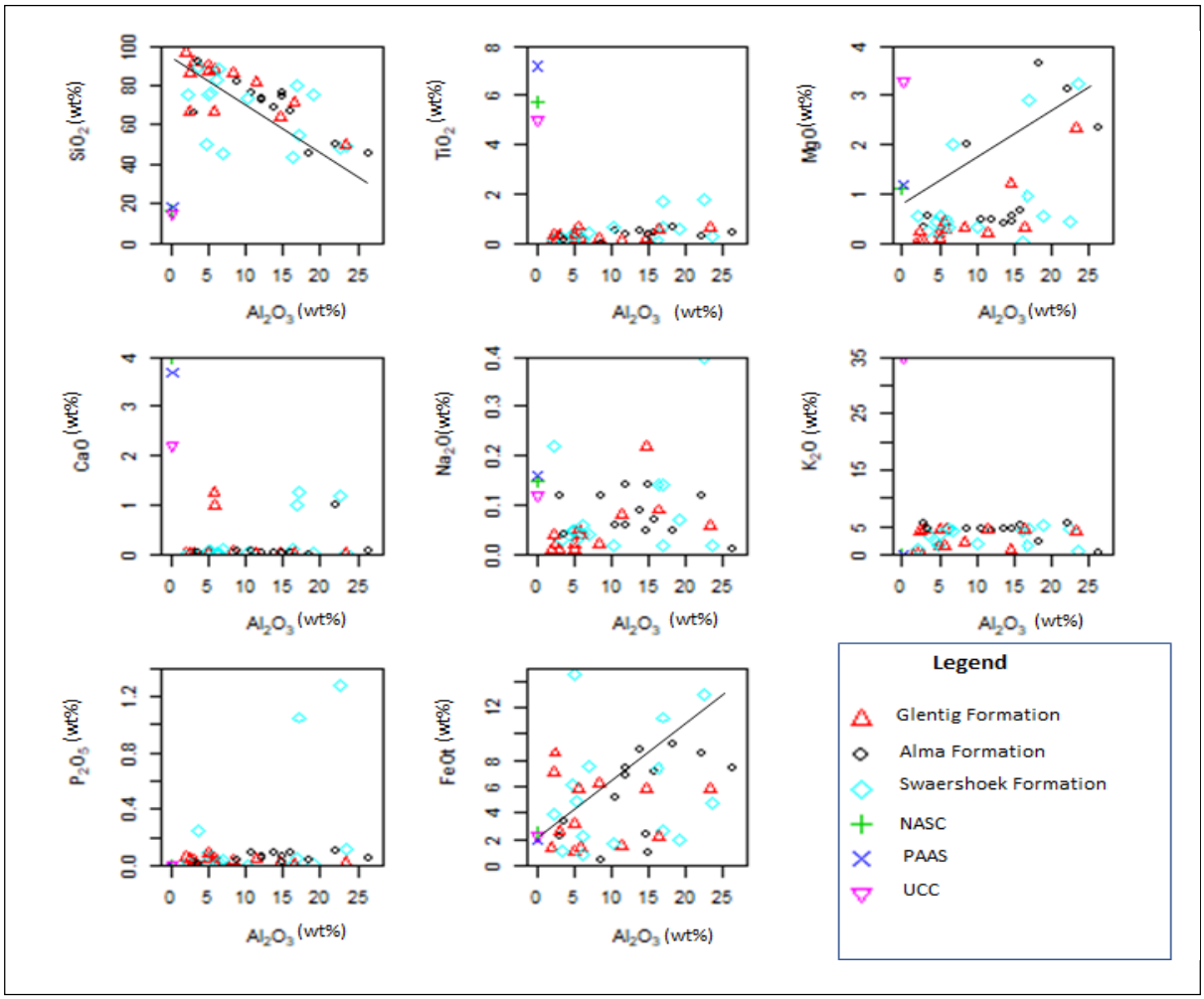

Figure 6.1: Binary plot of major elements versus Al_2O_3 showing the distribution of samples from Glentig, Alma and Swaershoek Formations (McLennan et al., 1993). The average UCC, PAAS and NASC data were included for comparison.

Al_2O_3 shows a positive correlation with MgO and Fe_2O_3. TiO_2, CaO, Na_2O, and P_2O_5 shows no trend. The positive correlation of MgO and Fe_2O_3 with Al_2O_3 perhaps suggests that they are associated with micaceous/clay minerals. The aforementioned 2 samples were normalised to UCC and PAAS (Figure 6.1). The major elements show

variations in the analysed samples, but still comparable with the average composition of UCC (Upper Continental Crust), NASC (North American Shale Composite), and PAAS (Post-Archean Australian Shale) (Table 6.1). The average concentration of Na_2O in this study is low as compared to those of UCC, PAAS and NASC, this could be due to the low amounts of Na-rich plagioclase in all the samples.

Table 6.1: Comparison of the average major elements composition of this study with those of the standard values.

Oxide (Wt%)	This study Sandstones	UCC	PAAS	NASC
SiO_2 (%)	71,40	66,6	62,40	64,82
TiO_2 (%)	0,40	0,64	0,99	0,80
Al_2O_3 (%)	10,90	15,40	18,78	17,05
Fe_2O_3 (%)	5,59	5,04	7,18	5,70
MnO (%)	0,04	0,10	0,11	0,00
MgO (%)	0,84	2,48	2,19	2,83
CaO (%)	0,20	3,59	1,29	3,51
Na_2O (%)	0,07	3,27	1,19	1,13
K_2O (%)	3,47	2,80	3,68	3,97
P_2O_5 (%)	0,11	0,12	0,16	0,15

The average K_2O/Na_2O ratio is 46, this indicates that there is a relatively high alteration of the feldspars. Jolayemi (2015) reported the average K_2O/N_2O for the Rooiberg Group to be just greater >1, which perhaps indicates the presence of albite that has been altered slightly. In this study, the average K_2O/Na_2O is greater than >5 which for albite represents a high degree of alteration. The K_2O enrichment also suggests the presence of illite and sericite, which are further proof of high weathering of the feldspars. Likewise, K_2O is higher as compared to that of UCC and is slightly lower as

compared to that of PAAS and NASC. The MgO average concentration is lower as compared to those of NASC, UCC and PAAS.

In the binary plot variation diagram of major elements against SiO_2 (Figure 6.2), MgO, TiO_2, Al_2O_3 and $FeO_{(t)}$ show a negative correlation to SiO_2, while there is no trend for the other major elements. The increase in SiO_2 marks a maturity in the sandstone, resulting in a decrease of feldspars and volcanic rock fragments. The negative correlation of SiO_2 with the other major elements is attributable to most of the silica being sequestered in quartz. Also, the samples were normalised to UCC, PAAS and NASC, as shown in Figures 6.4 – 6.5. Most samples from the Glentig, Alma and Swaershoek Formations are lower as compared to the UCC and NASC concentrations. Although, two samples from the Swaershoek Formation shows a positive correlation and enrichment of P_2O_5. The spider plot also shows a remarkable depletion of CaO. The other samples in the contextual information showed the values that were close to that of the NASC and almost the same values or concentrations of potassium feldspar (Figure 6.3). The Fe_2O_3 content, though slightly lower in one sample of from the Alma Formation, most of the recorded concentrations are similar to those of NASC and UCC.

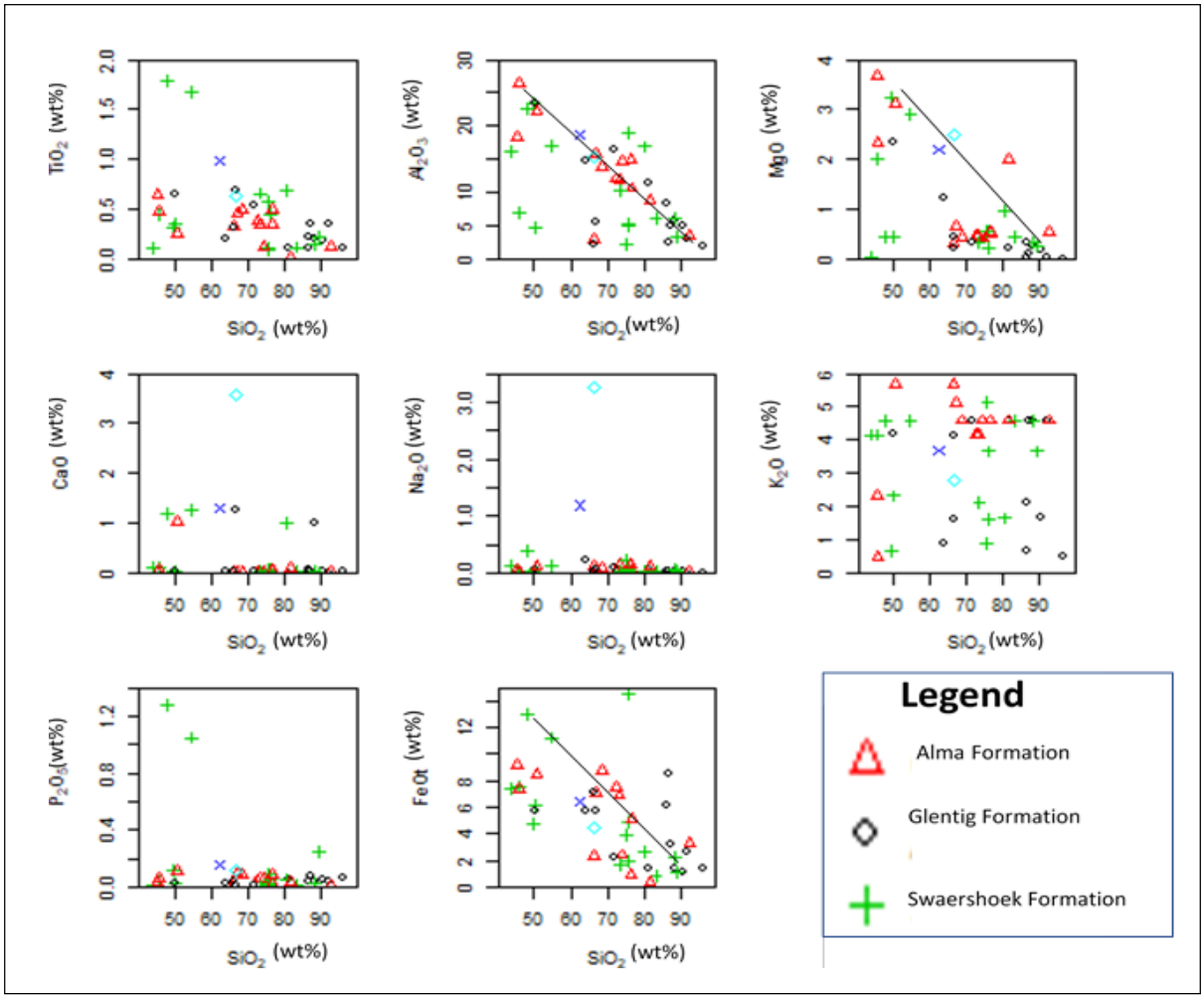

Figure 6.2: Binary plot of major elements against SiO_2 variation diagrams for the Glentig, Alma and Swaershoek Formations.

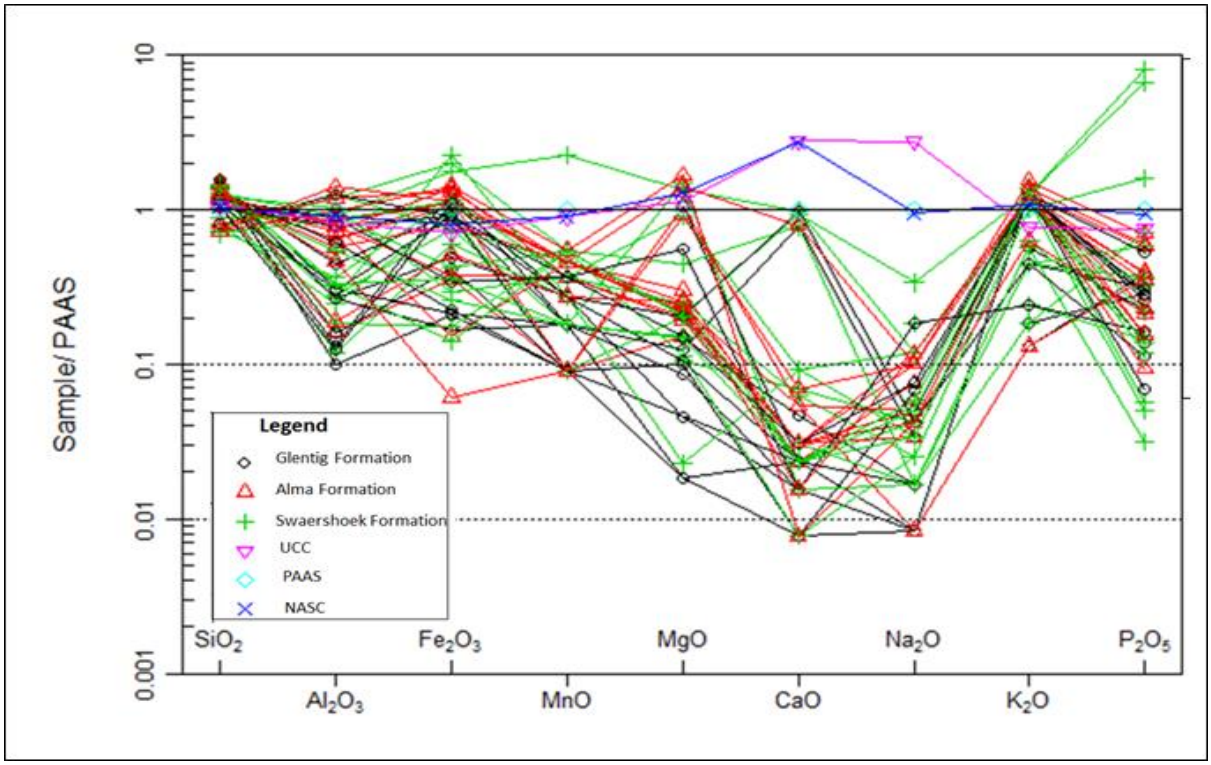

Figure 6.3: Spider plot of major elements normalised against PAAS (after McLennan, 1983; Rudnick and Gao, 2013).

The Spider plot of major elements normalized against UCC shows a depletion of CaO in all the samples. Although, there is a slight increase in the enrichment of potassium feldspar, which could be attributed to the presence of potassium-rich rocks around the area or from the source area. Generally, the concentrations of CaO in the analyzed samples are comparable or the same with the concentrations of the PAAS and the NASC (Figure 6.4). Despite the plot of major elements against NASC showing a depletion of CaO which is consistent with the other spider diagrams. The plot shows a slight enrichment of Fe_2O_3 which is consistent with previous plots. Samples from Glentig Formation also shows a slight depletion of MgO (Figure 6.5). Only one sample from the Swaershoek Formation exhibits depletion in the concentration of TiO_2.

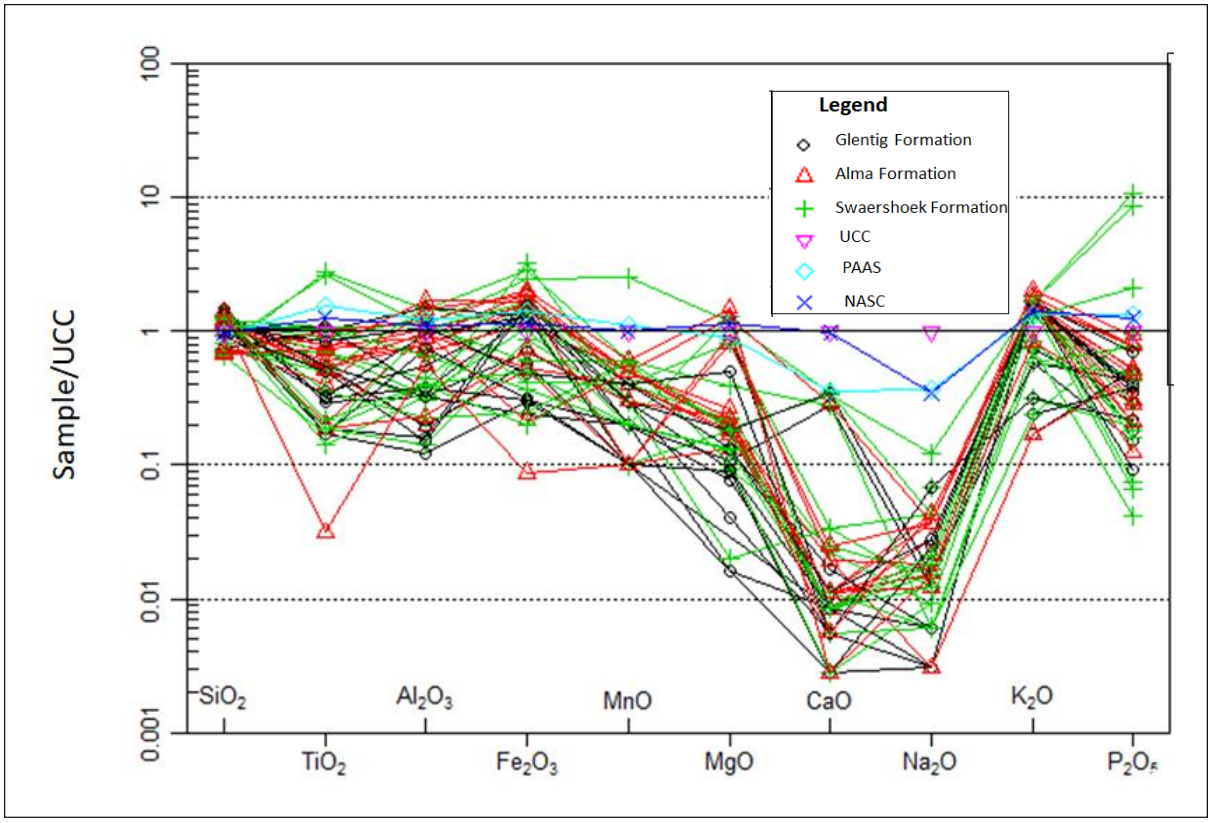

Figure 6.4: Spider plot of major elements normalised against UCC (after McLennan, 1983; Rudnick and Gao, 2013).

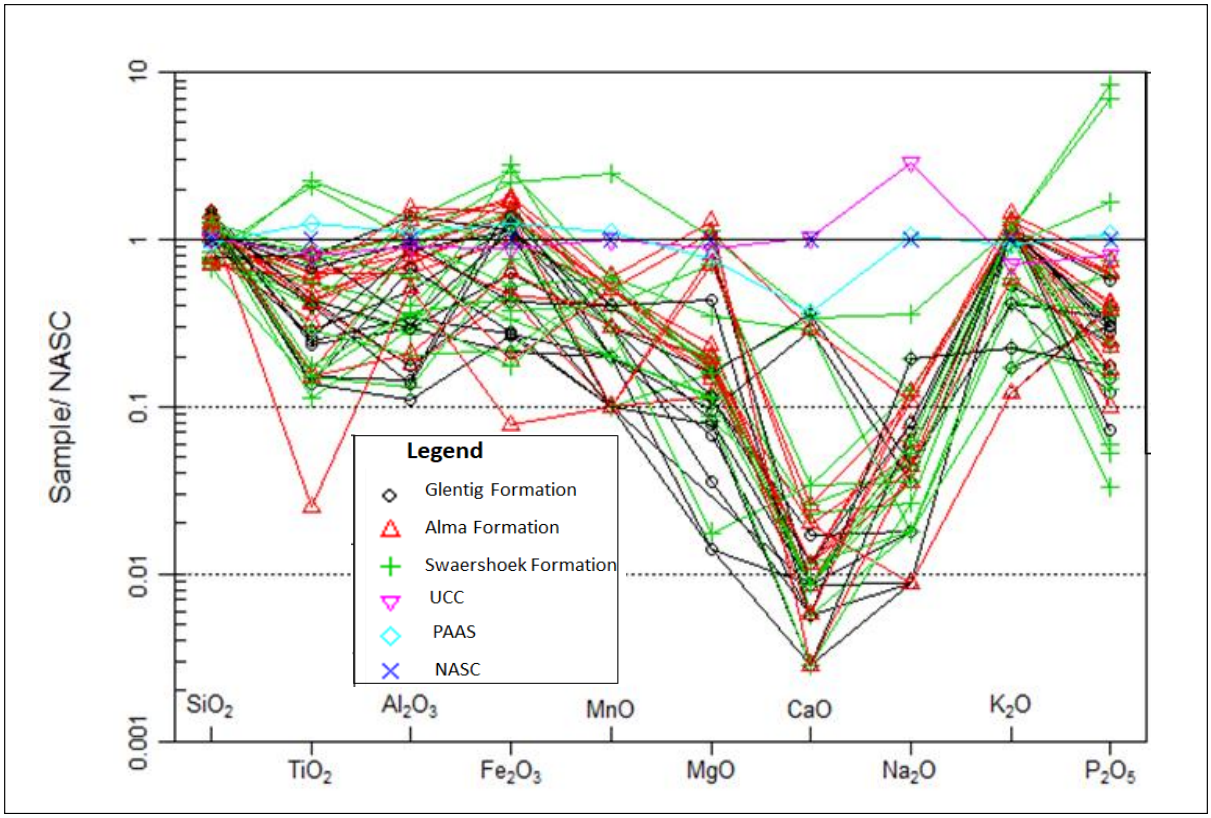

Figure 6.5: Spider plot of major elements normalised against NASC (after McLennan, 1983; Rudnick and Gao, 2013).

6.2.2 Trace elements

The processes controlling the trace element composition in sedimentary rocks may be investigated using normalization diagrams (spider diagrams). Trace elements concentration in the sandstones of the Glentig, Alma and Swaershoek Formations are presented in Appendix D. Just like the major elements, the concentrations of these trace elements are compared with the average concentration of those of UCC, PAAS and NASC. The spider plot of trace elements normalised against UCC (Figure 6.6) shows the depletion of Rb, V and Zn. The concentration of large ion lithophile elements (LILE) ranges from 2.80 to 3290 ppm for Ba, 2.01 to 618 ppm for Rb, 2.10 to 240 ppm for Sr, 1.18 to 216 ppm for Th, and 0.1 to 8.9 ppm for U. Samples oog 8 and oog 14

have the highest concentrations of Rb, while the lowest concentration of Rb was recorded for samples oog 23 and oog 33. Ba shows a higher concentration of all the LILE with a concentration of 390 ppm in samples oog 11 and oog 18.

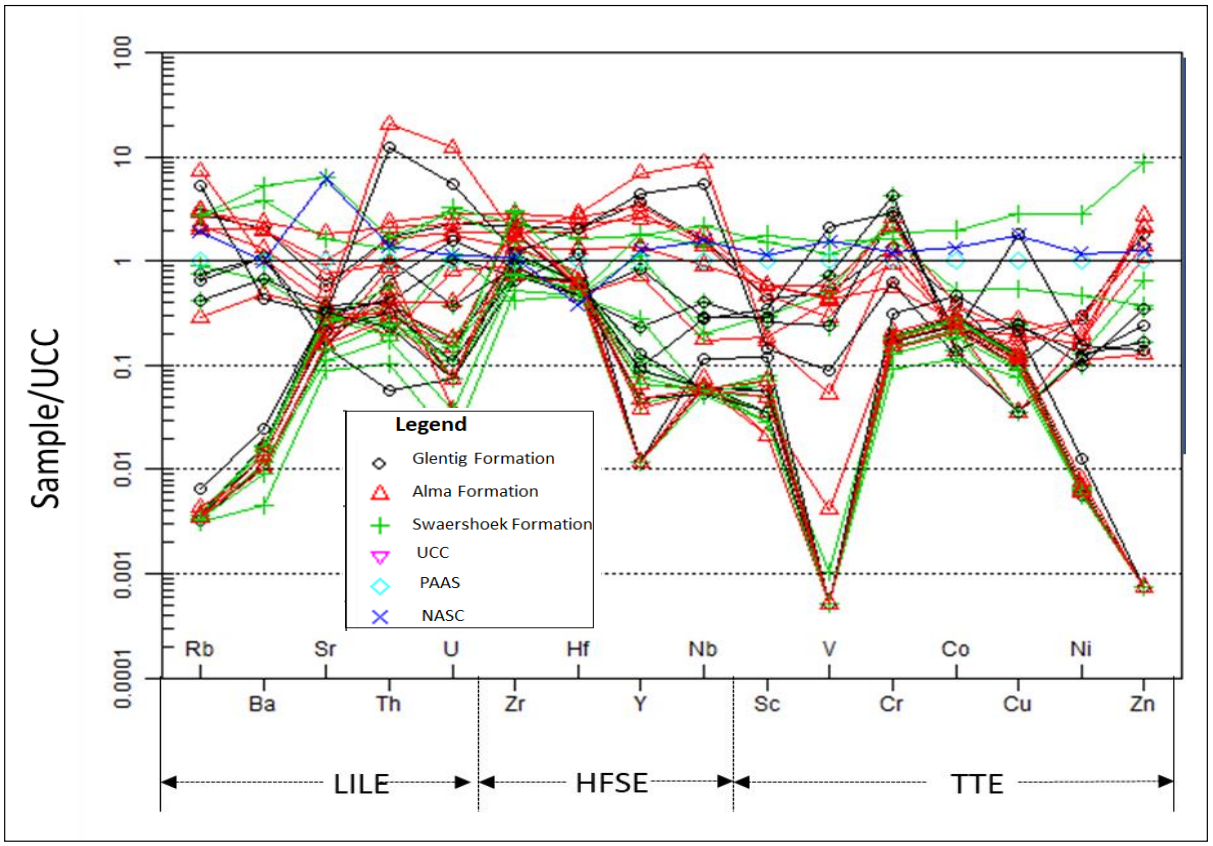

Figure 6.6: Spider plot of trace element normalised with UCC. PAAS and NASC were included in the analysis for comparison. Tace element fields were grouped into LILE (large ion lithophile elements), HFSE (high field strength elements) and TTE (transition trace elements).

Among the high field strength elements (HFSE) like Zr, Hf, Y and Nb, Zr has the highest concentrations ranging from 82 to 596 ppm. The concentration of Zr is highest in sample oog 32 of the Swaershoek Formation and lowest in sample oog 7 of the same formation. The concentration of Hf ranges from 2.76 to 14 ppm. The concentration of Y ranges from 0.5 to 146 ppm, the highest concentration of Y is

recorded in sample oog 20. Nb concentration ranges from 0.62 to 65 ppm. The concertation of Zr is higher when compared to those of UCC and PAAS.

The transition trace elements (TTE) like Sc, V, Cr, Ni, and Zn show variable concentrations. Zn has the highest concentration of 596 ppm in sample oog 32 from the Swaershoek Formation. V has the lowest concentration of less than 0.1ppm for samples from all formations under consideration. Sc concentrations range from 0.30 to 25 ppm with the highest concentration in sample oog 14 of Alma Formation, while the lowest concentration of Sc is displayed by sample oog 34 also from the same formation. The spider plot (Figure 6.7) shows that most samples have the lowest concentration of V. The TTE concentrations in the studied samples are compared with those of the UCC and the PAAS. Also, the identified trace elements were normalised and plotted against the PAAS for comparison (Figure 6.8). The LILE shows a depletion of Rb for Swaershoek Formation and slightly higher for samples from the Glentig and Alma Formations. The HFSE concentration shows depletion of Y, while an enrichment was recorded for Hf for the Glentig Formation.

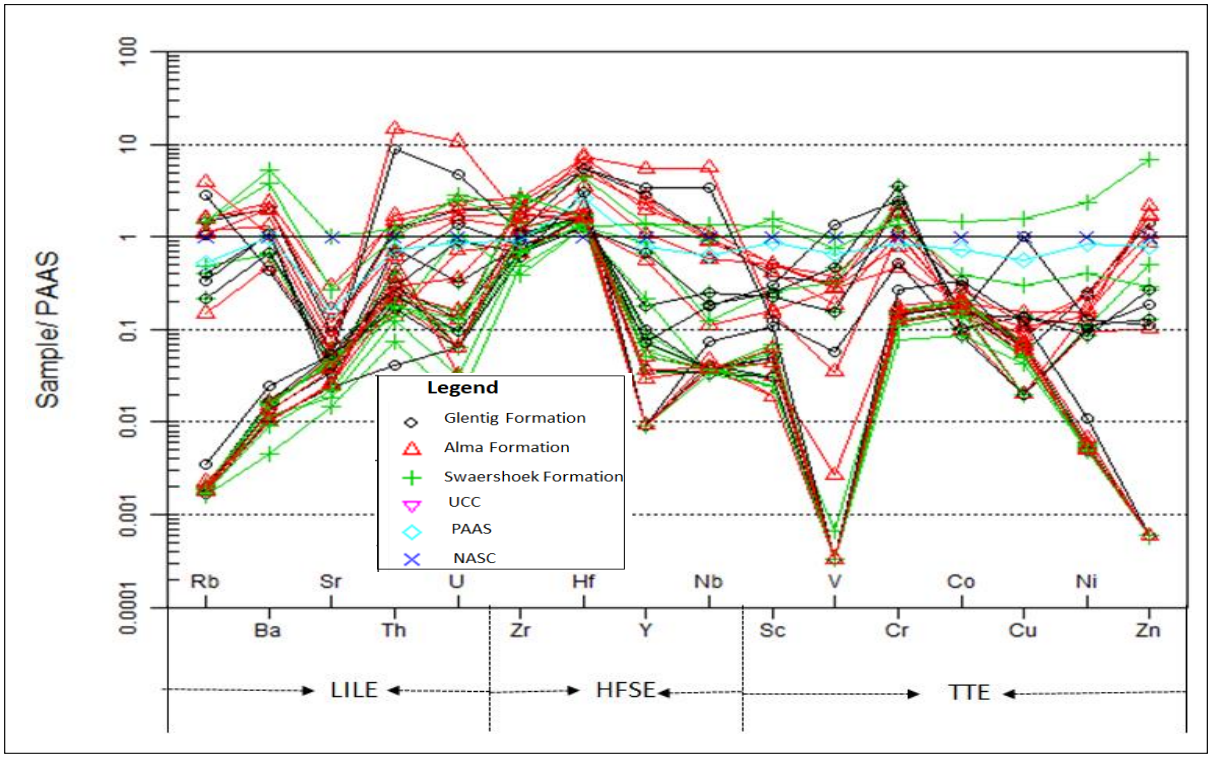

Figure 6.7: Trace element plot normalised with PAAS.

6.2.3 Source rock provenance

The concentration of major elements analysed for this study was used to determine the source rock provenances. Folk (1954) defined provenance as a term that has been used to include all factors involving the production or birth of sediments. Weltje and von Eynatten (2004) further expanded the definition of provenance to encompass all factors related to sediment production, with “specific reference to the composition of the parent rocks as well as the physiography and climate of the source area” (Mclennan, 1983). In this study, provenance discriminant analysis was used to differentiate between the four major provenances (mafic igneous, intermediated, felsic igneous and quartzose sedimentary or recycled provenances) as proposed by Nesbitt and Young (1982). The discriminant function plot infers that the sediments from the Swaershoek and Alma Formations have been derived from felsic and intermediate

igneous provenances (Figure 6.8). These sediments could have been derived from the whining stages of the emplacement of the Bushveld igneous complex.

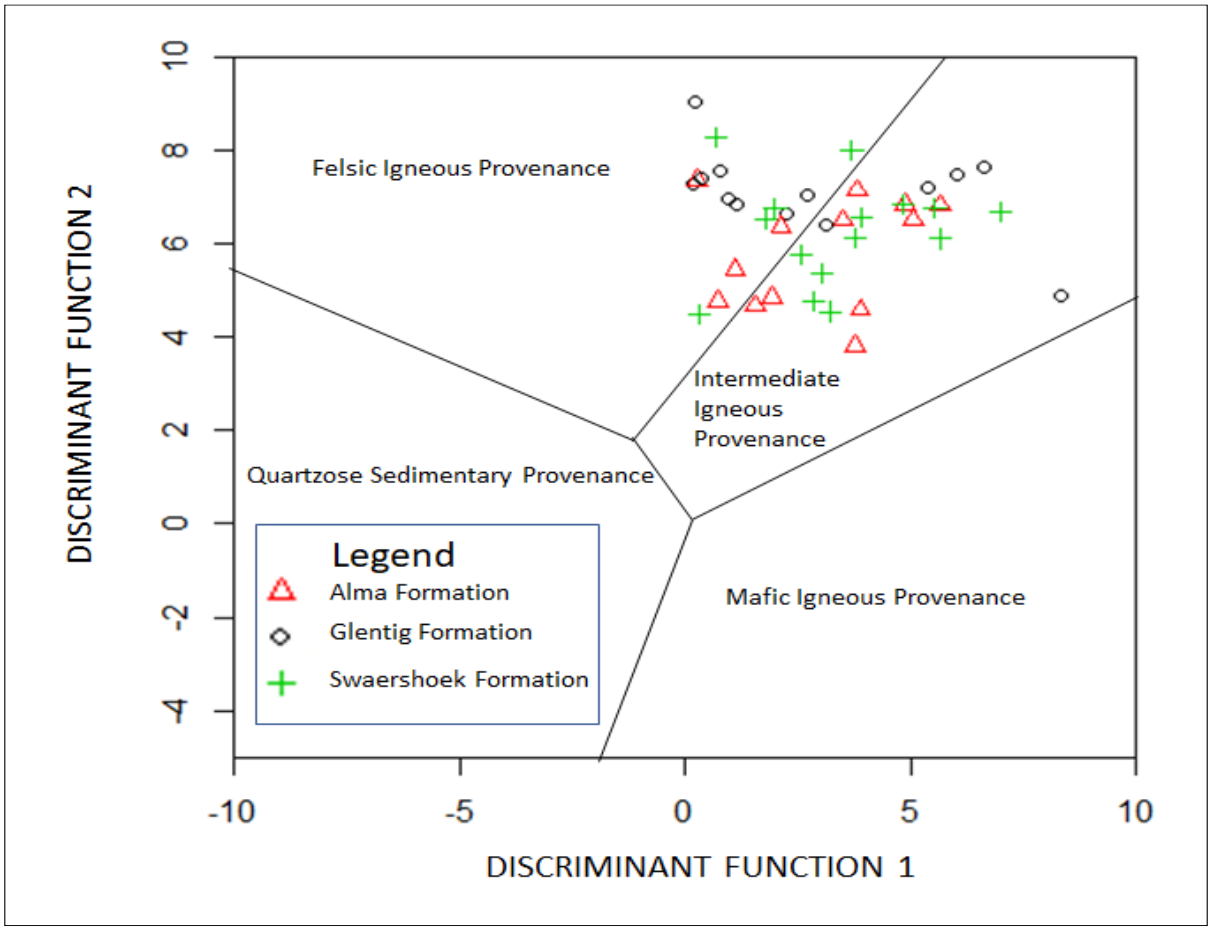

Figure 6.8: Major elements discrimination function diagram for sedimentary provenance. The Discriminant functions are: DISCRIMINANT FUNCTION 1= (-1.773 TiO_2) + (0.607 Al_2O_3) + (0.760 Fe_2O_3) +(-1.500 MgO) + (0.616 CaO) + (0.509 Na_2O) + (-1.224 K_2O) + (-9.090); DISCRIMINANT FUNCTION 2 = (0.445 TiO_2) + (0.070 Al_2O_3) + (-0.250 Fe_2O_3) + (-1.142 MgO) + (0.438 CaO) + (1.475 Na_2O) +(-1.426 K_2O) + (-6.861) (after Nesbitt and Young, 1982).

Similarly, the binary plot of TiO_2 vs Zr indicates that the samples were derived from intermediate and felsic rocks (Figure 6.9). However, one sample from the Swaershoek

Formation was the outlier that plotted in the mafic igneous rocks, this could suggest that some of the sediments were derived from the mafic layers of the Bushveld Igneous Complex. Likewise, the binary plots of TiO_2 versus Ni revealed that the samples are mostly of acid or felsic provenance (Figure 6.10). The binary plot of Log(K_2O/Na_2O) against SiO_2 for the Swaershoek, Alma and Glentig Formations shows that the studied samples are derived from a passive continental margin and active continental margin (Figure 6.11).

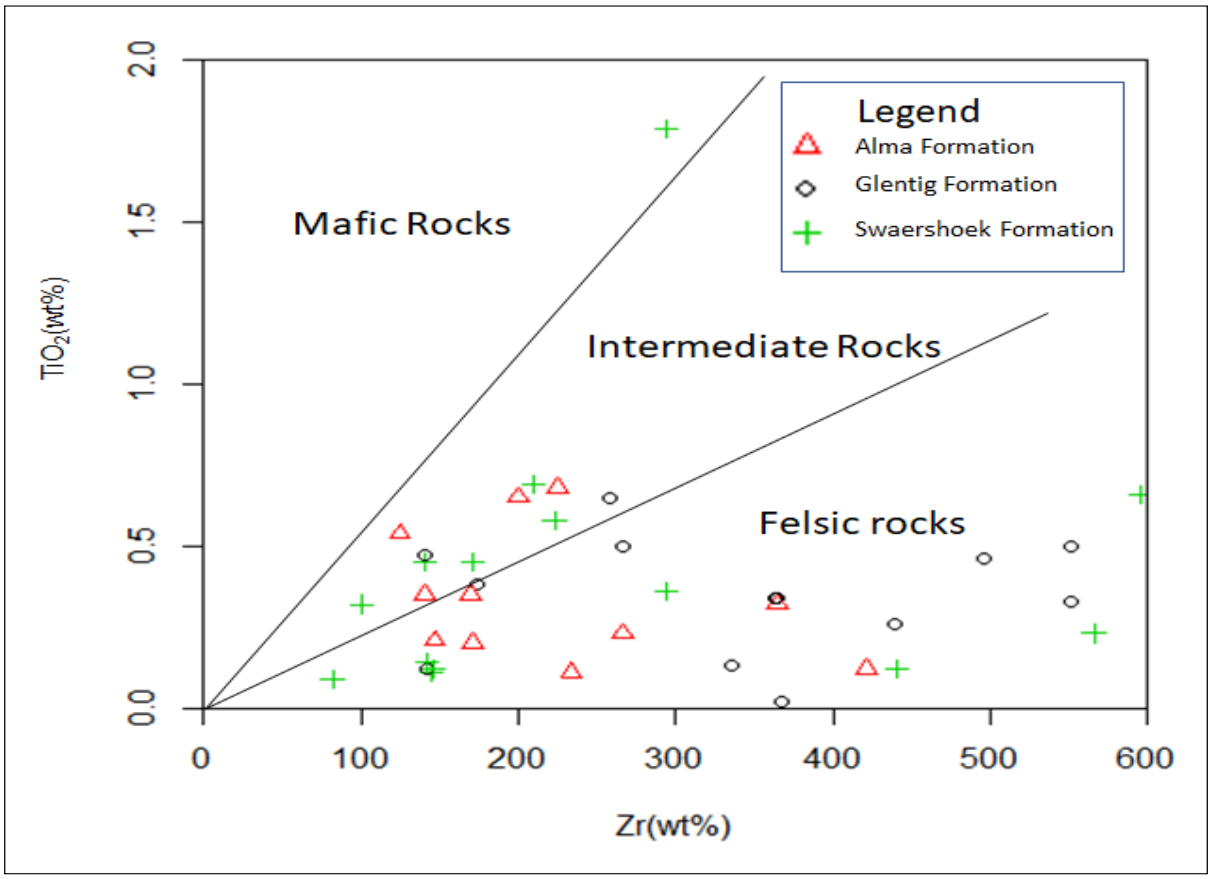

Figure 6.9: Binary plot of TO_2 versus Zr for samples from the Glentig, Alma and Swaershoek Formations.

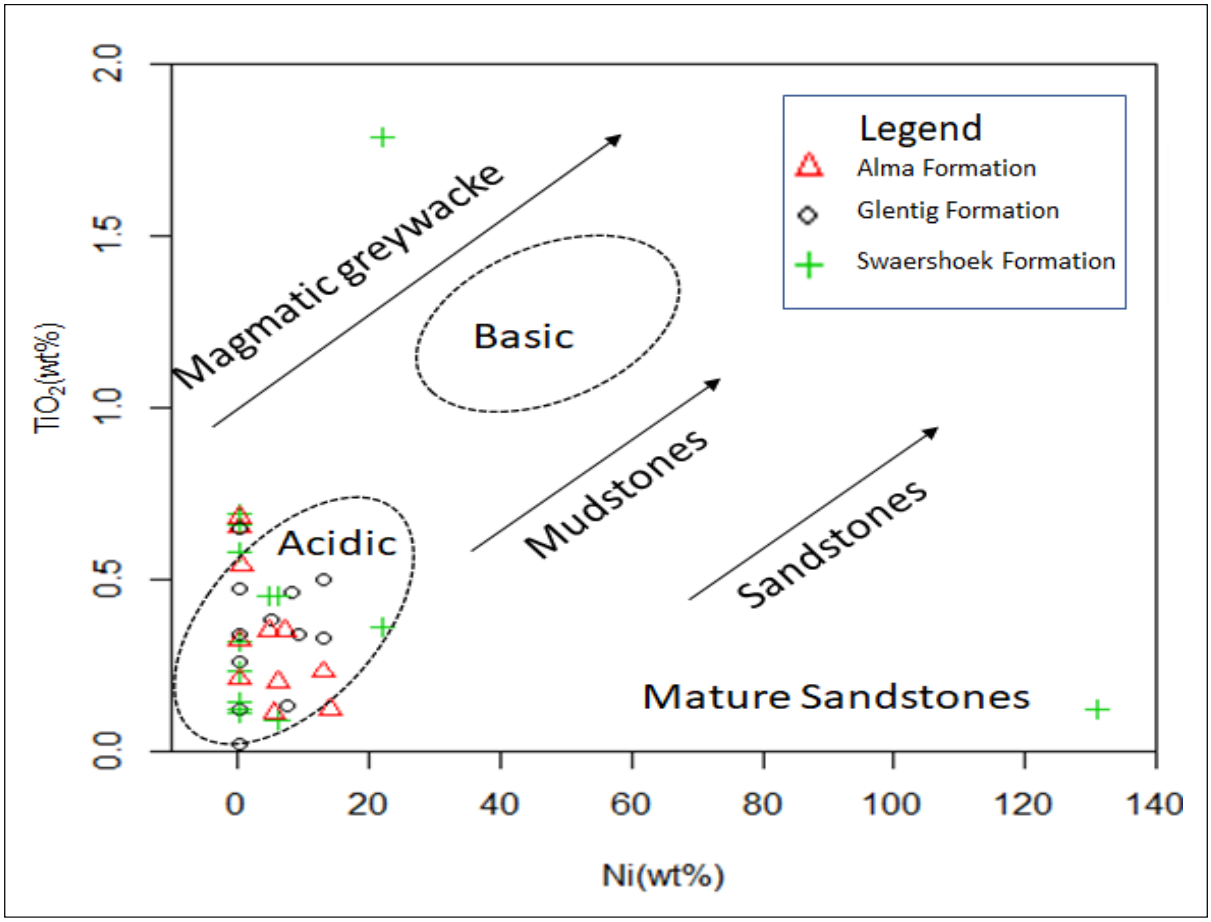

Figure 6.10 The binary plot of TiO_2 against Ni showing the different clastic sediments and an acidic provenance.

6.2.4 Tectonic setting

Several researchers like Bhatia (1983), Bhatia and Crook (1986) and Roser and Korsch (1986) documented that the chemical compositions of siliciclastic sedimentary rocks are considerably controlled by plate tectonic settings of their provenances and depositional basins. Thus, siliciclastic rocks originating from different tectonic settings possess terrain-specific geochemical signatures. McLennan et al. (1993) documented that tectonic setting discrimination diagrams offer reliable results for siliciclastic rocks that have not been highly affected by post-depositional physical weathering, chemical weathering and metamorphic process. Bivariate plots of major and trace element

geochemistry have been used to determine the tectonic setting of sandstones (i.e. Bhatia, 1983; Roser and Korsch, 1986; McCann, 1991; Toulkeridis et al., 1999). The binary plot of SiO_2 versus Log(K_2O/Na_2O) indicated that the sediments had been derived from a passive margin and an active continental margin (Figure 6.11). Three samples from the Glentig and Alma Formations plotted within the active continental margin. Six samples from the Swaershoek Formation plotted within the active continental margin. Twenty-eight samples from the three formations plotted within the passive continental margin.

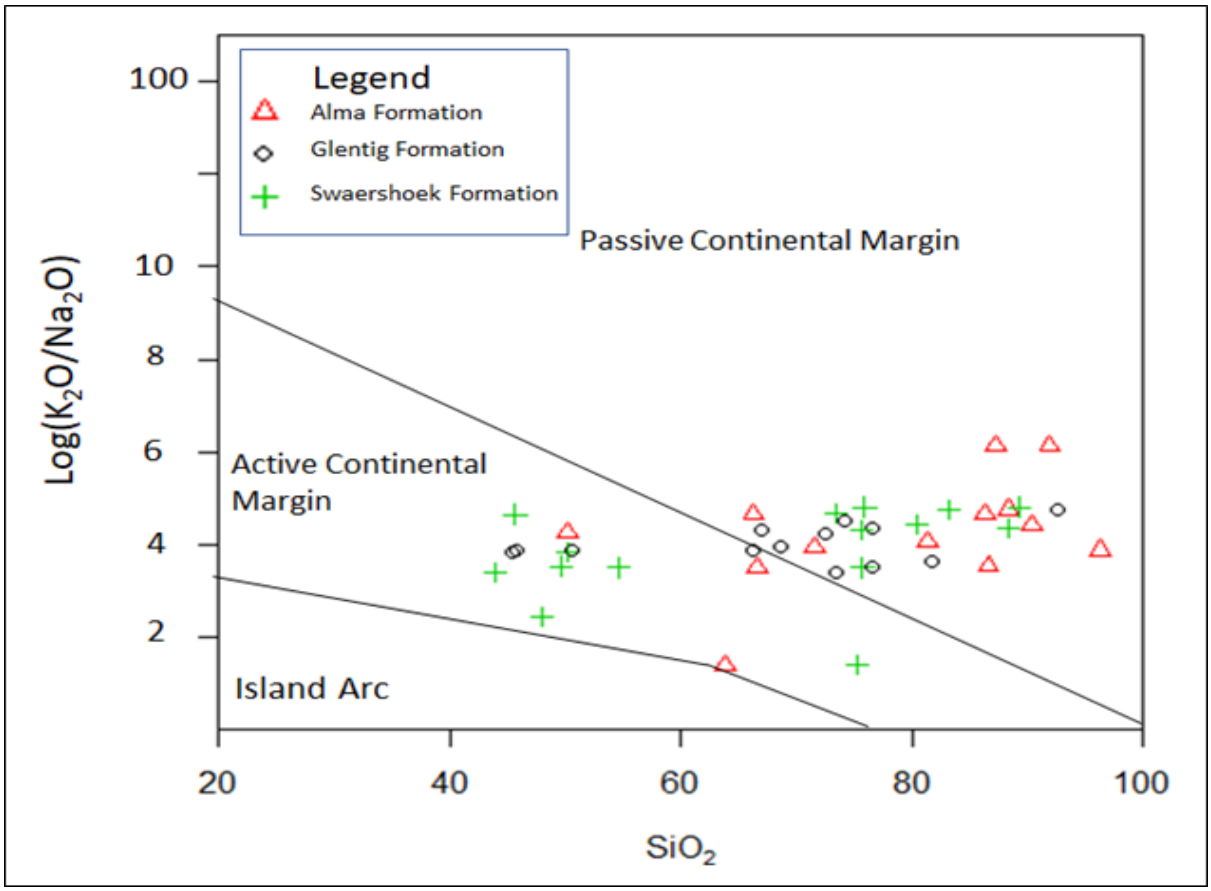

Figure 6.11: Binary plot of log(K_2O/Na_2O) versus SiO_2 for the Swaershoek, Alma and Glentig Formations.

6.2.5 Paleo-weathering conditions

The degree of weathering of the source rock depends mainly on the nature of the source rock, period of weathering, climatic conditions and rates of tectonic upliftment of the source region. Calcium (Ca^{2+}), sodium (Na^{+}) and potassium (K^{+}) cations are mainly removed during weathering, the relative concentration of these elements left in the samples serve as the indicators of the degree of weathering. As the intensity of weathering increases, the concentration of Ca^{2+}, Na^{+}, K^{+} and Sr decreases, such depletion can be attributed to the alteration of feldspars. The decrease in these ions gives rise to an increase in Fe^{+}, Al^{3+} and Ti. Fiantis et al. (2010) indicated that weathering indices help to determine or unravel how much of the original concentration has been altered compared to the remaining concentration (Table 6.2).

Table 6.2: Weathering index with optimum values for a fresh sample and weathered samples.

Index	Optimum fresh value	Optimum weathered value
CIA	≤ 50	100
PIA	≤ 50	100
CIW	≤ 50	100

The provenance studies have indicated that the source rock of this sediments is acidic and according to Nesbitt and Young (1982a), the alkali contents of siliciclastic sediments are prone to deposition alteration. The ratios of K_2O/Na_2O and the sum of K_2O+Na_2O are reliable indicators of the degree of weathering. The molecular proportions of mobile and immobile oxides have been used for the determination of source rock weathering. Source rock weathering indices used in this study are the

chemical index of weathering, (CIW), the chemical index of alteration (CIA) and plagioclase index of alteration (PIA). The calculated values for these weathering indices are shown in Table 6.3.

According to Nesbitt and Young (1982b), the CIA is defined by the formula for the evaluation of the degree of weathering:

$$\mathrm{CIA} = [\mathrm{Al_2O_3}/(\mathrm{Al_2O_3} + \mathrm{CaO^*} + \mathrm{Na_2O} + \mathrm{K_2O})] * 100.$$

Wherein CaO* is the content of CaO incorporated in the silicate fraction.

The chemical index of alteration indicates the proportion of the former minerals to the secondary minerals. The CIA values for less weathered or rather the least weathered rocks range from 50-100 and this value increases when the rocks are subjected to more weathering (Nesbitt and Young, 1982a). The CIA values for the studied samples ranges from 34.16 to 97.93, averaging 63.88 (Table 6.4). These CIA values revealed that the samples have undergone moderate to the high degree of weathering. This in line with the proximity of the source of the rocks which is the Bushveld Igneous Complex. The CIW of the analysed samples ranges from 81.32 to 99.83, averaging 96.61 (Table 6.4). These values indicate a high degree of chemical weathering. According to Nesbitt and Young (1982b), the CIW formula is given by:

$$\mathrm{CIW} = \left[\frac{\mathrm{Al_2O_3}}{\mathrm{Al_2O_3} + \mathrm{CaO} + \mathrm{Na_2O}}\right] 100$$

The CIW is better as compared to other weathering indices because it involves fewer components and entails components that contain consistent geochemical demeanour during weathering. The observed CIW values show high altered samples. The plagioclase index of alteration (PIA) assesses the source area weathering and

redistribution during diagenesis. This is attained by monitoring and quantifying progressive weathering of feldspars to clay minerals and according to Nesbitt and Young (1982b), the formula is given as:

$$\mathrm{PIA} = \left[\mathrm{Al_2O_3} - \frac{\mathrm{K_2O}}{\mathrm{Al_2O_3} + \mathrm{CaO} + \mathrm{Na_2O} - \mathrm{K_2O}}\right] * 100$$

The PIA values range from 54.98 to 122.22, averaging 96.16 (Table 6.4). This indicates moderate to intensive weathering of the feldspars. When weathering occurs, calcium is leached first then followed by potassium and then sodium (Figure 6.12).

The plagioclase index of alteration (PIA) denotes that, if the determined value after the calculation is ≤ 50 then the sample fairly fresh and less alteration, thus it has not been subjected to intense weathering (Nesbitt and Young, 1982a). While a PIA value between 50 and 100 does show some degree of weathering, thus close to 50 is least altered and close to 100 shows a high degree of alteration (Table 6.3). The PIA values range from 54.98 to 122.22, indicating that most of the samples are altered, except for one sample being the least altered (MEL 0012). The bivariate diagrams show a weak correlation of the feldspars with the PIA (Figure 6.12). Nesbitt and Young (1984b) reported that the weak correlation of the feldspars with PIA could be attributed to potassium leaching.

Table 6.3: Indices of weathering calculated from the major elements.

Samples	CIA	PIA	CIW
PEB 001	77,04	97,25	98,00
PEB 002	73,84	98,75	99,18
PEB 003	73,44	97,76	98,52
PEB 004	75,23	99,08	99,37
PEB 005	74,59	98,81	99,20
PEB 006	78,33	97,22	97,92
PEB 007	73,59	95,95	97,25
PEB008	34,16	106,45	94,97
PEB009	58,06	93,41	97,94
PEB010	79,18	98,73	99,05
PEB011	66,47	84,81	90,24
PEB012	66,01	96,69	98,31
PEB013	61,43	94,44	97,73
PEB 016	74,49	98,71	99,13
MEL 0012	51,00	54,98	84,93
MEL 0015	69,31	97,90	98,80
MEL 0016	74,02	89,96	92,46
MEL 0017	78,47	91,82	93,38
MEL 0018	39,50	101,28	99,34
MEL 026	76,00	99,13	99,40
MELS 0016	52,02	93,33	99,40
MEL 0025	70,95	98,70	99,22
MEL 0019	97,03	99,83	99,83
MEL0020	84,56	99,53	99,62
MEL0021	78,61	97,89	98,42
MEL0022	78,45	99,29	99,48
MEL0023	86,34	93,72	94,30
MEL0024	97,93	99,69	99,70
MEL0026	65,81	75,56	81,32

MEL0027	76,56	93,56	95,12
MEL0028	48,18	122,22	98,85
MEL0029	82,47	99,26	99,42
MEL0030	92,90	98,29	98,39
MEL0031	88,52	99,63	99,67
MEL0032	35,52	103,98	97,08
MEL0033	77,69	98,91	99,22
MEL0034	43,19	108,33	97,80
MEL0035	57,06	94,77	98,57
MEL0036	75,80	98,47	98,94
MEL0037	56,73	95,60	98,87
MEL0038	64,50	95,16	97,65

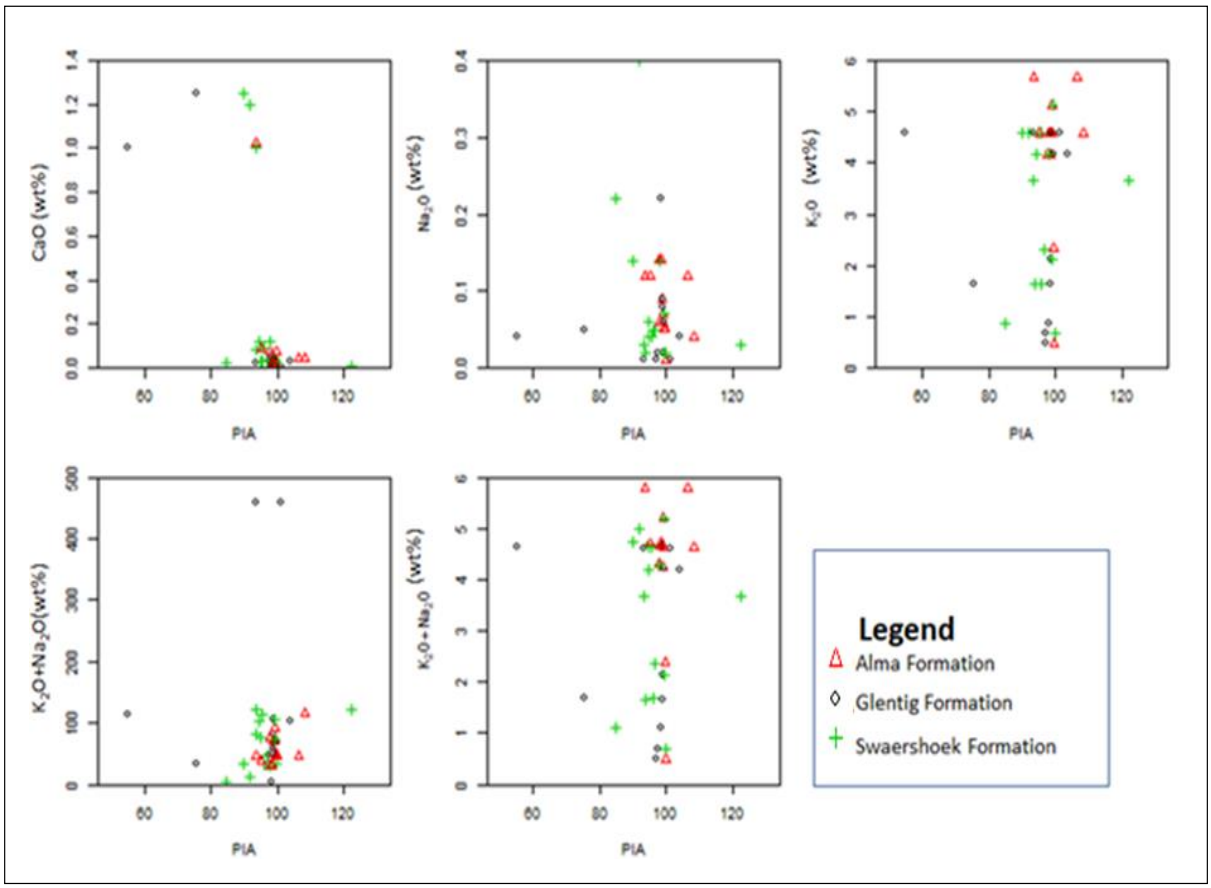

Figure 6.12 Bivariate diagrams showing the mobility of elements during weathering of feldspars (PIA) in the samples from Glentig, Alma and Swaershoek Formations.

The Al_2O_3–($CaO+Na_2O$)–K_2O (represented as A–CN–K) ternary diagram of Nesbitt and Young (1984a) is another useful approach for assessing the composition of source rock and mobility of elements during chemical weathering of source material and post-depositional chemical modifications. The A–CN–K ternary plot of the sandstones were plotted to unravel the compositional changes of the sandstones that are related to chemical weathering, diagenesis and source rock composition. The Al_2O_3–($CaO+Na_2O$)–K_2O composition of the studied samples were plotted on the A-CN-K ternary diagram background fields of Nesbitt and Young (1984a).

The A–CN–K diagrams of the sandstones show that all the samples plotted above the line joining plagioclase and K-feldspar (Figure 6.13). The weathering trendline of the sandstones is closer to the A–K boundary, signifying the silicates (i.e. feldspar) have experienced intense or high weathering resulting in the leaching of Ca and Na out of plagioclase. Also, the weathering trendline (red dotted arrow in Figure 6.13) of the sandstones is relatively closer to the A–K boundary, indicating that K-feldspar is the first to be weathered, out of which Ca and Na leached rapidly, whereas plagioclase is relatively stable. In the sandstones, kaolinite, illite and smectite are the main weathering products.

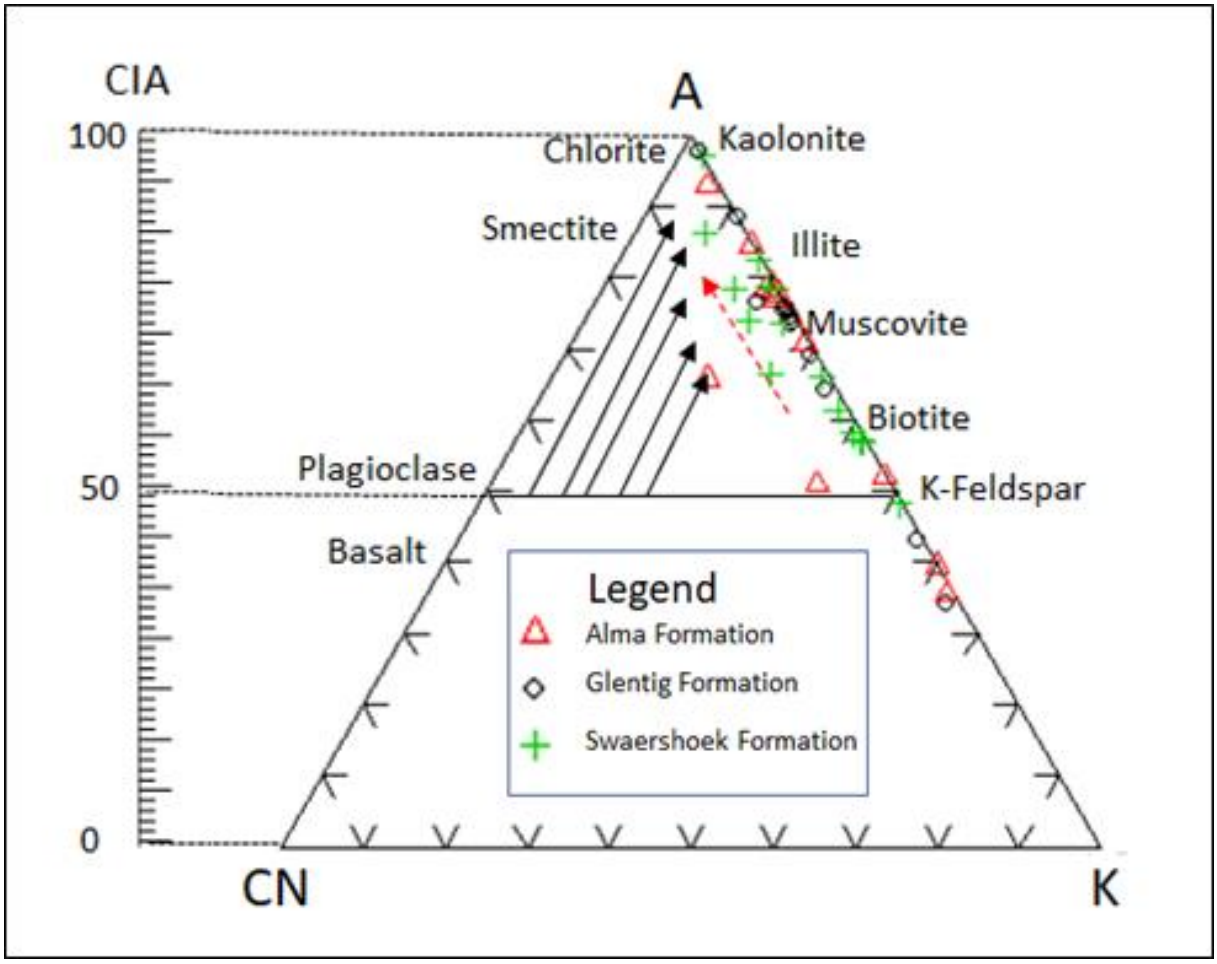

Figure 6.13: A-CN-K ternary diagram of molecular proportions of Al_2O_3-($CaO+Na_2O$)-K_2O for Swaershoek, Alma and Glentig Formations (after Nesbitt and Young, 1984). The CIA scale shown at the left side is for comparison.

CHAPTER 7

GENERAL DISCUSSION, CONCLUSIONS AND RECOMMENDATIONS

7.1 General discussion

The purpose of this research project is to investigate the geology and geochemistry of the Glentig, Alma and Swaershoek Formations to provide information on their source rock characteristics, provenance and tectonic setting. Although, the Alma and Swaershoek Formations had been studied in the past. The previous studies only cover the upper parts of the Waterberg Group, perhaps due to the challenges in accessing the game reserves and farms where the Waterberg Group outcrops, which is also a major challenge in this study.

In the study area (northeast of Modimolle town), the Glentig Formation is about 400 m thick and is made up of sandstone, conglomerate and quartz-feldspar porphyry (volcanic igneous rock). The Swaershoek Formation attained a thickness of approximately 300m. This formation consists mainly of sandstones and conglomerates with minor quartz-feldspar porphyry. The Alma Formation is composed of sandstone and conglomerate and attains a maximum thickness of about 190m. Based on the lithological similarity through the three formations. The stratigraphy of the Swaershoek Formation, Alma Formation and Glentig Formation can be correlated. However, the prominent thick quartz-feldspar porphyry in the Glentig and Swaershoek Formations is absent in the Alma Formation. Based on their correlation the Swaershoek and Glentig Formations were deposited around the same time.

A total of six main lithofacies were identified in the Glentig, Alma and Swaershoek Formations, which are categorized into two distinct facies associations (FAs). These facies associations are Conglomerate and massive sandstone (FA 1; Gmc + Gmp + Sm) and planar cross-bedded sandstone, and planar bedded sandstone (FA 2; Sp + St + Scp). Sedimentological characteristics of the identified facies associations suggested as grain-flow. The facies analysis of the Swaershoek, Alma and Glentig Formations have indicated that these formations were deposited in a fluvial environment and that environment was as a result of the uplifting of the surrounding area and/ thermal subsidence of the Bushveld Igneous Complex (BIC).

The petrographic study of sandstones from the Swaershoek, Alma and Glentig Formations indicated that they are poorly to moderately sorted, and immature. Modal composition analysis of the sandstones indicates that the detrital components of the sandstones are dominant. The sandstones of the Swaershoek, Alma and Glentig Formations can be classified as subarkosic arenite and lithic arkosic arenite. Provenance analysis indicates that the sandstones are largely derived from felsic igneous provenance and intermediate igneous provenance. The QFL tectonic provenance diagrams show that the sandstones are largely derived from granites and granite–gneisses of a continental block tectonic provenance (craton interior and transitional continental), in a continental margin basin setting, suggesting that the sandstones were derived from stable shields and uplifted areas. The aforementioned characteristics indicate that the sandstones were deposited on a passive continental margin that received an enormous amount of immature detritus from the hinterland areas. Also, the modal composition data plot of the studied formations on the background ternary diagram of Yerino and Maynard (1984) shows that the

sandstones are related to trailing edge setting, which is tectonically inactive and where the continental margin is facing a spreading centre or rifting resulting in the development of the Waterberg Basin on the trailing edge of the continent.

The major oxide and trace element concentrations in the sandstones show significant variation in composition across the samples but still comparable with those of NASC, UCC and PAAS. The discriminant function plot and binary plot of TiO_2 versus Zr revealed that the studied rocks are derived from felsic and intermediate igneous provenances. These sediments could have been derived from the whining stages of the emplacement of the Bushveld igneous complex. The A-CN-K ternary diagram and indices of weathering revealed that the studied rocks had been subjected to moderate to the high degree of chemical weathering.

7.2 Conclusions

The provenance, tectonic setting and paleoweathering conditions of the sandstones from the from Glentig, Alma and Swaershoek Formations has been assessed using inorganic geochemical studies. Based on the major oxide compositions, the sandstones could be classified as subarkose and sub-lithic arenite. The major oxide and trace element concentrations in the sandstones show significant variation in composition across the samples but still comparable with those of NASC, UCC and PAAS. The tectonic setting discrimination diagrams support the passive-active continental margin setting of the provenance. The CIA and PIA values, as well as the A-CN-K ternary plots, suggest that the source area of the sandstones were subjected to moderate to intense weathering conditions.

7.3 Recommendations

The main hindrance or limitation of this study was that access to other farms where the investigated formations outcrops were not granted. Hence, a further detailed geological study of these formations in those farms/game reserves is recommended. The current study indicated the presence of quartz-porphyry in all the formations, such units have been known to contain zircons and thus this can be used to ideally place, in brackets, the age of the deposition of the Alma, Swaershoek, and the Glentig Formations. Also, the correlation between the currently studied formations and the Loskop Formation and the Rust de Winter Formation is recommended because it is of pivotal importance since this will add knowledge about the whining stages of the Bushveld Igneous Complex (BIC).

REFERENCES

Baiyegunhi, C. (2017). Sedimentary, geochemical and geophysical study of the Ecca Group, Karoo Supergroup and its hydrocarbon potential in the Eastern Cape Province, South Africa. PhD thesis, University of Fort Hare, 526pp.

Barker, O.B., Brandl, G., Callaghan, C.C., Eriksson, P.G., and van der Neut, M., (2006). The Soutpansberg and Waterberg Groups and the Blouberg Formation, in Johnson, M.R., Anhaeusser, C.R., Thomas, R (ed) The Geology of South Africa. Johannesburg: Council for Geoscience, pp. 301–318.

Bhatia, M. (1983a). Plate tectonics and geochemical compositions of sandstones, Journal of geology, 91, pp. 611–627.

Bhatia, M. (1983b). Plate tectonics and geochemical compositions of sandstones, The Journal of Geology, 91(6), pp. 611–627.

Bhatia, M. R., and Crook, K. A. W. (1986). Mineralogy and Trace element characteristics of greywackes and tectonic setting discrimination of sedimentary basins. pp. 181–193.

Boggs, S, J. (2009). Petrology of Sedimentary Rocks. State-wide Agricultural Land Use Baseline 2015. Second ed. New York: Cambridge University Press.

Bracciali, L., Marroni, M., Pandolfi, L., and Rocchi, S. (2007). Geochemistry and Petrography of Western Tethys Cretaceous sedimentary covers (Corsica and Northern Apennines): from source areas to configuration of margins, Geological Society of America. Geological Society of America Special Paper.

Chang, K. H. (1975). Unconformity-bounded stratigraphic units, Geological Society of America Bulletin, 86(51107), pp. 1544–1552.

Callaghan, C.C. (1986). The Waterberg Basin: its evolution, sedimentation and mineralisation, in Geological Society of South Africa, pp. 759–762.

Callaghan, C.C. (1993). The Geology of the Waterberg Group in the southern portion of the Waterberg Basin, Bulletin of Geological Survey of South Africa, 104, p. 83.

Catuneanu, O., Wopfner, H., Eriksson, P. G., Cairncross, B., Rubidge, B. S., Smith, R., and Hancox, P. J. (2005). The Karoo basins of south-central Africa, Journal of African Earth Sciences, 43(1–3), pp. 211–253.

Cheney, E.S., and Twist, D. (1986). The Waterberg “Basin” - a reappraisal. 89, 353-360, Transactions of the Geological Society of South Africa, 89, pp. 353–360.

Coertze, J. F., Jansen, H., and Walraven, F. (1977). The Transition from the Transvaal Sequence to the Waterberg Group’, Trans. Geol. Soc. S. Afr, 80, pp. 145–156.

Condie, K. C., Des Marais, D. J., and Abbott, D. (2001). Precambrian superplumes and supercontinents: a record in black shales, carbon isotopes, and paleoclimates, Precambrian Research. Elsevier, 106(3–4), pp. 239–260.

Cullers, R.L. (2000). The geochemistry of shales, siltstones and sandstones of Pennsylvanian–Permian age, Colorado, USA: implications for provenance and metamorphic studies, Lithos, 51(3), pp. 181–203.

De Kock, M.O. (2006). Palaeomagnetism of the lower two unconformity-bounded sequences of the Waterberg Group, South Africa: Towards a better-defined apparent polar wander path, 109(1986), pp. 157–182.

De Vries, S. T. (1969). Early Archean sedimentary basins: depositional environment and hydrothermal systems. Examples from the Barberton and copping gap greenstone belts Geologie Ultraiectina, 244 160 pp

De Vries, W.C.P. (1973): Sedimentary structures in the southern and central portions of the Waterberg area, north-western Transvaal: Ann. geol. Surv. S. Afr., 7. 56-73.

Dickinson, W.R. and Suczek, T, A. (1979). Plate tectonics and sandstone compositions, The American Association of Petroleum Geologists Bulletin, 63(12), p. 2164-2182.

Dickinson, W. R. (1983). Compositions of Sandstones in Circum-Pacific Subduction Complexes and Fore-Arc Basins, AAPG Bulletin, 66(2), pp. 121–137.

Dickinson, W.R., Beard, L. S., Brakenridge, G.R., Erjavec, J.L., Ferguson, R.C., Inman, K.F., Knepp, R.A., Lindberg, F. A. and Ryberg, P.T. (1983). The provenance of North American Phanerozoic sandstones concerning the tectonic setting, Geological Society of America Bulletin, 94(2), p. 222.

Dorland, H. C. (2006). Precise SHRIMP U-Pb zircon age constraints on the lower Waterberg and Soutpansberg Groups, South Africa', South African Journal of Geology, 109(1–2), pp. 139–156.

Dorland, H.C., Beukes, N.J., Gutzmer, J. and Armstrong, R.A. (2006). Precise SHRIMP U-Pb zircon age constraints on the lower Waterberg and Soutpansberg Groups, South Africa, South African Journal of Geology, 109(1–2), pp. 139–156.

Du Plessis, C. (1987). New perspectives on early Waterberg Group sedimentation from Gatkop area, north-western Transvaal South African Journal of Geology, 90, pp. 395–408.

Eriksson, Patrick., Long, Darrel., Bumby, Adam., Eriksson, Kenneth., Simpson, Edward., Long, Darrel., Bumby, Adam., Eriksson, Kenneth., Simpson, Edward.,

Classen, Marko., Mtimkulu, Mtimkulu., Mudziri, Kenneth., Brümer, Jacobus., and van der Neut, Markus. (2008). Palaeohydrological data from the c. 2. 0 to 1. 8 Ga Waterberg Group, South Africa: discussion of a possibly unique Palaeoproterozoic fluvial style, 111, pp. 281–304.

Eriksson, P.G., Catuneanu, O., Sarkar, S., and Tirsgaard, H. (2005). Patterns of sedimentation in the Precambrian, Sedimentary Geology, 176(1–2), pp. 17–42.

Eriksson, P.G., Bumby, A.J., Brümer, J.J., and van der Neut, Markus. (2006). Precambrian fluvial deposits: Enigmatic palaeohydrological data from the c. 2 – 1. 9 Ga Waterberg Group, South Africa, 190, pp. 25–46.

Eriksson, P. G., Hattingh, P. J., and Altermann, W. (1995). An overview of the geology of the Transvaal Sequence and Bushveld Complex, South Africa, Journal of for sedimentary research 111.

Eriksson, P. G., and Reczko, B.F.F. (1997). The economic mineral potential of the mid-Proterozoic Waterberg Group, northwestern Kaapvaal craton, South Africa, Minerilium deposita, 32, pp. 401–409.

Eriksson, P.G., Schreiber, U.M., Reczko, B.F.F., and Snyman, A.N. (1994). Petrography and geochemistry of sandstones interbedded with the Rooiberg Felite Group (Transvaal, South Africa): Implications for provenance and tectonic setting, Journal for sedimentary research, A64(4), pp. 836–846.

Fiantis, D., Nelson, M., Shamshuddin, J., Goh, T. B., and Van Ranst, E. (2010). Determination of the Geochemical Weathering Indices and Trace Elements Content of New Volcanic Ash Deposits from Mt. Talang (West Sumatra) Indonesia, Eurasian Soil Science, 43(13), pp. 1477–1485.

Floyd, P.A. and Leveridge, B.E. (1987). A tectonic environment of the Devonian Gramscatho basin, south Cornwall: framework mode and geochemical evidence from turbiditic sandstones, Journal of the Geological Society, 144(4), pp. 531–542.

Floyd, P. A., Winchester, J. A. and Park, R. G., (1989). 'Geochemistry and tectonic setting of Lewisian clastic metasediments from the Early Proterozoic Loch Maree Group of Gairloch, NW Scotland', Precambrian Research. Elsevier, 45(1–3), pp. 203–214.

Folk, R. (1954). The Distinction between Grain Size and Mineral Composition in Sedimentary-Rock Nomenclature Author (s): Robert L. Folk Source: The Journal of Geology, Vol. 62, No. 4 (Jul. 1954), pp. 344-359 Published by The University of Chicago Press Stab, The Journal of Geology, 62(4), pp. 344–359.

Folk, R. L. (1974). Petrology of sedimentary rocks, Hemphill Publishing Company, Austin, p. 170.

Gressly, A. (1838). Observations géologiques sur le Jura soleurois. Nouveaux mémoires de la Société Helvetique des Sciences Naturelles, Neuchâtel, 349 (2), 1-14.

Hatano, N., Yoshida, K. and Sasao, E. (2019). Effects of grain size on the chemical weathering index: A case study of Neogene fluvial sediments in southwest Japan, Sedimentary Geology. Elsevier, 386, pp. 1–8.

Hayashi, K. I., Fujisawa, H., Holland, H.D. and Ohmoto, H., (1997). Geochemistry of ~1.9 Ga sedimentary rocks from northeastern Labrador, Canada, Geochimica et Cosmochimica Acta. Pergamon, 61(19), pp. 4115–4137.

Hessler, A.M. and Lowe, D.R. (2006). Weathering and sediment generation in the Archean: An integrated study of the evolution of siliciclastic sedimentary rocks of the 3.2 Ga Moodies Group, Barberton Greenstone Belt, South Africa, Precambrian Research. Elsevier, 151(3–4), pp. 185–210.

Jansen, H. (1970). Precambrian basins on the Transvaal craton and their sedimentological and structural features, Transactions of geological Society of South Africa, 78, pp. 25–23.

Johnson, M.R., Vuuren, C.J., Van Visser, J.N.J., Cole, D.I., Wickens, H., De V., Christie, A.D.M. and Roberts, D.L. (1997). Chapter 12 The foreland Karoo basin, South Africa, Sedimentary Basins of the World, 3, pp. 269–317.

Johnson, M.R., Anhaeusser, C.R. and Thomas, R.J. (2006). The geology of South Africa. Pretoria; Johannesburg: Council for Geoscience; Geological Society of South Africa and Council for Geoscience.

Jolayemi, O. O. (2015). Chemical evolution of the Paleoproterozoic Rooiberg Group, Kaapvaal Craton, South Africa: new insights into the formation of a silicic large igneous province (SLIP), University of Pretoria.

Kent, L., (1980). The Stratigraphy of South Africa: South Africa Geological Survey Handbook 8. handbook 8. Geological Survey.

Kinnaird, J. (2006). The Bushveld Large Igneous Province Igneous Complex, South African Journal of Geology 48 (62), pp. 72-80.

Lenhardt, N. and Eriksson, P.G. (2011). Volcanism of the Palaeoproterozoic Bushveld Large Igneous Province: The Rooiberg Group, Kaapvaal Craton, South Africa, Precambrian Research. Elsevier.

Maré, L.P. (2003). A paleomagnetic study of selected formations in the Waterberg Group, South Africa. The University of Pretoria.

Maré, L. P., Eriksson, P.G. and Améglio, L. (2006). A palaeomagnetic study of the lower part of the Palaeoproterozoic Waterberg Group, South Africa, Journal of African Earth Sciences, 44(1), pp. 21–36.

Martini, J.E.J. (1998). The Loskop Formation and its relationship to the Bushveld Complex, South Africa, Journal of African Earth Sciences, 27(2), pp. 193–222.

Masango, S.M. (2014). Physical volcanology of the Rooiberg Group near Loskop Dam, Mpumalanga, South Africa. The University of Pretoria.

McCann, N. (1991). Subsurface Geology of the Lough Neagh-Larne Basin, Northern Ireland, Irish Journal of Earth Sciences, 11(1), pp. 53–64.

McLennan, S.M., Taylor, S.R., McCulloch, M.T. and Maynard, J.B. (1990). Geochemical and Nd/Sr isotopic composition of deep-sea turbidites: Crustal evolution and plate tectonic associations, Geochimica et Cosmochimica Acta, 54(7), pp. 2015–2050.

Mclennan, S.M., (1983). Continental Crust, Scientific American, 249(3).

McLennan, S.M., Hemming, S., McDaniel, D.K. and Hanson, G. N., (1993a) 'Geochemical approaches to sedimentation, provenance, and tectonics', pp. 21–40.

Miall, A.D. (1978). Paleocurrent analysis of alluvial sediments; a discussion of directional variance and vector magnitude, Journal of Sedimentary Research, 44(4), pp. 1174–1185.

Miall, A.D. (1985). Architectural-element analysis: A new method of facies analysis applied to fluvial deposits, Earth-Science Reviews, 22(4), pp. 261–308.

Miall, A.D. (1992). Hierarchies of Architectural Units in Terrigenous Clastic Rocks, and Their Relationship to Sedimentation Rate, Society for Sedimentary Geology, (D), pp. 6–12.

Miall, A.D. (1999). In defence of Facies Classifications and Models, Journal of Sedimentary Research, 69(1), pp. 2–5.

Miall, A.D. (2006). Reconstructing the architecture and sequence stratigraphy of the preserved fluvial record as a tool for reservoir development: A reality check, AAPG Bulletin, 90(7), pp. 989–1002.

Mtimkulu, M.N. (2009) A provisional basinal study of the Waterberg-Karoo, South Africa, The University of Pretoria.

Nesbitt, H., and Young, G. (1984a). Prediction of some weathering trends of plutonic and volcanic rocks based on thermodynamic and kinetic considerations, Geochimica et Cosmochimica Acta. Pergamon, 48(7), pp. 1523–1534.

Nesbitt, H.W., Young, G.M., McLennan, S.M. and Keays, R.R. (1996). Effects of Chemical Weathering and Sorting on the Petrogenesis of Siliciclastic Sediments, with Implications for Provenance Studies, The Journal of Geology, 104(5), pp. 525–542.

Nesbitt, H.W., and Young, G.M. (1982a). Early proterozoic climates and plate motions inferred from major element chemistry of lutites, Nature, 299(5885), pp. 715–717.

Osman, M. (1996). Recent to Quaternary River Nile Sediments: A Sedimentological Characterization on Samples from Aswan to Naga Hammadi, Egypt (Unpublished doctoral dissertation). University of Vienna, Vienna

Pinotti, A, E., D′Eramo L., Castro F., Rabbia A., Coniglio O., Demartis J., Hernando M., Cavarozzi I., Aguilera C, E.., and Yolanda E. (2013). 'The Farallon-Aluk ridge collision with South America: Implications for the geochemical changes of slab window magmas from fore- to back-arc', Geoscience Frontiers, 4(4), pp. 377–388.

Pettijohn, F. (1954). Classification of Sandstones, The Journal of Geology, 62(4), pp. 360–365.

Roser, B.P. and Korsch, R.J. (1986). Determination of Tectonic Setting of Sandstone-Mudstone Suites Using SiO_2 Content and K_2O/Na_2O ratio, The Journal of Geology, 94(5), pp. 635–650.

Roser, B.P. and Korsch, R.J. (1988). Provenance signatures of sandstone-mudstone suites determined using discriminant function analysis of major-element data, Chemical Geology, 67(1), pp. 119–139.

Rudnick, R.L. and Gao, S. (2013). Composition of the Continental Crust. 2nd ed, Treatise on Geochemistry: Second Edition. Elsevier Ltd.

Russell, H, P. (1997). 'The Geology, Geochemistry and Metallogeny of the felsic rocks of the Bushveld Complex, North of Bronkhorstspruit, South Africa. The University of Witwatersrand.

Salvador, A. (1949). Unconformity-bounded stratigraphic units, Geological Society of America Bulletin, 98(51107), pp. 1544–1552.

Salvador, A. (1987). Unconformity-bounded stratigraphic units, Geological Society of America Bulletin, 98, pp. 232–237.

Schweitzer, J.K. and Hatton, C. J. (1995). Chemical alteration with the volcanic of rocks of the Bushveld Complex, Economic Geology, 90(8), pp. 2218–2231.

South African Committee of Stratigraphy (1980) Stratigraphy of South Africa. Part 1 (Comp. L.E. Kent). Lithostratigraphy of South Africa, South West Africa/Namibia, and the Republics of Bophuthatswana, Transkei and Venda. Handbook of Geological Survey of South Africa.

Thirlwall, M.F. (1991). X-ray Fluorescence in the Geological Sciences: Advances in Methodology. (Geological Association of Canada, Short course 7), 1990, 297, Mineralogical Magazine, 55(380), pp. 487–487.

Toulkeridis, T., Clauer, N., Kröner, A., Reimer, T., and Wolfgang, T., (1999). Characterization, provenance, and tectonic setting of Fig Tree greywackes from the Archaean Barberton Greenstone Belt, South Africa, Sedimentary Geology, 124(1–4), pp. 113–129.

Twist, D. and French, B.M. (1983). Voluminous acid volcanism in the Bushveld Complex; a review of the Rooiberg Felsite. 46, 225–242. Ukstins, Bulletin Volcanologique, 46, pp. 225–242.

Van der Nuet, M., Eriksson, P.G., and Callaghan, C.C. (1991). Distal alluvial fan sediments in the early Proterozoic red beds of the Wilgerevier Formation, Waterberg Group, South Africa, Journal of African Earth Sciences, 12, pp. 537–547.

Walraven, F. and Hattingh, E. (1993). Geochronology of the Nebo Granite, Bushveld Complex, South African Journal of Geology, 96(112), pp. 31–41.

Weltje, G. J. and von Eynatten, H. (2004). Quantitative provenance analysis of sediments: Review and outlook, Sedimentary Geology, 171(1–4), pp. 1–11.

Whittaker, A., Cope, J.C.W., Cowie, J.W., Gibbons, W., Hailwood, E.A., House, M.R., Jenkins, D.G., Rawson, P.F., Rushton, A.W.A., Smith, D.G., Thomas, A.T. and Wimbledon, W. A. (1991). Guide to the stratigraphical procedure, Journal of Geological Society, London, 148, pp. 813–824.

Yerino, L.N. and Maynard, J. (1984). Petrography of modern marine sands from the Peru-Chile Trench and adjacent areas, The Journal of International Association of Sedimentologists, 31(1)(Mm), pp. 1–18.

Zeh, A., Wilson, A. H. and Ovtcharova, M. (2016). Source and age of upper Transvaal Supergroup, South Africa: Age-Hf isotope record of zircons in Magaliesberg quartzite and Dullstroom lava, and implications for Paleoproterozoic (2.5–2.0 Ga) continent reconstruction, Precambrian Research. Elsevier, 278, pp. 1–21.

APPENDICES

APPENDIX A

Sample location

Name	Type	Date Time	Elevation (m)	Lithology	Longitude	Latitude
AM0027	WPT	2016-10-14 09:22:18	1473.38	Quartz arenite	28˚37'71	-24.46 ' 36
AM0028	WPT	2016-10-14 09:43:26	1491.20	CONG PEB 300CM X 200CM	28˚37'73	-24.46 ' 44
AM0029	WPT	2016-10-14 09:47:58	1491.21	CONGLOMERATE	28˚37'73	-24.46 ' 44
AM0030	WPT	2016-10-14 09:51:00	1489.14	SHARP CONTAC BAND OF SAND10M	28˚37 ' 72	-24.46 ' 45
AM0031	WPT	2016-10-14 09:55:09	1495.05	SANDSTONE	28 ˚.37 ' 73	-24.46 ' 45
AM0032	WPT	2016-10-14 10:07:53	1502.58	CONGLOMERATE	28 ˚.37 ' 75	-24.46 ' 48
AM0034	WPT	2016-10-14T10:25:16	1506.63	MONO POLOMICTIC	28 ˚.37 ' 78	-24.46 ' 50
AM0035	WPT	2016-10-14 10:51:01	1481.70	CONT GLEN AND ROOIB	28 ˚.37 ' 82	-24.46 ' 59
AM0037	WPT	2016-10-14 11:32:30	1481.03	CONNT	28 ˚.37 ' 73	-24.46 ' 36
AM0038	WPT	2016-10-14 11:36:35	1495.22	THIN BAND OF SANDSTONE	28 ˚.37 ' 72	-24.46 ' 33
AM0039	WPT	2016-10-13T08:38:47Z	1485.92	SHPC CONG/SANDT	28 ˚.37 ' 64	-24.46 ' 33
AM0040	WPT	2016-10-13 08:50:10	1420.69	SANDSTONE WITH SPARODIC PEBBLES	28 ˚.37 ' 62	-24.46 ' 34
AM0041	WPT	2016-10-13 08:52:21	1421.22	SANDSTONE WITH SPARODIC PEBBLES	28 ˚.37 ' 63	-24.46 ' 34
AM0044	WPT	2016-10-13 09:10:09	1431.91	Massive Sandstone	28 ˚.37 ' 71	-24.46 ' 24
AM0045	WPT	2016-10-13 09:17:39	1443.70	Massive Sandstone	28 ˚.37 ' 73	-24.46 ' 20
AM0046	WPT	2016-10-13 10:26:35	1453.87	CONTACT GLEN & WATERBERG	28 ˚.37 ' 81	-24.46 ' 23
AM0047	WPT	2016-10-12 07:33:18	1456.95		28 ˚.38 ' 54	-24.45 ' 69
AM0048	WPT	2016-10-12 07:47:42	1448.08		28 ˚.38 ' 55	-24.45 ' 69
AM0049	WPT	2016-10-12 08:03:10	1455.56		28 ˚.38 ' 56	-24.45 ' 71
AM0050	WPT	2016-10-12 08:05:09	1452.33		28 ˚.38 ' 56	-24.45 ' 70
AM0051	WPT	2016-10-12 08:06:02	1454.59		28 ˚.38 ' 56	-24.45 ' 70
AM0052	WPT	2016-10-12 08:32:34	1489.81		28 ˚.38 ' 62	-24.45 ' 78

AM0053	WPT	2016-10-12 08:37:18	1494.47		28 ˚.38 ˈ 62	-24.45 ˈ 79
AM0054	WPT	2016-10-12 08:42:32	1495.65		28 ˚.38 ˈ 62	-24.45 ˈ 80
AM0055	WPT	2016-10-12 08:46:28	1503.31		28 ˚.38 ˈ 62	-24.45 ˈ 81
AM0056	WPT	2016-10-12 08:49:27	1490.63		28 ˚.38 ˈ 61	-24.45 ˈ 82
AM0057	WPT	2016-10-12 10:25:54	1545.84	xcutting sandstone	28 ˚.38 ˈ 61	-24.45 ˈ 88
AM0058	WPT	2016-10-12 10:28:54	1551.23	pebble sandstone	28 ˚.38 ˈ 61	-24.45 ˈ 89
AM0059	WPT	2016-10-12 10:59:24	1569.63	sandstone	28 ˚.38 ˈ 61	-24.45 ˈ 91
AM0060	WPT	2016-10-12 11:04:25	1574.93	LAVA CONTACT Rooiberg	28 ˚.38 ˈ 63	-24.46 ˈ 00
AM0061	WPT	2016-10-12 11:14:37	1563.86	quartzite	28 ˚.38 ˈ 71	-24.46 ˈ 03
AM0062	WPT	2016-10-12 11:39:24	1559.13	sandstone	28 ˚.38 ˈ 73	-24.46 ˈ 10
AM0063	WPT	2016-10-12 12:17:34	1544.84	SANDSTONE	28 ˚.38 ˈ 86	-24.46 ˈ 10
AM0064	WPT	2016-10-12 13:19:12	1552.19	CONGLOMERATE	28 ˚.38 ˈ 87	-24.46 ˈ 09
AM0065	WPT	2016-10-12 13:21:07	1555.36	CONGLOMERATE	28 ˚.38 ˈ 86	-24.46 ˈ 08
AM0066	WPT	2016-10-12 13:22:39	1556.38	SANDSTONE	28 ˚.38 ˈ 86	-24.46 ˈ 07
AM0067	WPT	2016-10-12 13:26:19	1557.90	CONFUP3M	28 ˚.38 ˈ 86	-24.46 ˈ 06
AM0068	WPT	2016-10-12 13:33:16	1568.47	CONGLOMERATE	28 ˚.38 ˈ 84	-24.45 ˈ 99
AM0069	WPT	2016-10-12 13:41:37	1560.79	SANDSTONE	28 ˚.38 ˈ 82	-24.45 ˈ 93

APPENDIX B

Facies architecture

Architectural Element	Facies code	Lithofacies	Sedimentary structures	Interpretation
CH	Sp, St, Sr, Gm, and Sh	Sp (sand, medium to v. course, maybe pebbly)	solitary (alpha) or grouped (omikron) planar cross-beds	Linguoid, transverse bars, sand waves (lower flow regime)
		St (sand, medium to v. course, maybe pebbly)	solitary (theta) or grouped (pi) trough cross-beds	Dunes (lower flow regime)
		Sr (sand, very fine to coarse)	Ripple marks of all types	Ripples (lower flow regime)
		Gm (massive or crudely bedded gravel)	Horizontal bedding (imbrication)	Longitudinal bars, lag deposits, sieve deposits
		Sh (sand, medium to v. course, maybe pebbly)	Horizontal laminations, parting or streaming lineation	Planar bed flow (I. and U. flow regime)
LA	St	St (sand, medium to v. course, maybe pebbly)	solitary (theta) or grouped (pi) trough cross-beds	Dunes (lower flow regime)
SG	Gms and Sg	Gms (massive, matrix-supported gravel)	none	Debris flow deposits
GB	Gm and Gp	Gm (massive or crudely bedded gravel)	Horizontal bedding (imbrication)	Longitudinal bars, lag deposits, sieve deposits
		Gp (gravel, stratified)	Planar cross-beds	Minor channel fills
Fm		Mud and silt	Massive, desiccation cracks	Overbank or drape deposits
		Sp (sand, medium to v. course, maybe pebbly)	solitary (alpha) or grouped (omikron)	Linguoid, transverses bars, sand

SB	Sp, St, Sr, Gm, and Sh		planar cross-beds	waves (lower flow regime)
		St (sand, medium to v. course, maybe pebbly)	solitary (theta) or grouped (pi) trough cross-beds	Dunes (lower flow regime)
		Sr (sand, very fine to coarse)	Ripple marks of all types	Ripples (lower flow regime)
		Gm (massive or crudely bedded gravel)	Horizontal bedding (imbrication)	Longitudinal bars, lag deposits, sieve deposits
		Sh (sand, medium to v. course, maybe pebbly)	Horizontal laminations, parting or streaming lineation	Planar bed flow (I. and U. flow regime)
LS	Sh	Sh (sand, very fine to the very course may be pebbly)	Horizontal laminations, parting or streaming lineation	Planar bed flow (I. and U. flow regime)
OF	Fl	Fl (Sand, silt and mud)	Fine lamination, very small ripples	Overbank or waning flood deposits

APPENDIX C

Major elements

Farm	Formations	Samples	SiO2	TiO2	Al2O3	Fe2O3	MnO	MgO	CaO	Na2O	K2O	P2O5	Cr2O3	LOI
oog 1	Glentig Formation	PEB 001	86,61	0,12	2,45	9,5	0,02	0,04	0,03	0,02	0,68	0,046	0,113	0,46
oog 2	Alma Formation	PEB 002	72,55	0,38	12,05	8,28	0,05	0,48	0,04	0,06	4,17	0,056	0,022	1,89
oog 3	Alma Formation	PEB 003	73,34	0,34	12	7,64	0,05	0,47	0,04	0,14	4,16	0,063	0,008	1,71
oog 4	Alma Formation	PEB 004	67,03	0,46	15,88	7,85	0,05	0,66	0,03	0,07	5,13	0,096	0,009	2,78
oog 5	Glentig Formation	PEB 005	90,4	0,19	4,96	1,21	0,02	0,19	0,02	0,02	1,65	0,051	0,058	0,73
oog 6	Glentig Formation	PEB 006	96,23	0,11	1,88	1,5	0,01	0	0,03	0,01	0,48	0,061	0,057	0,27
oog 7	Swaershoek Formation	PEB 007	75,71	0,09	4,96	16,15	0,03	0,23	0,09	0,05	1,64	0,093	0,018	0,67
oog 8	Alma Formation	PEB008	66,3	0,33	3,02	2,56	0,01	0,33	0,04	0,12	5,66	0,025	0,112	2,18
oog 9	Swaershoek Formation	PEB009	75,9	0,45	5,22	5,41	0,05	0,55	0,08	0,03	3,66	0,052	0,253	0,82
oog 10	Glentig Formation	PEB010	86,36	0,23	8,33	6,88	0,02	0,32	0,06	0,02	2,11	0,036	0,005	1,58
oog 11	Swaershoek Formation	PEB011	75,32	0,12	2,22	4,33	0,03	0,56	0,02	0,22	0,88	0,023	0,026	3,32
oog12	Swaershoek Formation	PEB012	50,21	0,36	4,66	6,88	0,01	0,45	0,03	0,05	2,32	0,024	0,034	3,23
oog13	Swaershoek Formation	PEB013	45,66	0,45	6,88	8,32	0,04	2,01	0,12	0,04	4,16	0,035	0,045	0,47
oog 14	Alma Formation	PEB 016	68,62	0,5	13,75	9,8	0,04	0,42	0,03	0,09	4,59	0,093	0,011	2,18
oog 15	Glentig Formation	MEL 0012	88,32	0,2	5,86	1,54	0,02	0,27	1	0,04	4,59	0,046	0,015	0,82
oog 16	Alma Formation	MEL 0015	76,63	0,5	10,66	5,73	0,05	0,5	0,07	0,06	4,59	0,094	0,022	1,58
oog 17	Swaershoek Formation	MEL 0016	54,64	1,68	17,04	12,5	0,25	2,91	1,25	0,14	4,59	1,05	0,025	3,32
oog 18	Swaershoek Formation	MEL 0017	47,95	1,79	22,56	14,4	0,06	0,46	1,2	0,4	4,59	1,28	0,019	3,23
oog 19	Glentig Formation	MEL 0018	91,92	0,35	3,01	2,96	0,01	0,04	0,01	0,01	4,59	0,042	0,037	0,47
oog 20	Alma Formation	MEL 026	74,25	0,13	14,82	2,68	0,04	0,45	0,04	0,05	4,59	0,061	0,011	2,16

oog 21	Glentig Formation	MELS 0016	87,22	0,35	5,01	3,54	0,03	0,1	0,02	0,01	4,59	0,085	0,018	0,9
oog 22	Glentig Formation	MEL 0025	81,36	0,11	11,43	1,61	0,01	0,22	0,01	0,08	4,59	0,048	0,008	1,76
oog23	Swaershoek Formation	MEL 0019	49,66	0,32	23,54	5,33	0,02	3,22	0,02	0,02	0,68	0,113	0,046	2,18
oog24	Glentig Formation	MEL0020	50,21	0,65	23,33	6,44	0,01	2,33	0,03	0,06	4,17	0,022	0,056	0,82
oog25	Swaershoek Formation	MEL0021	43,88	0,11	16,24	8,21	0,03	0,05	0,12	0,14	4,16	0,008	0,063	1,58
oog26	Swaershoek Formation	MEL0022	75,65	0,58	19,04	2,12	0,04	0,54	0,03	0,07	5,13	0,009	0,096	3,32
oog27	Swaershoek Formation	MEL0023	80,36	0,69	16,88	3,01	0,06	0,98	1	0,02	1,65	0,058	0,051	3,23
oog28	Alma Formation	MEL0024	45,75	0,47	26,44	8,21	0,01	2,33	0,07	0,01	0,48	0,057	0,061	0,47
oog29	Glentig Formation	MEL0026	66,63	0,68	5,66	6,44	0,03	0,45	1,25	0,05	1,64	0,018	0,093	2,18
oog30	Alma Formation	MEL0027	50,65	0,26	22,21	9,44	0,05	3,11	1,02	0,12	5,66	0,112	0,025	0,82
oog31	Swaershoek Formation	MEL0028	89,21	0,23	3,44	1,25	0,06	0,25	0,01	0,03	3,66	0,253	0,052	1,58
oog32	Swaershoek Formation	MEL0029	73,44	0,66	10,21	1,88	0,02	0,33	0,04	0,02	2,11	0,005	0,036	3,32
oog33	Glentig Formation	MEL0030	63,88	0,21	14,66	6,44	0,04	1,22	0,02	0,22	0,88	0,026	0,023	3,23
oog34	Alma Formation	MEL0031	45,36	0,65	18,36	10,22	0,06	3,66	0,01	0,05	2,32	0,034	0,024	0,47
oog35	Glentig Formation	MEL0032	66,32	0,32	2,33	7,88	0,03	0,23	0,03	0,04	4,16	0,045	0,035	2,16
oog36	Glentig Formation	MEL0033	71,63	0,54	16,44	2,44	0,04	0,33	0,04	0,09	4,59	0,011	0,093	0,9
oog37	Alma Formation	MEL0034	92,54	0,12	3,55	3,69	0,03	0,55	0,04	0,04	4,59	0,015	0,046	1,76
oog38	Swaershoek Formation	MEL0035	88,36	0,14	6,22	2,55	0,02	0,32	0,03	0,06	4,59	0,022	0,094	0,46
oog39	Alma Formation	MEL0036	76,54	0,34	14,88	1,08	0,05	0,56	0,02	0,14	4,59	0,025	1,05	1,89
oog40	Swaershoek Formation	MEL0037	83,22	0,12	6,11	1,01	0,06	0,45	0,03	0,04	4,59	0,019	1,28	1,71
oog41	Alma Formation	MEL0038	81,63	0,02	8,72	0,44	0,01	2,01	0,09	0,12	4,59	0,037	0,042	2,78
UCCC	UCC		66,6	0,64	15,4	5,04	0,1	2,48	3,59	3,27	2,8	0,12		
PAAS	PAAS		62,4	0,99	18,78	7,18	0,11	2,19	1,29	1,19	3,68	0,16		
NASC	NASC		64,82	0,8	17,05	5,7	0,1	2,83	3,51	1,13	3,97	0,15		
		Avarage	71,40122	0,39878	10,90024	5,593902	0,038293	0,843415	0,199024	0,074878	3,469512	0,106405	0,102244	1,74122
		Standard deviation	15,45575	0,360119	7,058832	3,857323	0,037875	0,985613	0,389524	0,074233	1,607851	0,247917	0,248922	1,014365
		Minmum	43,88	0,02	1,88	0,44	0,01	0	0,01	0,01	0,48	0,005	0,005	0,27
		Maximum	96,23	1,79	26,44	16,15	0,25	3,66	1,25	0,4	5,66	1,28	1,28	3,32

APPENDIX D

Trace elements

Samples	As	Ba	Ce	Co	Cr	Cu	Ga	Hf	La	Mo	Nb	Nd	Ni	Pb	Rb	Sc	Sn	Sr	Ta	Th	Tl	U	V	W	Y	Yb	Zn	Zr
PEB 001	68	1277	244	6,9	127	2,8	22	11	135	2,1	19	110	14	35	236	6,1	5,3	19	<2	18	3	6,1	49	<5	78	5,2	121	421
PEB 002	7,6	303	68	2,3	239	<2	2,7	<5	33	2,2	2,1	28	5,3	19	24	2,6	<3	11	<2	2	2,4	2,2	41	11	15	<4	8,6	174
PEB 003	74	833	135	3,9	118	<2	18	10	93	2	17	73	9,2	33	185	6,6	3,9	16	<2	17	<2	5,2	28	<5	61	5,3	146	365
PEB 004	31	1493	122	4,4	51	7,7	22	12	78	2,7	22	55	8,4	61	248	8,2	5,9	59	4,2	22	<2	6,2	42	<5	53	<4	73	496
PEB 005	NA	NA	NA	NA	NA	NA	NA	NA	NA	NA	NA	NA	NA	NA	NA	NA	NA	NA	NA	NA	NA	NA	NA	NA	NA	NA	NA	NA
PEB 006	NA	NA	NA	NA	NA	NA	NA	NA	NA	NA	NA	NA	NA	NA	NA	NA	NA	NA	NA	NA	NA	NA	NA	NA	NA	NA	NA	NA
PEB 007	22	402	47	3,4	255	<2	8,5	<5	22	2,7	2,4	25	6	24	77	4,2	3,5	8,9	3,8	2	2,1	3,2	48	7,6	24	<4	43	82
PEB008	25	1221	236	4	87	4,3	23	14	163	3	18	130	13	65	260	8,3	6,2	33	2,5	25	<2	7,6	43	<5	71	7,4	142	551
PEB009	4,3	671	49	3,4	253	6,7	6,9	<5	25	2	4,8	15	6,1	8,7	64	3,6	<3	6,7	<2	11	<2	<2	23	13	4,9	<4	11	171
PEB010	10	1260	86	6,4	203	5,8	15	7	43	2,2	11	41	13	47	171	8,2	<3	24	<2	10	<2	4,8	56	7,6	29	<4	93	267
PEB011	28	2421	204	34	175	79	21	8,7	88	2,9	26	62	131	41	234	21	3,1	53	<2	14	<2	8,9	114	9,3	37	<4	586	441
PEB012	11	3290	338	8,9	150	15	22	<5	137	2,8	17	113	22	65	234	25	4,8	204	4,2	18	<2	7,9	149	<5	38	<4	25	294
PEB013	4,6	429	64	2,4	393	7	4,5	<5	36	<2	3,5	31	4,7	13	35	4	<3	12	<2	4,2	<2	2,8	70	7	18	<4	23	141
PEB 016	25	1221	236	4	87	4,3	23	14	163	3	18	130	13	65	260	8,3	6,2	33	2,5	25	<2	7,6	43	<5	71	7,4	142	551
MEL 0012	4,3	671	49	3,4	253	6,7	6,9	<5	25	2	4,8	15	6,1	8,7	64	3,6	<3	6,7	<2	11	<2	<2	23	13	4,9	<4	11	171
MEL 0015	10	1260	86	6,4	203	5,8	15	7	43	2,2	11	41	13	47	171	8,2	<3	24	<2	10	<2	4,8	56	7,6	29	<4	93	267
MEL 0016	28	2421	204	34	175	79	21	8,7	88	2,9	26	62	131	41	234	21	3,1	53	<2	14	<2	8,9	114	9,3	37	<4	586	441
MEL 0017	11	3290	338	8,9	150	15	22	<5	137	2,8	17	113	22	65	234	25	4,8	204	4,2	18	<2	7,9	149	<5	38	<4	25	294
MEL 0018	4,6	429	64	2,4	393	7	4,5	<5	36	<2	3,5	31	4,7	13	35	4	<3	12	<2	4,2	<2	2,8	70	7	18	<4	23	141
MEL 026	41	657	364	3,8	117	5,4	35	15	226	<2	106	115	7,5	23	618	2,4	17	12	8,3	216	4,2	33	5,2	6,4	146	22	184	335
MELS 0016	<3	694	54	3,4	266	51	6,5	<5	22	3,4	3,4	11	7,2	618	54	4,8	<3	4,7	<2	6,9	2,1	4,2	202	5	<4	<4	9,3	170
MEL 0025	11	276	61	2	57	<2	21	11	22	<2	65	19	5,6	12	453	2	9,1	10	7,1	128	<2	15	8,7	<5	93	13	16	234

MEL 0019	1,10	2,80	15,1	1,98	8,60	2,15	0,74	2,47	0,43	2,71	0,62	1,79	0,27	1,66	0,26	0,40	146,40	2,90	33,40	1,10	<0.1	<0.1	<0.1	<0.1	5,90	<0.01	<0.1	101,00
MEL0020	4,50	10,30	39,4	4,75	17,40	3,50	0,88	3,44	0,55	3,46	0,77	2,17	0,32	2,09	0,32	0,50	65,60	9,70	85,00	4,50	<0.1	0,20	<0.1	<0.1	<0.5	<0.01	<0.1	200,00
MEL0021	3,90	10,50	40	4,77	16,70	3,41	0,83	3,46	0,56	3,21	0,70	2,11	0,31	1,97	0,30	1,10	56,00	8,10	71,60	3,90	<0.1	0,20	<0.1	<0.1	0,90	<0.01	<0.1	145,00
MEL0022	5,80	10,30	39,7	4,70	17,30	3,57	0,82	3,41	0,56	3,29	0,70	2,05	0,30	2,06	0,30	0,90	63,60	9,30	77,80	5,80	<0.1	0,20	<0.1	<0.1	2,40	<0.01	<0.1	223,00
MEL0023	3,10	10,20	39,9	4,73	17,00	3,51	0,83	3,30	0,55	3,39	0,74	2,11	0,32	1,99	0,31	0,40	57,00	8,50	86,40	3,10	0,10	0,50	0,10	<0.1	<0.5	<0.01	<0.1	210,00
MEL0024	3,70	10,50	41,5	4,80	17,70	3,45	0,77	3,43	0,57	3,31	0,70	2,05	0,32	2,01	0,31	0,50	50,00	7,80	83,50	3,70	0,10	0,50	0,40	<0.1	0,80	<0.01	<0.1	141,00
MEL0026	4,20	10,60	39,6	4,86	17,50	3,42	0,80	3,36	0,56	3,61	0,71	2,13	0,32	2,02	0,32	0,80	64,00	10,70	79,80	4,20	<0.1	0,40	<0.1	<0.1	2,70	<0.01	<0.1	225,00
MEL0027	3,30	9,60	39,4	4,62	17,30	3,37	0,80	3,33	0,56	3,26	0,74	2,18	0,31	2,04	0,31	0,30	62,90	10,10	80,00	3,30	<0.1	0,40	<0.1	<0.1	<0.5	<0.01	<0.1	440,00
MEL0028	2,70	10,10	40,4	4,81	17,60	3,31	0,80	3,45	0,56	3,49	0,71	2,06	0,31	2,05	0,33	0,50	61,30	9,50	77,10	2,70	<0.1	0,30	<0.1	<0.1	1,90	<0.01	<0.1	566,00
MEL0029	2,40	9,70	37,6	4,62	16,60	3,22	0,84	3,27	0,52	3,31	0,67	2,03	0,30	2,04	0,30	0,70	56,20	8,90	67,50	2,40	<0.1	0,30	<0.1	<0.1	1,60	<0.01	<0.1	596,00
MEL0030	3,40	8,70	34	4,17	15,60	3,21	0,80	3,35	0,56	3,38	0,73	2,21	0,30	2,03	0,30	0,80	87,90	6,80	64,10	3,40	<0.1	0,30	<0.1	<0.1	1,90	0,01	<0.1	147,00
MEL0031	2,90	6,30	33,6	5,03	19,40	3,74	0,97	4,11	0,67	4,01	0,90	2,60	0,37	2,31	0,36	0,30	69,50	5,20	104,50	2,90	<0.1	0,20	<0.1	<0.1	<0.5	<0.01	<0.1	258,00
MEL0032	0,60	6,80	29,2	3,75	13,30	2,80	0,73	2,90	0,47	2,95	0,63	1,89	0,27	1,78	0,27	0,50	71,40	4,80	97,20	0,60	<0.1	0,20	<0.1	<0.1	1,00	<0.01	<0.1	365,00
MEL0033	2,40	15,40	65,9	7,84	29,20	6,15	1,40	6,17	1,02	6,32	1,40	4,11	0,60	3,75	0,55	1,70	169,50	10,50	42,00	2,40	<0.1	0,20	<0.1	0,10	<0.5	<0.01	<0.1	125,00
MEL0034	9,10	6,90	31	3,78	13,90	3,07	0,75	3,21	0,53	3,28	0,72	2,19	0,30	1,91	0,31	0,70	71,00	4,90	101,70	9,10	<0.1	0,10	<0.1	<0.1	1,40	<0.01	<0.1	142,00
MEL0035	1,80	7,30	30	3,68	13,90	2,59	0,70	2,82	0,47	2,92	0,63	1,88	0,27	1,77	0,27	1,00	68,30	3,60	94,20	1,80	<0.1	0,10	<0.1	<0.1	<0.5	<0.01	<0.1	142,00
MEL0036	5,60	6,40	27,6	3,48	13,30	2,74	0,76	3,04	0,50	3,34	0,71	1,99	0,28	1,82	0,29	1,00	70,10	5,10	96,60	5,60	<0.1	0,20	<0.1	<0.1	<0.5	<0.01	<0.1	364,00
MEL0037	2,60	5,80	25,7	3,14	11,80	2,50	0,66	2,76	0,47	2,89	0,69	2,03	0,28	1,69	0,28	0,40	54,90	4,40	156,70	2,60	<0.1	0,40	<0.1	<0.1	1,40	<0.01	<0.1	146,00
MEL0038	4,30	8,40	34,6	4,28	16,20	3,28	0,80	3,22	0,52	3,20	0,72	2,02	0,29	1,94	0,29	0,70	75,00	7,50	75,90	4,30	<0.1	1,10	<0.1	<0.1	1,00	<0.01	<0.1	368,00
		626,00		17,00	92,00	28,00	17,50	5,30			12,00		47,00	17,00	84,00	14,00		32,00		10,50		2,70	97		21,00		67	193,00
		628,00		23,00	110,00	50,00	20,00	2,00			19,00		55,00	20,00	160,00	16,00		200,00		14,60		3,10	150		27,00		85	

APPENDIX E

Discrimination function values

Samples	Dicriminant function 2	Dicriminant Function 1
PEB 001	-58,902	-65,880577
PEB 002	-60,775	-157,833205
PEB 003	-59,731	-157,721868
PEB 004	-60,688	-157,336541
PEB 005	-45,371	-65,56283
PEB 006	-44,968	-34,857571
PEB 007	-71,354	-96,248987
PEB008	-44,350	-34,20674
PEB009	-51,311	-157,93324
PEB010	-58,493	-65,876612
PEB011	-42,931	-96,010754
PEB012	-41,449	-33,695147
PEB013	-45,564	-126,069952
PEB 016	-63,642	-126,771404
MEL 0012	-51,930	-65,430444
MEL 0015	-56,519	-157,702351
MEL 0016	-54,393	-767,196618
MEL 0017	-59,377	-179,764445
MEL 0018	-54,072	-35,260704
MEL 026	-52,131	-126,444715
MELS 0016	-53,989	-96,384054
MEL 0025	-51,425	-34,344042
MEL 0019	-41,734	-63,486492
MEL0020	-51,506	-33,871937
MEL0021	-52,143	-94,944256
MEL0022	-54,121	-127,281265
MEL0023	-50,343	-188,650612
MEL0024	-48,431	-33,206235
MEL0026	-47,145	-96,126601
MEL0027	-60,563	-156,155875
MEL0028	-46,143	-187,385097
MEL0029	-42,580	-65,618718
MEL0030	-48,408	-126,418456
MEL0031	-50,200	-187,886192
MEL0032	-52,617	-95,999184
MEL0033	-51,022	-127,066141
MEL0034	-56,376	-96,936008
MEL0035	-53,691	-65,801482
MEL0036	-49,386	-157,725068
MEL0037	-47,976	-188,755114
MEL0038	-46,346	-34,275281